

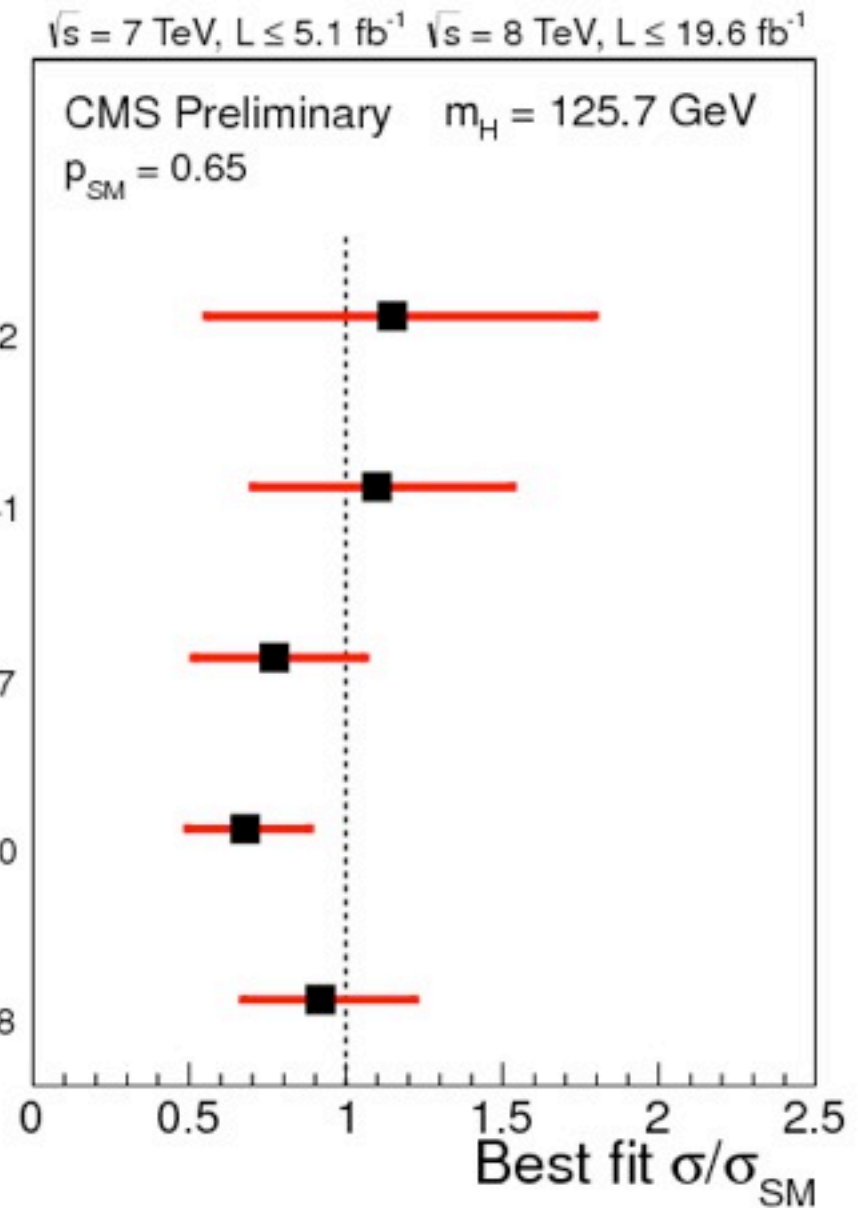
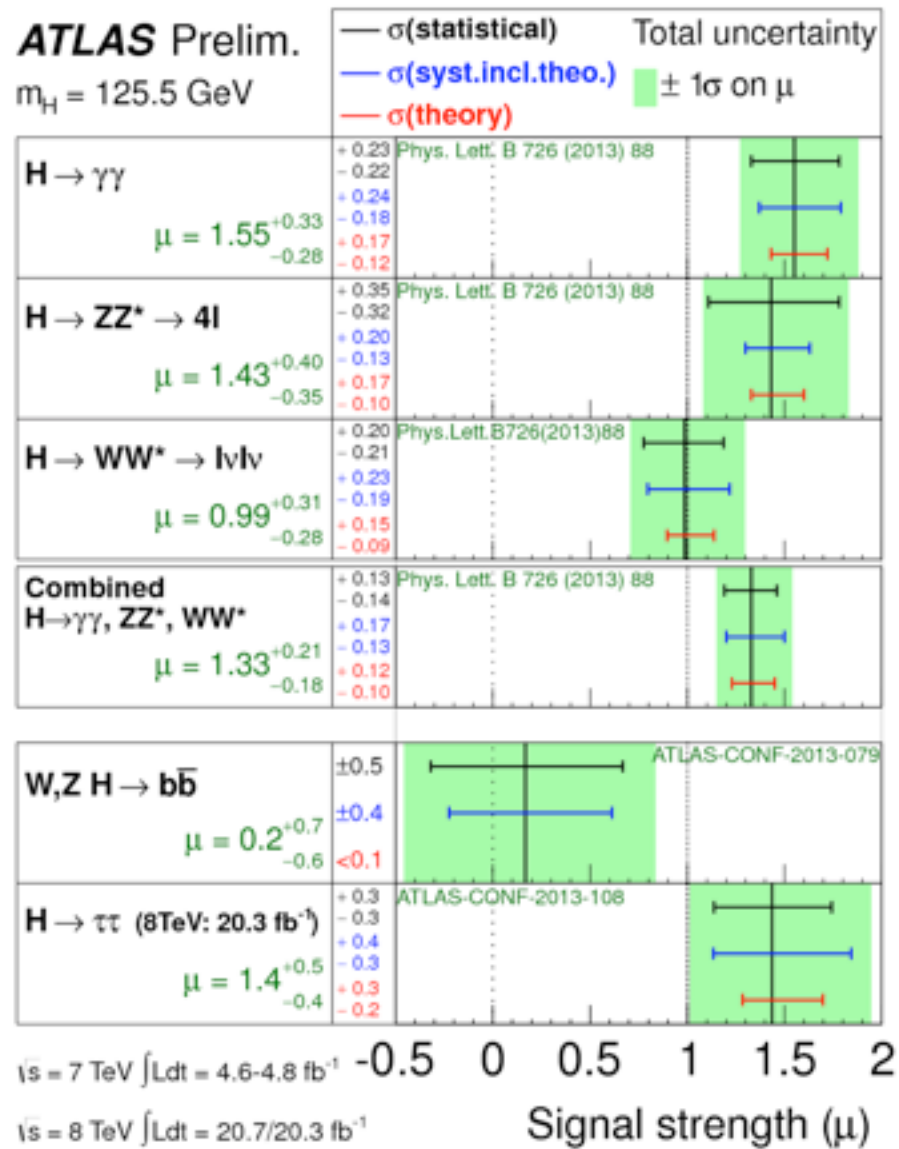
Precision QCD Confronts the Higgs

Jonathan Walsh, UC Berkeley



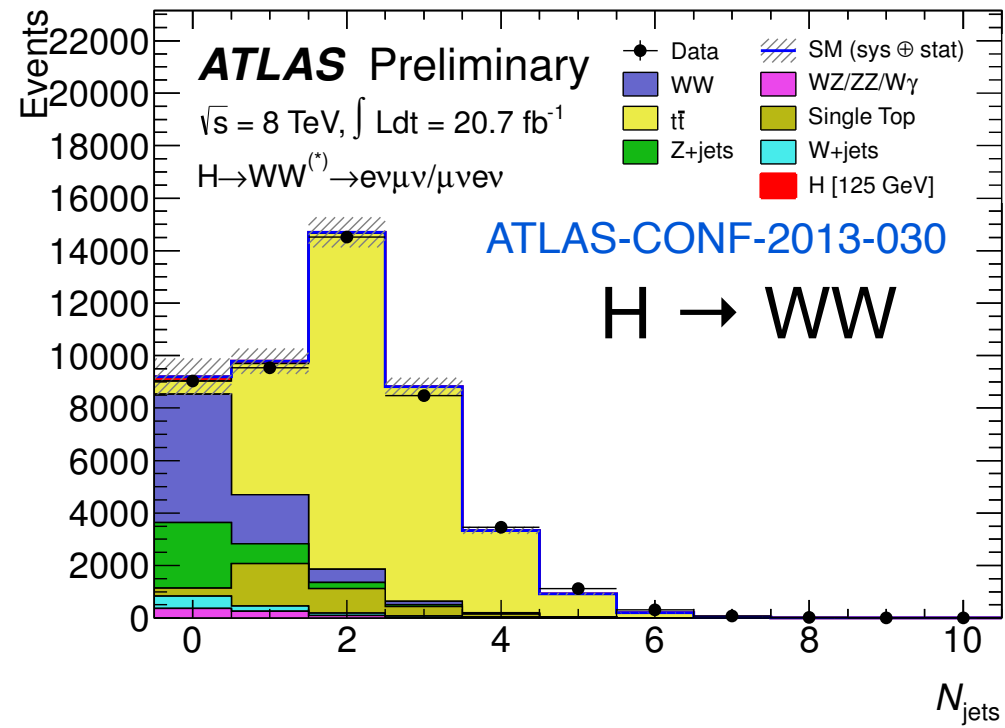
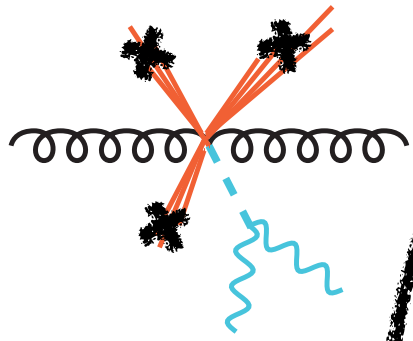
We are on the verge of uncovering the nature of the Higgs mechanism

ATLAS-CONF-2013-108

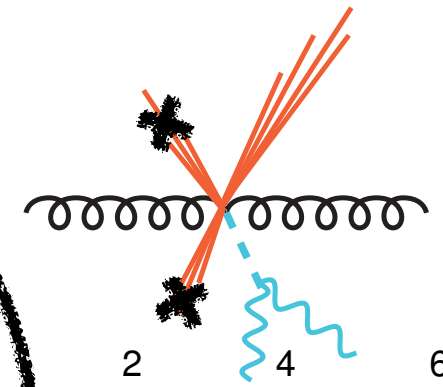


and precision QCD is necessary to maximize this opportunity

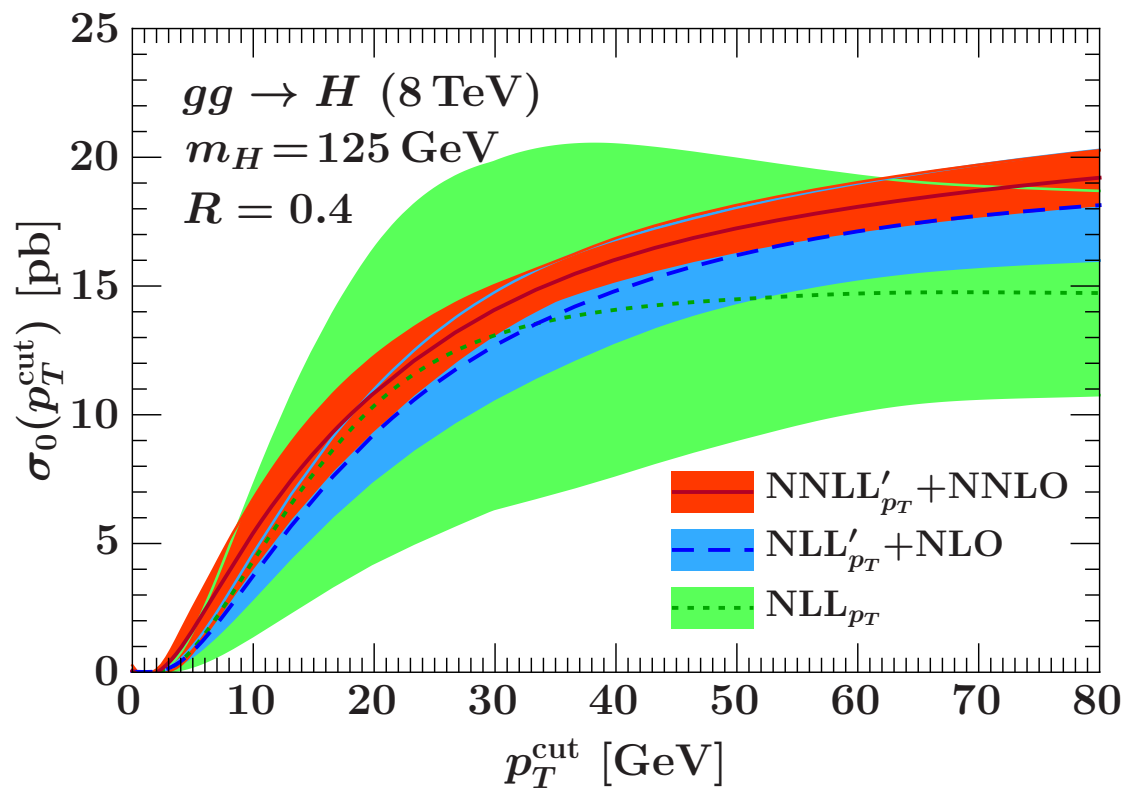
0-jet bin



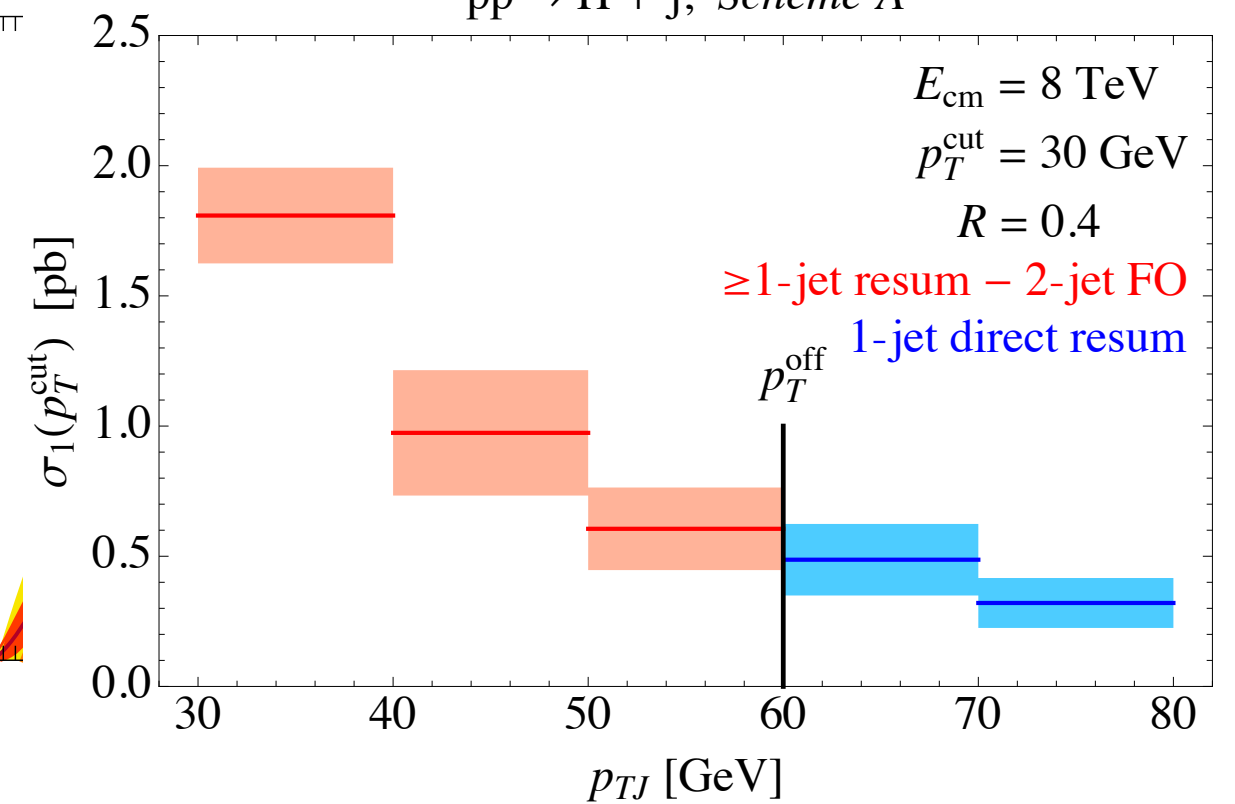
1-jet bin



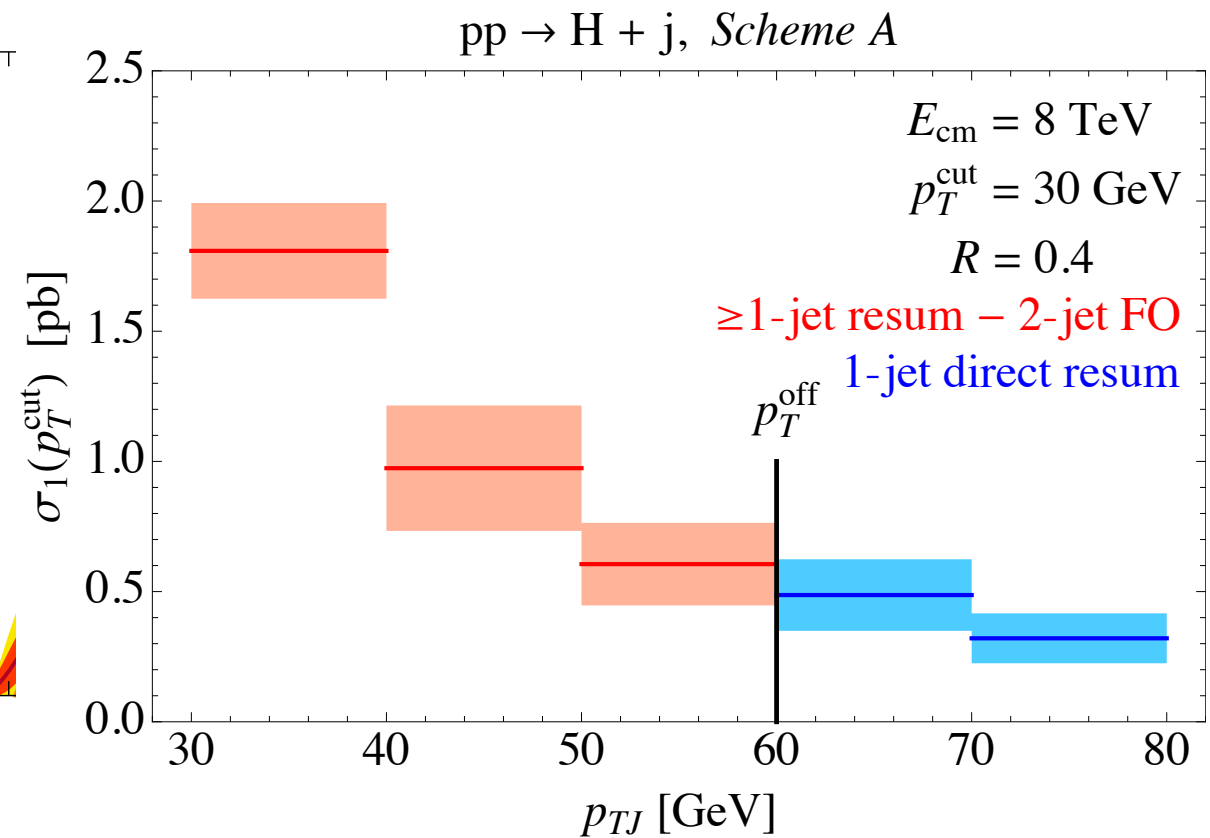
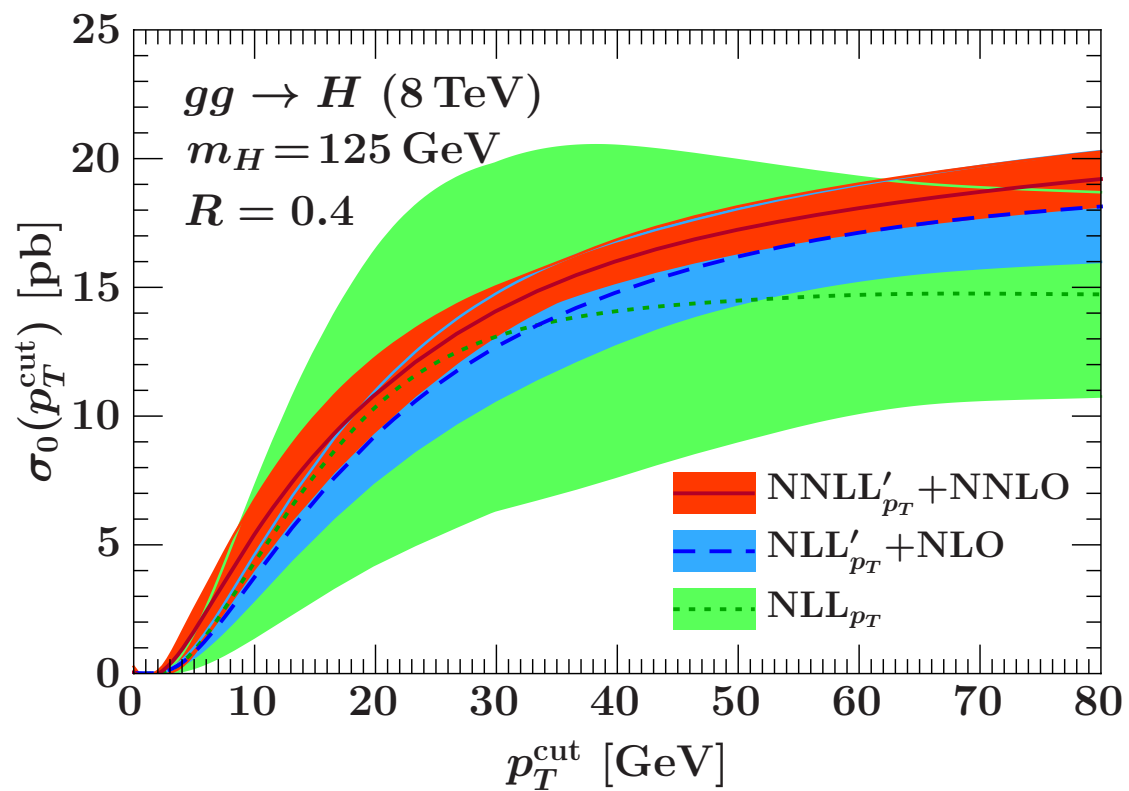
$pp \rightarrow H + j$, Scheme A



Stewart, Tackmann, JW, Zuberi, 1307.1808



Boughezal, Liu, Petriello, Tackmann, JW, 1312.4535



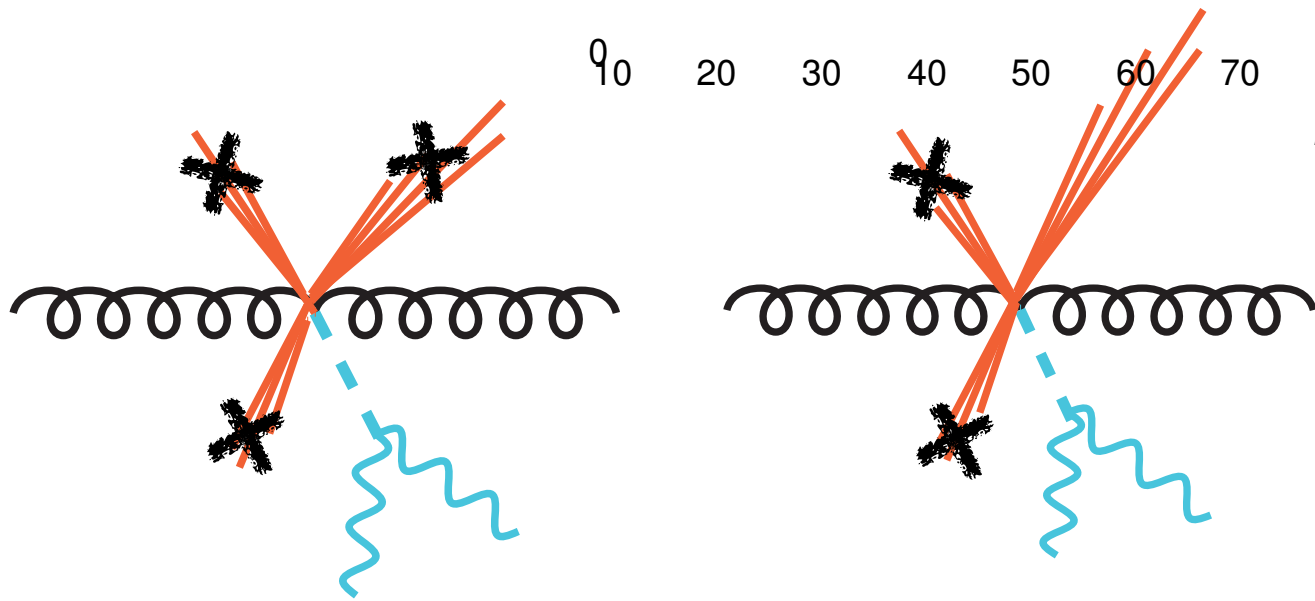
$$C_{\text{FO}}^{\text{ATLAS}} = \begin{pmatrix} 0 & 1 & \geq 2\text{-jet} \\ 4.24 & -1.99 & 0 \\ -1.99 & 5.23 & -3.24 \\ 0 & -3.24 & 3.24 \end{pmatrix} \text{pb}^2$$



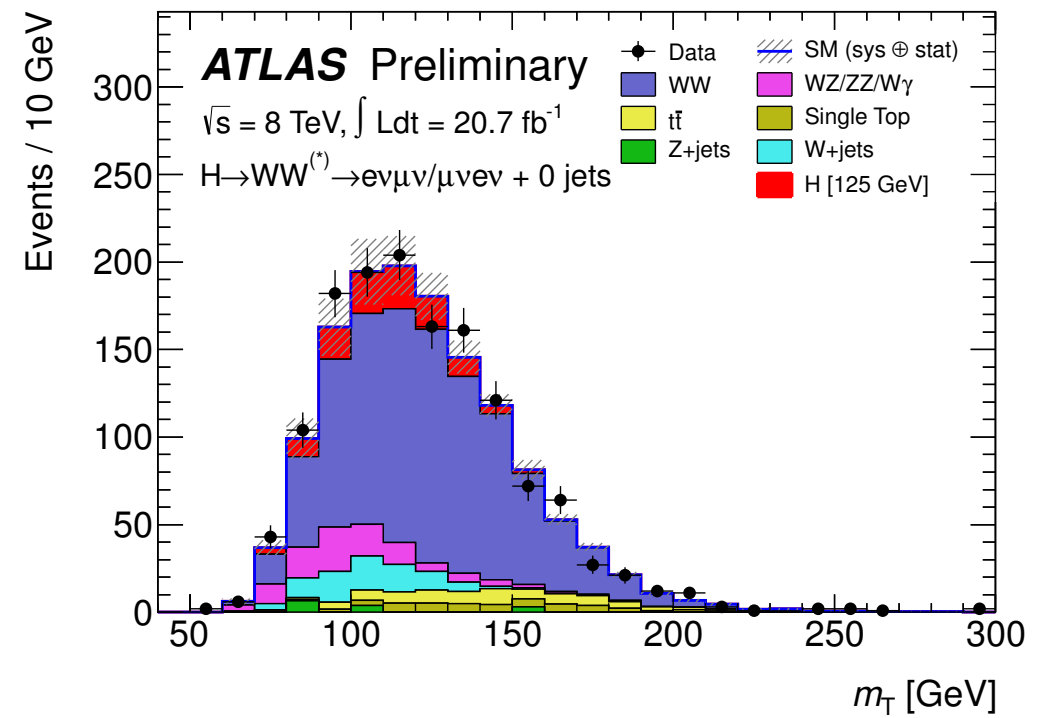
our resummed predictions dramatically
 improve theory uncertainties,
 roughly halving them

$$C^{\text{ATLAS}} = \begin{pmatrix} 1.49 & -0.39 & 0.20 \\ -0.39 & 0.88 & -0.04 \\ 0.20 & -0.04 & 0.32 \end{pmatrix} \text{pb}^2$$

The precision frontier and the Higgs



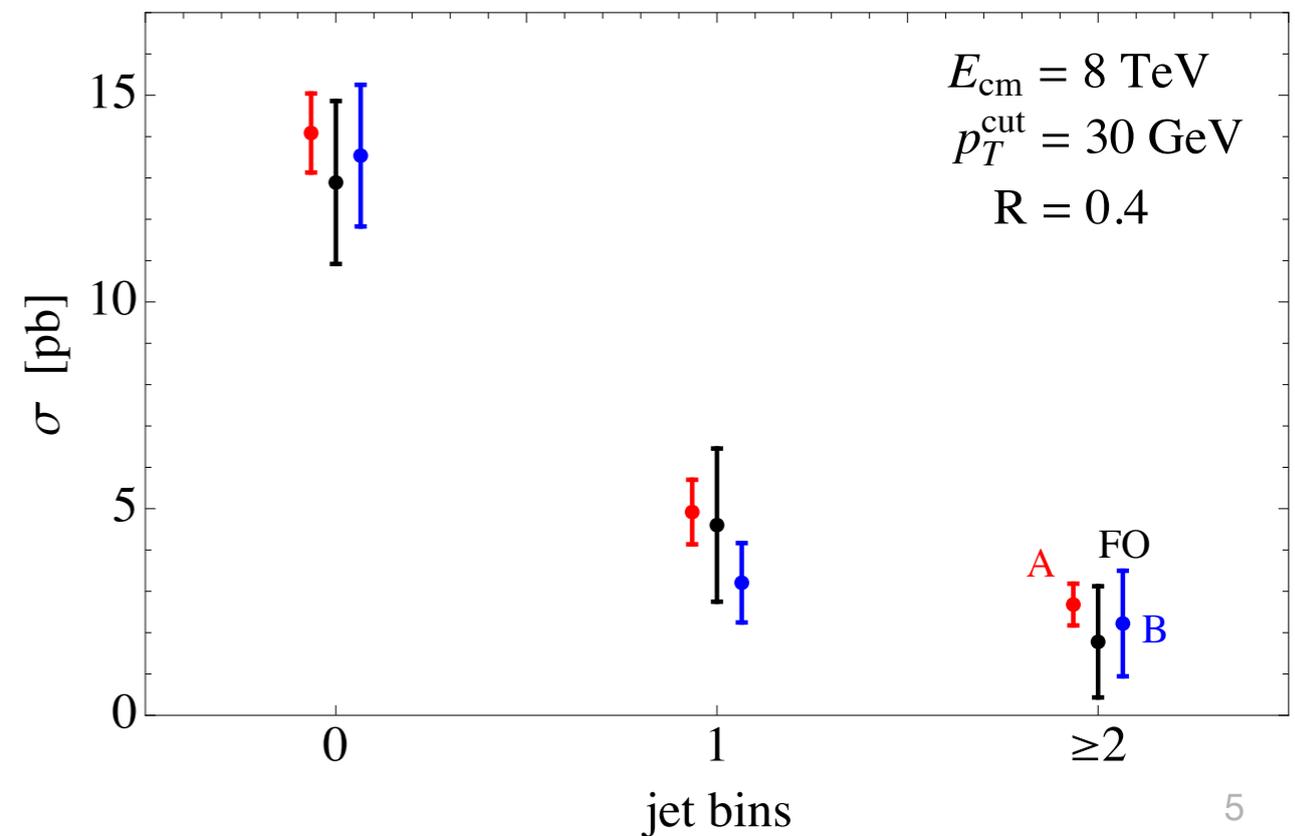
Implementation and future work



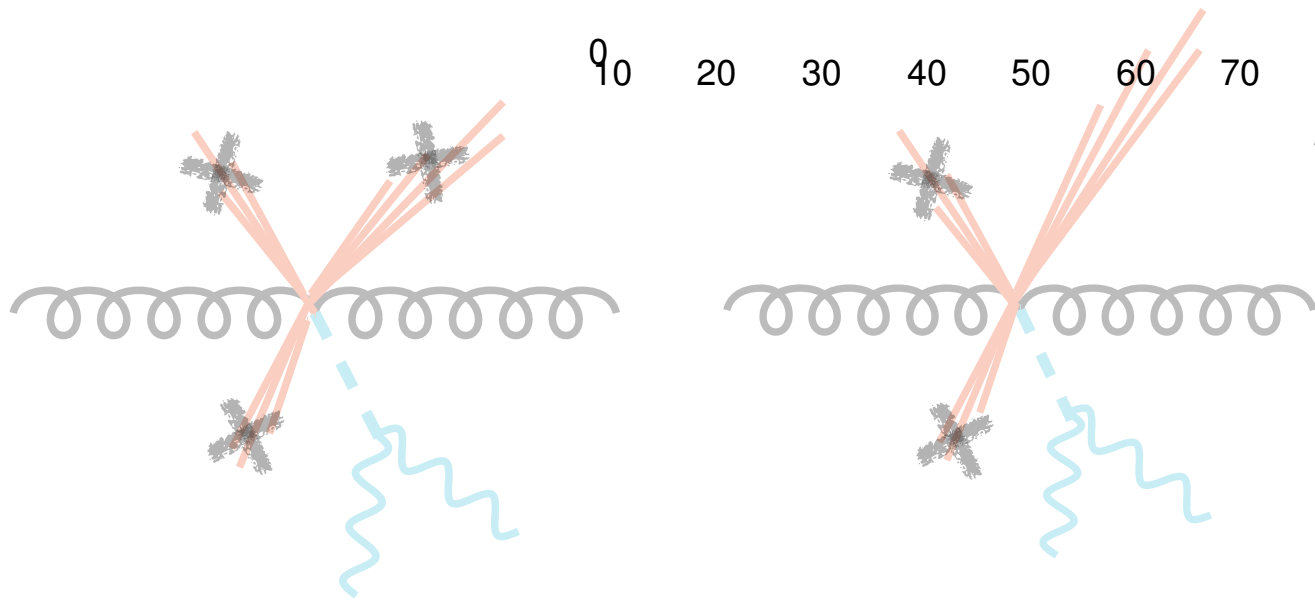
Exclusive jet cross sections

Stewart, Tackmann, JW, Zuberi, 1307.1808
 Boughezal, Liu, Petriello, Tackmann, JW, 1312.4535

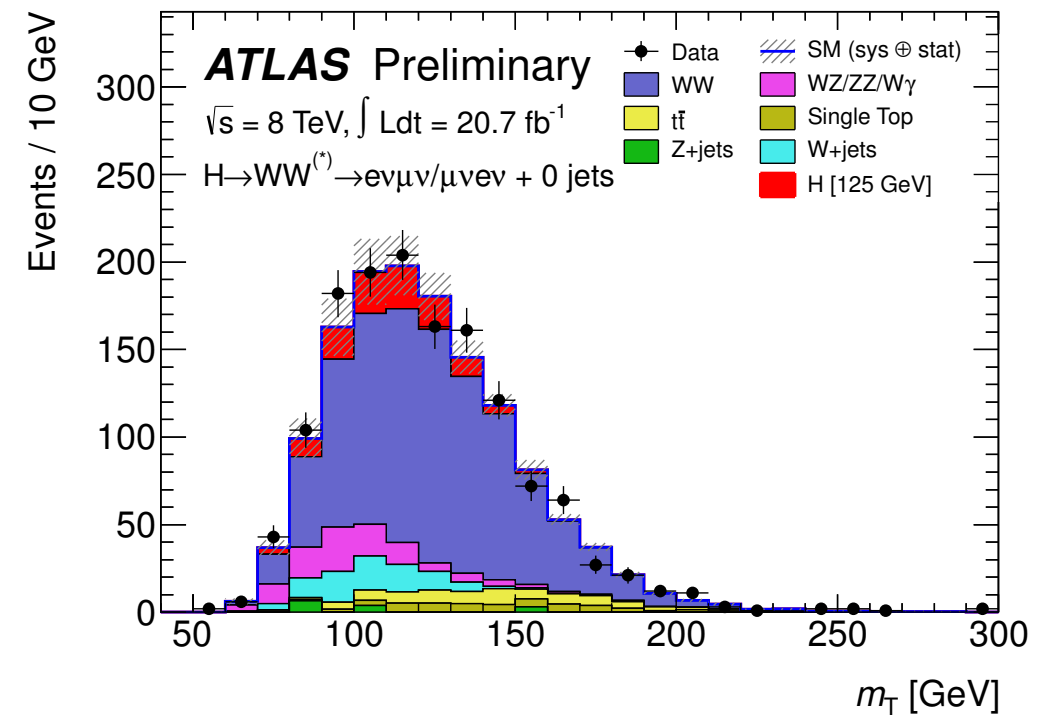
cross section in jet bins



The precision frontier and the Higgs



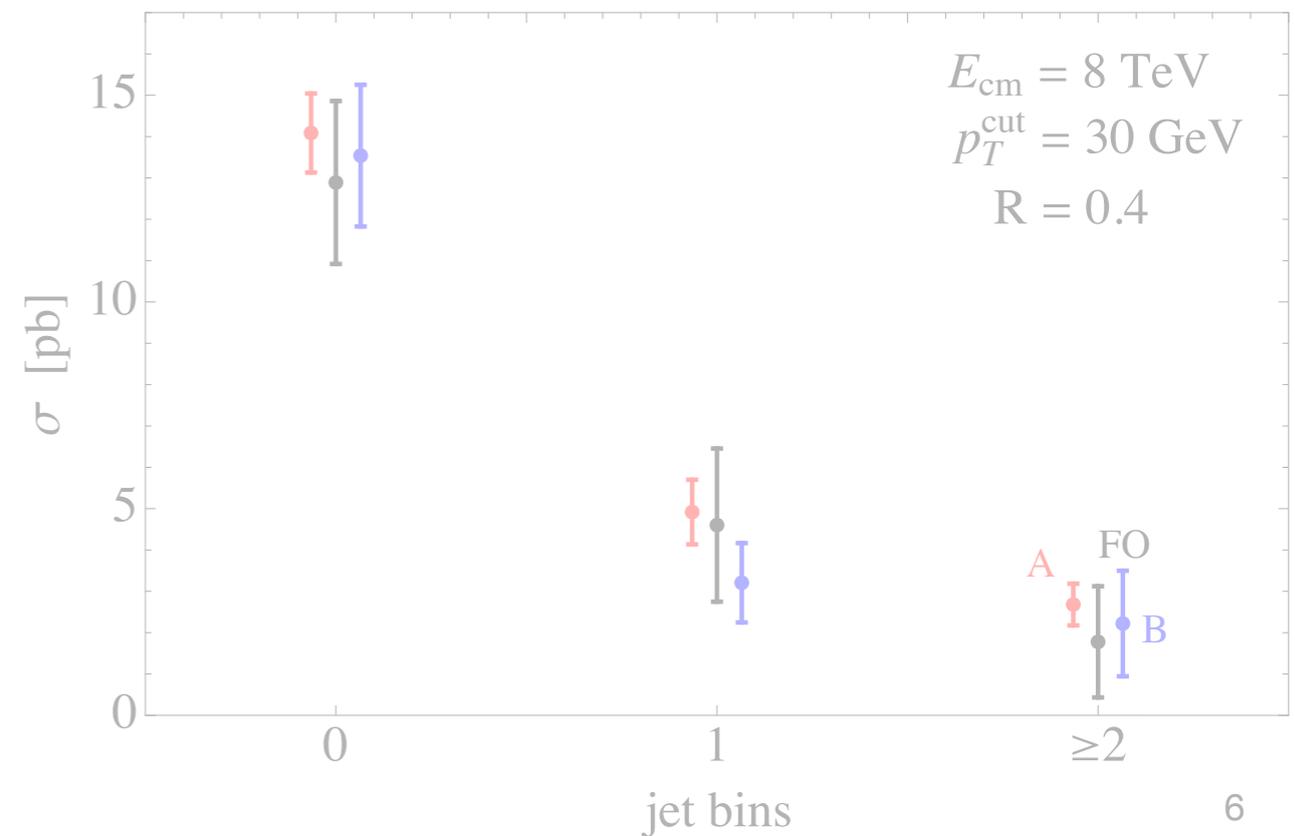
Implementation and future work



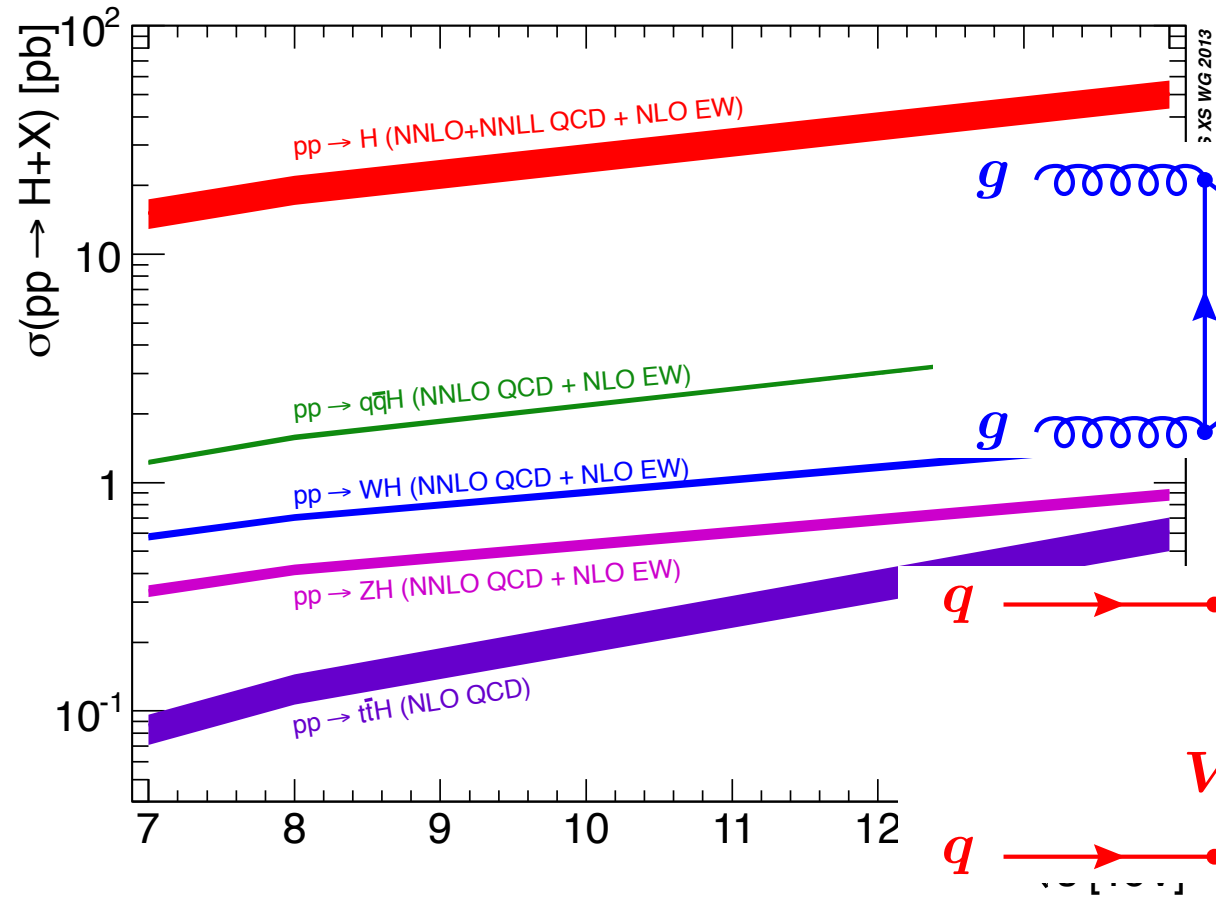
Exclusive jet cross sections

Stewart, Tackmann, JW, Zuberi, 1307.1808
 Boughezal, Liu, Petriello, Tackmann, JW, 1312.4535

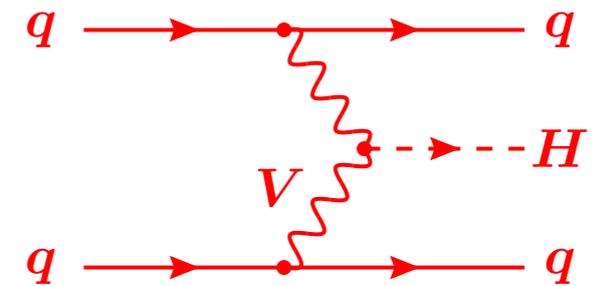
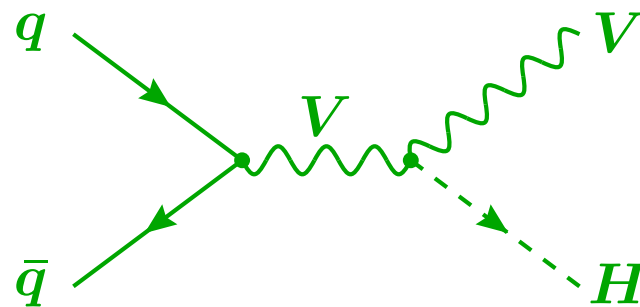
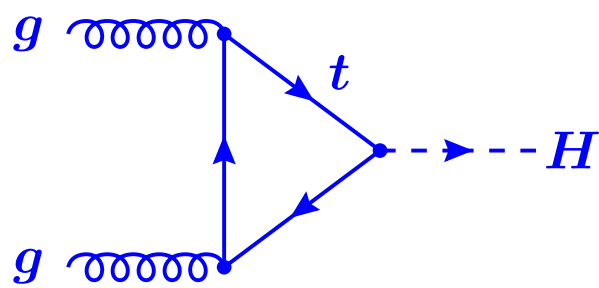
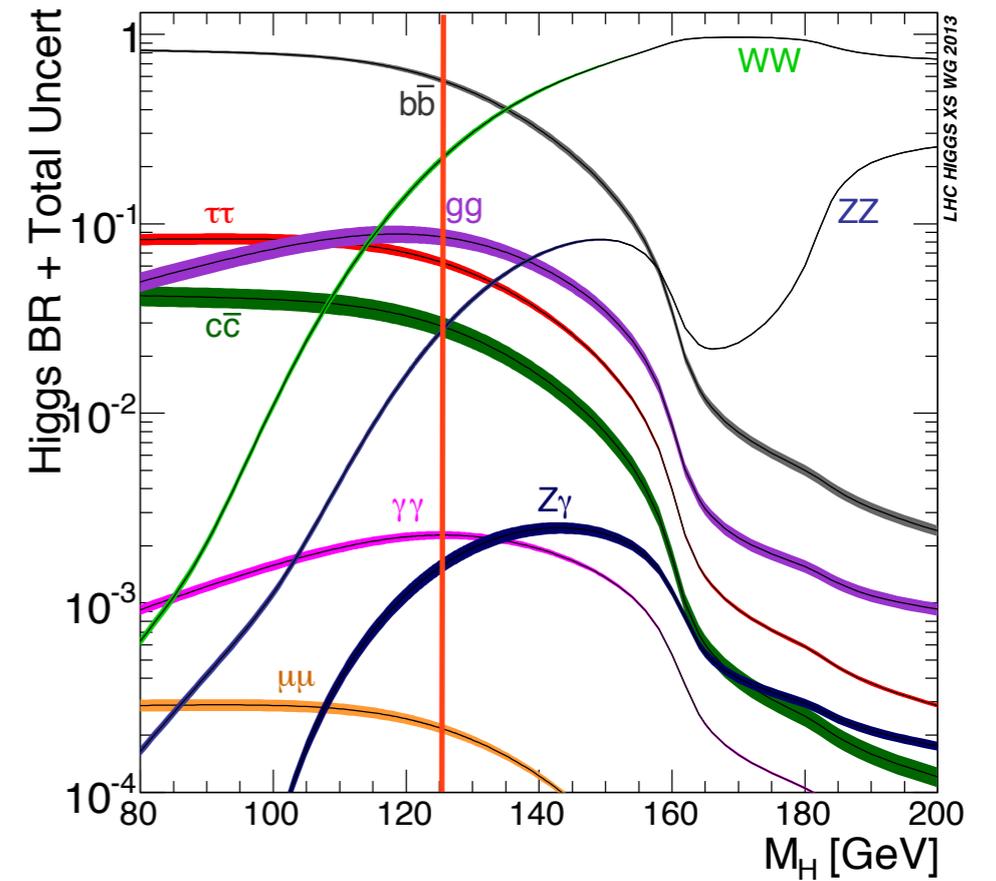
cross section in jet bins



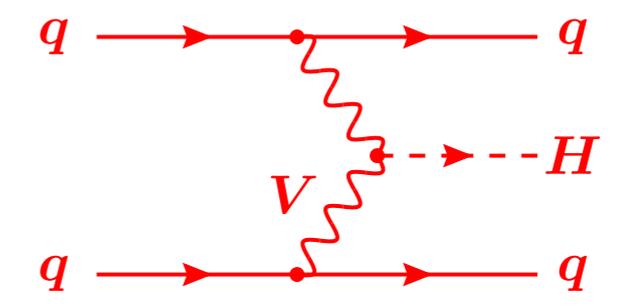
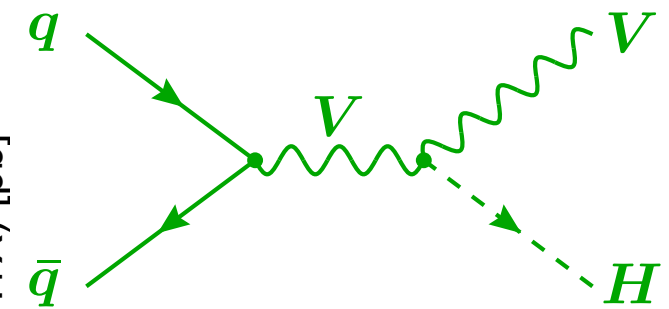
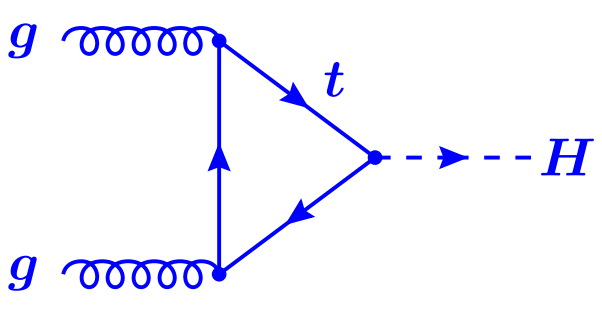
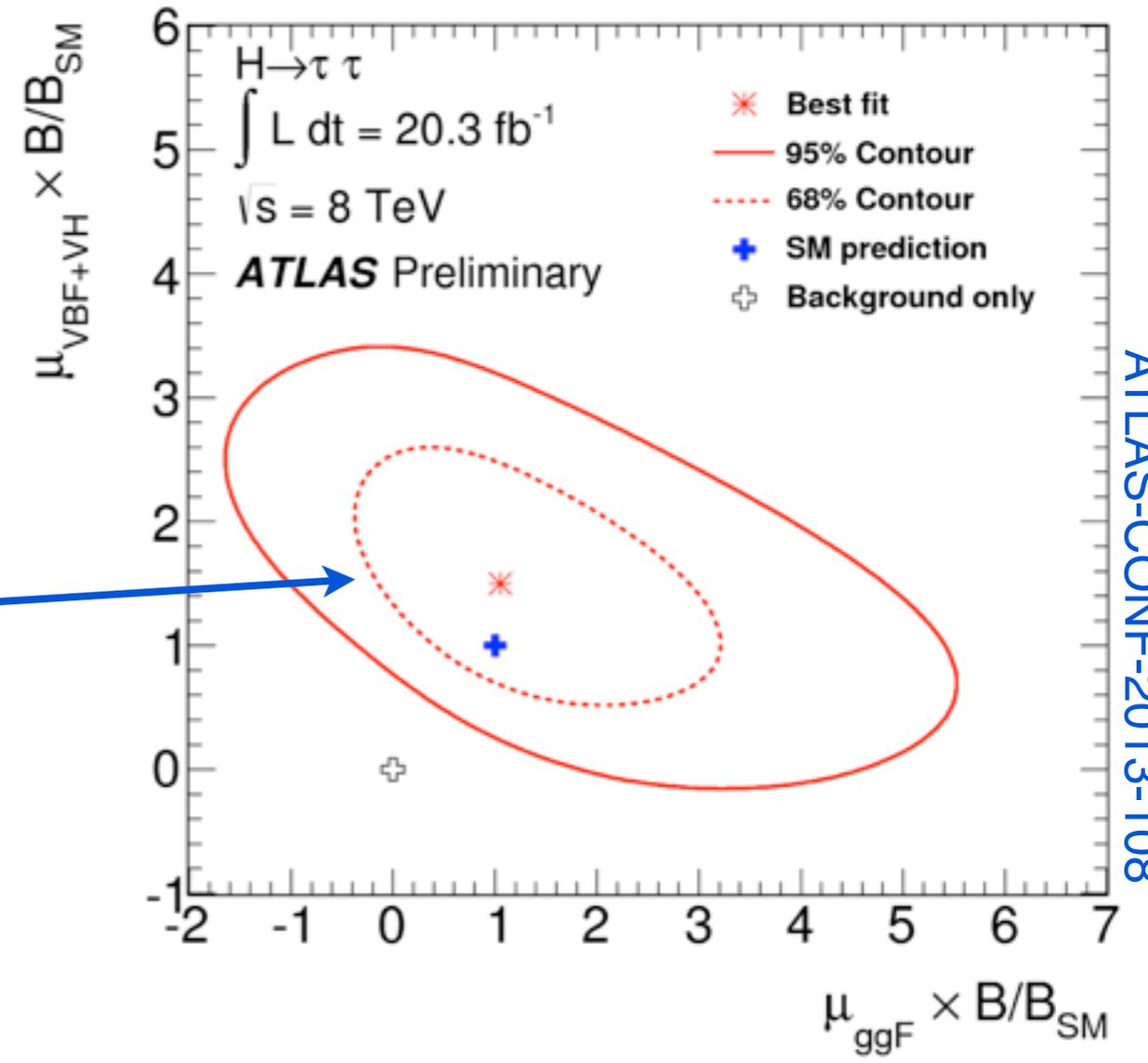
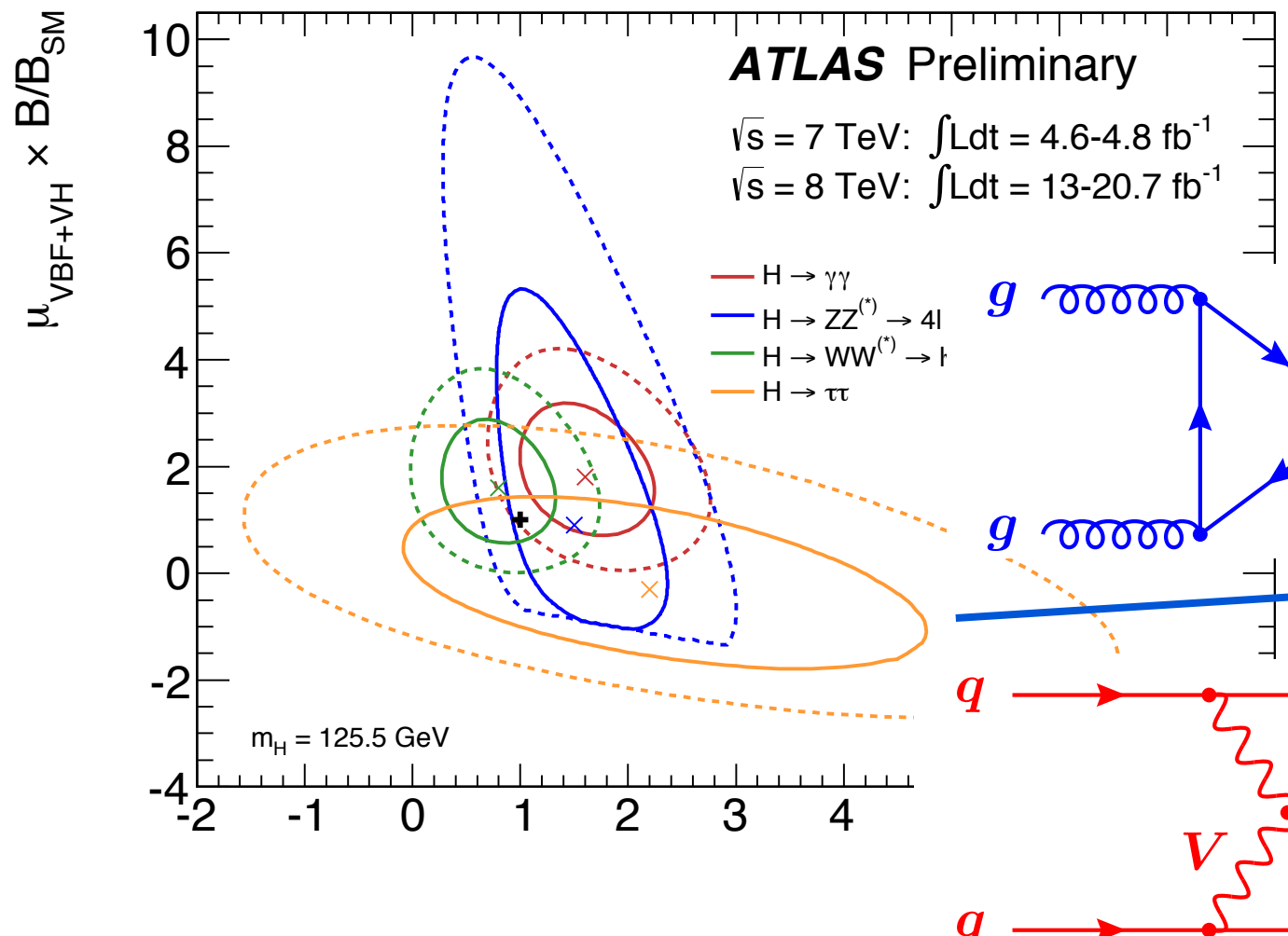
production



decay



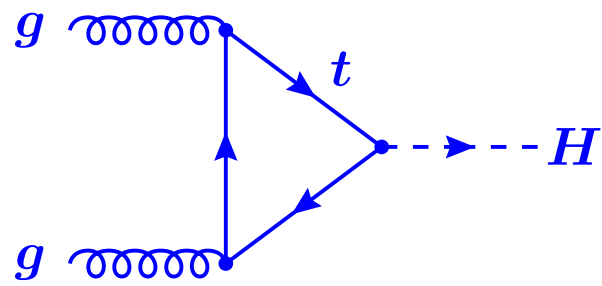
Production and decay channels sensitive to a wide variety of Higgs couplings



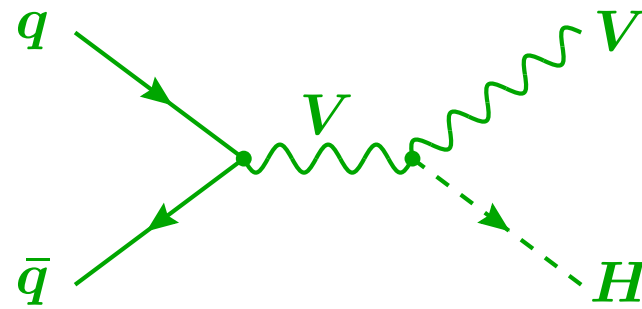
Precision Higgs measurements are a sensitive probe of these couplings, and we have significant opportunity for improvement

ATLAS-CONF-2013-108

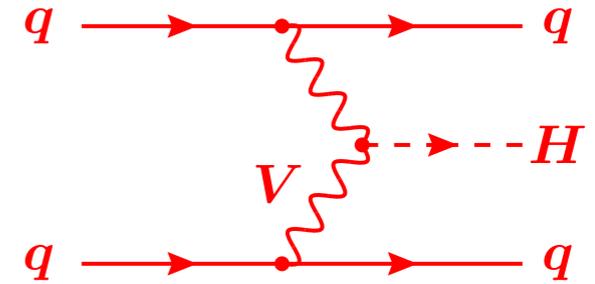
precision QCD in Higgs physics...



H @ NNLO (+NLO EW)
(Hj @ NLO, Hj \bar{j} @ NLO)

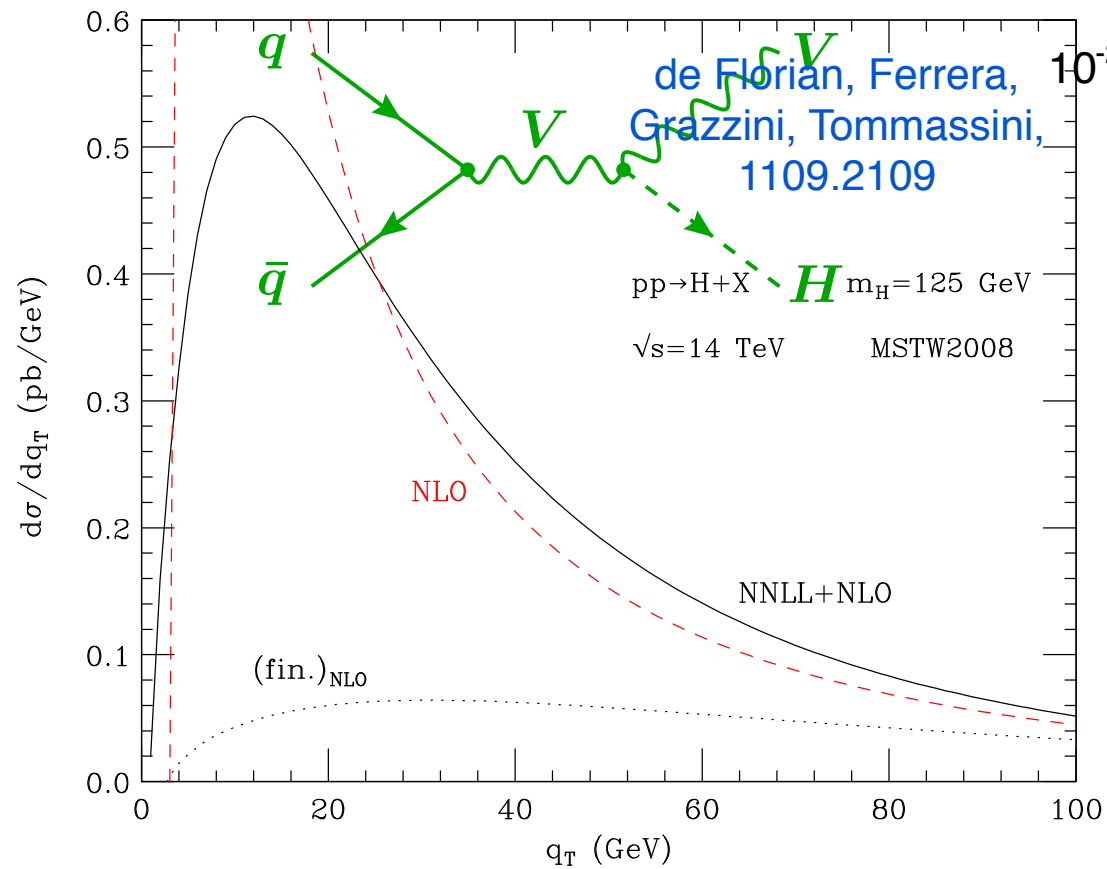


VH @ NNLO
(+NLO EW)

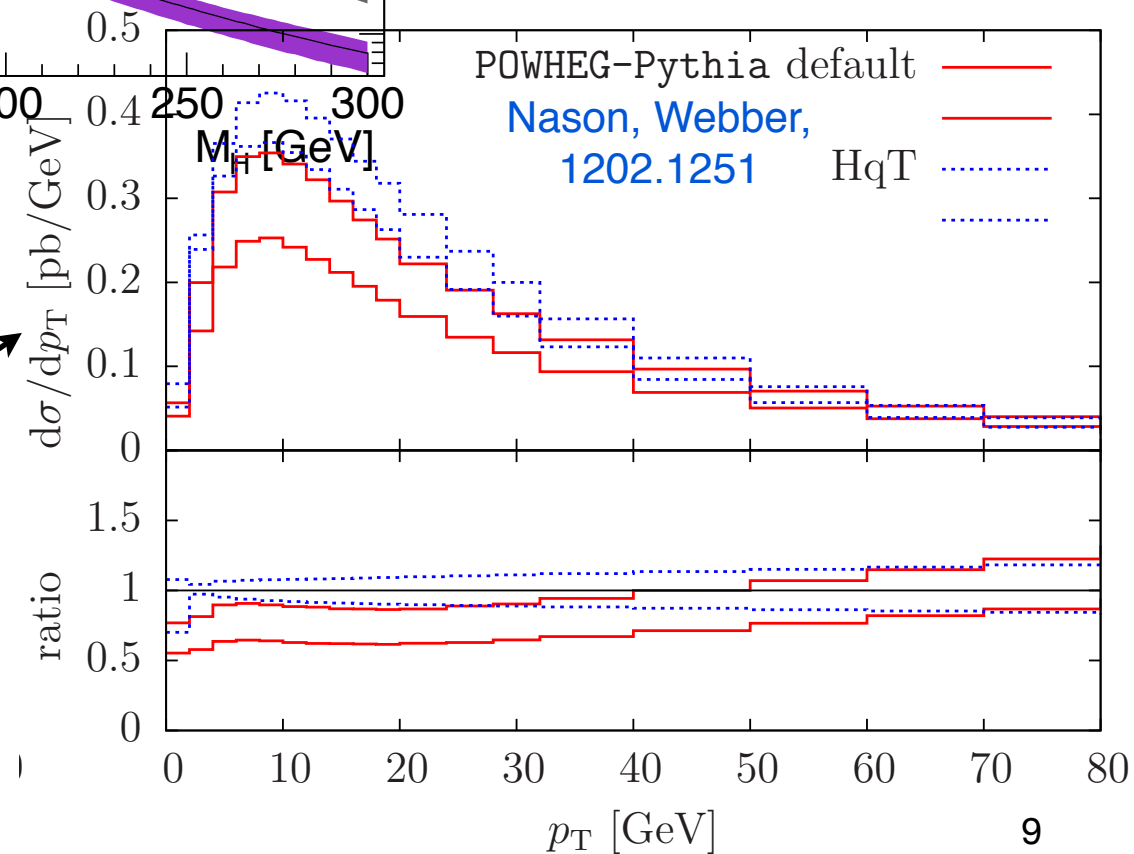


VBF @ NNLO
(total rate)

+ NNLL threshold resummation



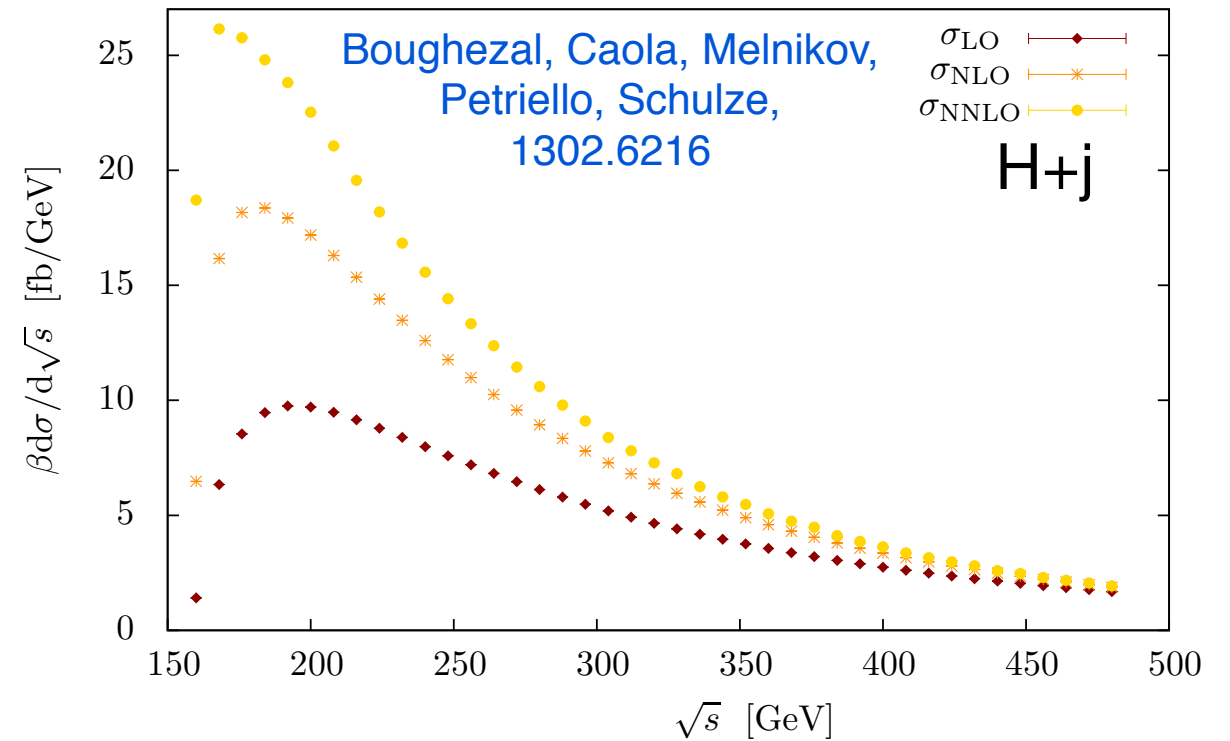
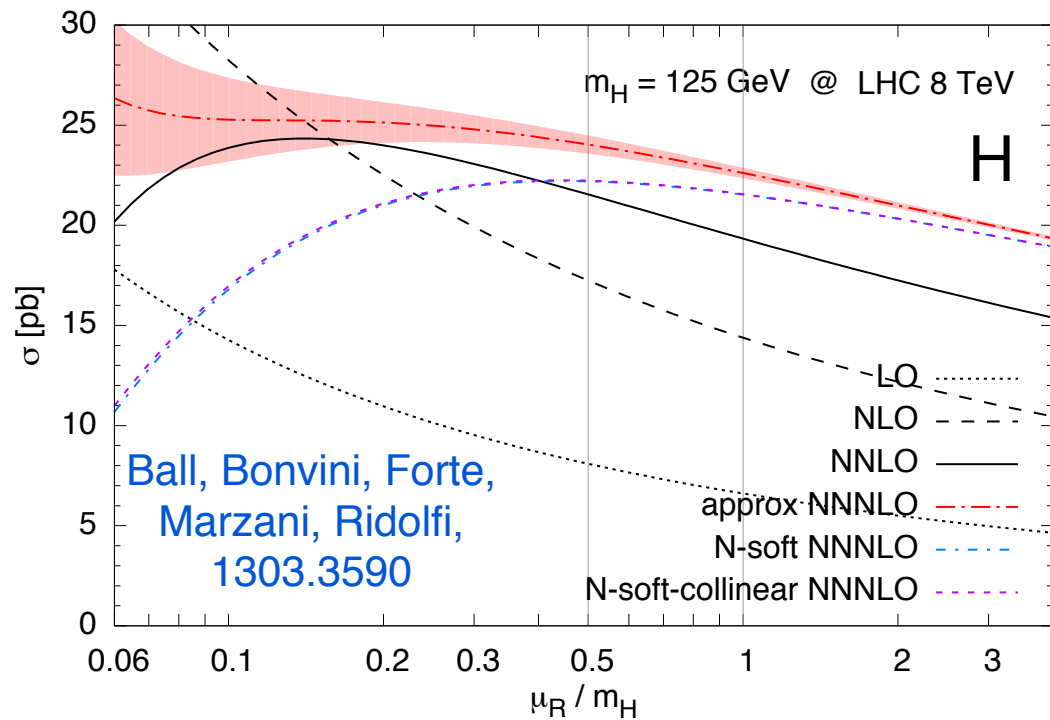
Higgs p_T
analytic
NLO MC



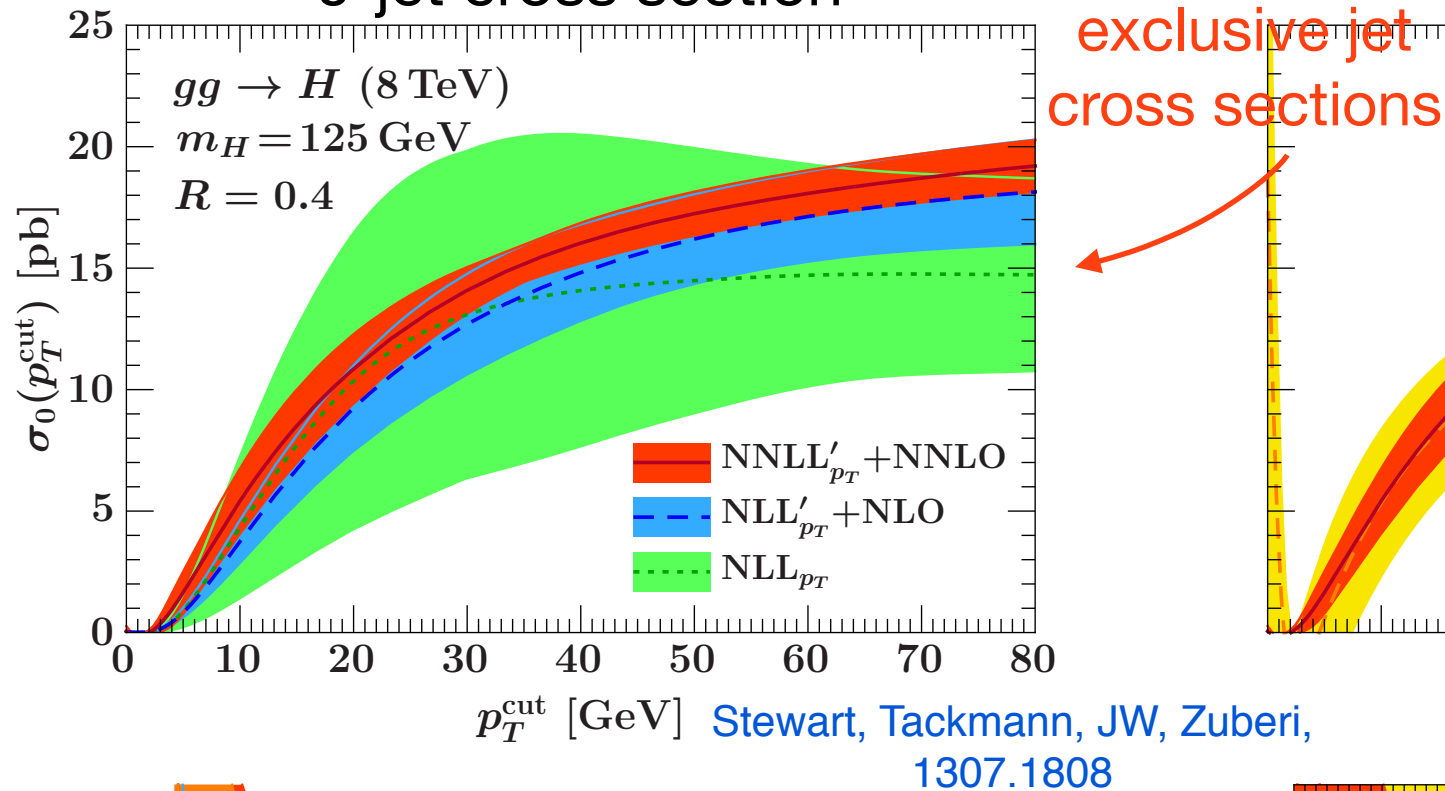
...continues to develop

upcoming/new results for gluon fusion: N³LO total rate, NNLO H+j, NLO H+3j (done)

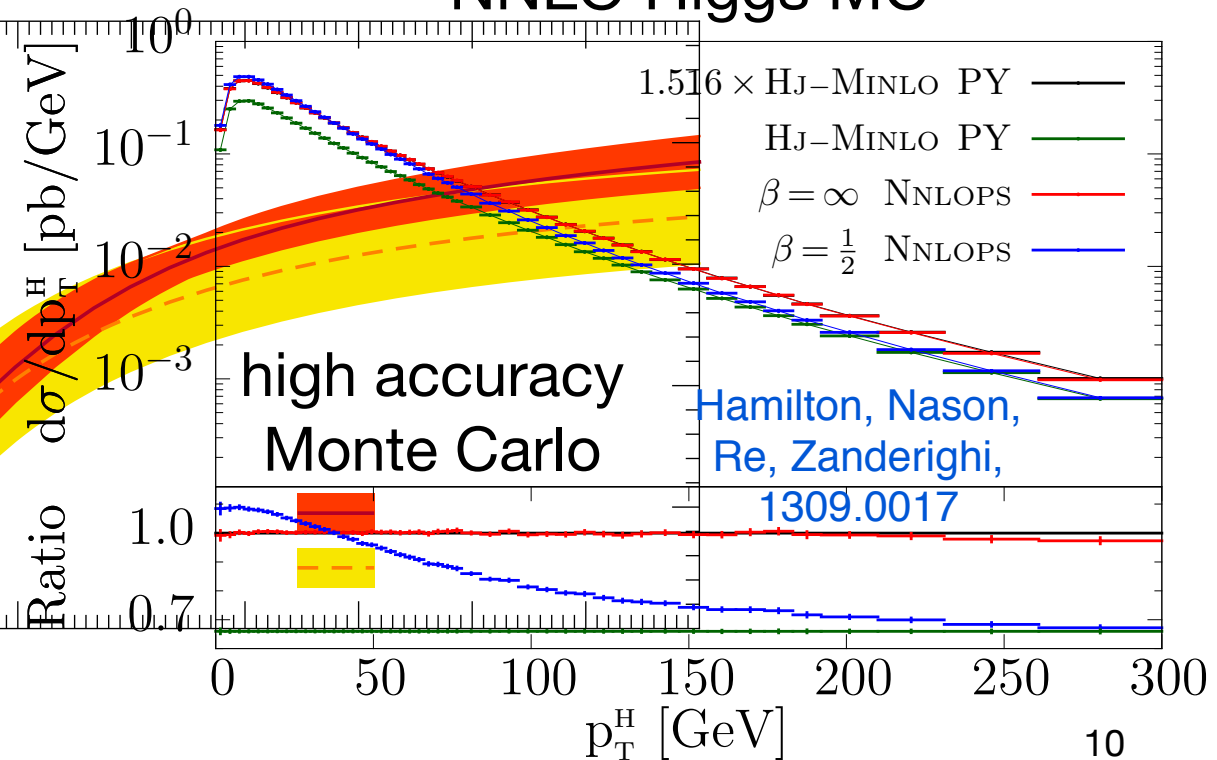
Higgs hadron-level cross section



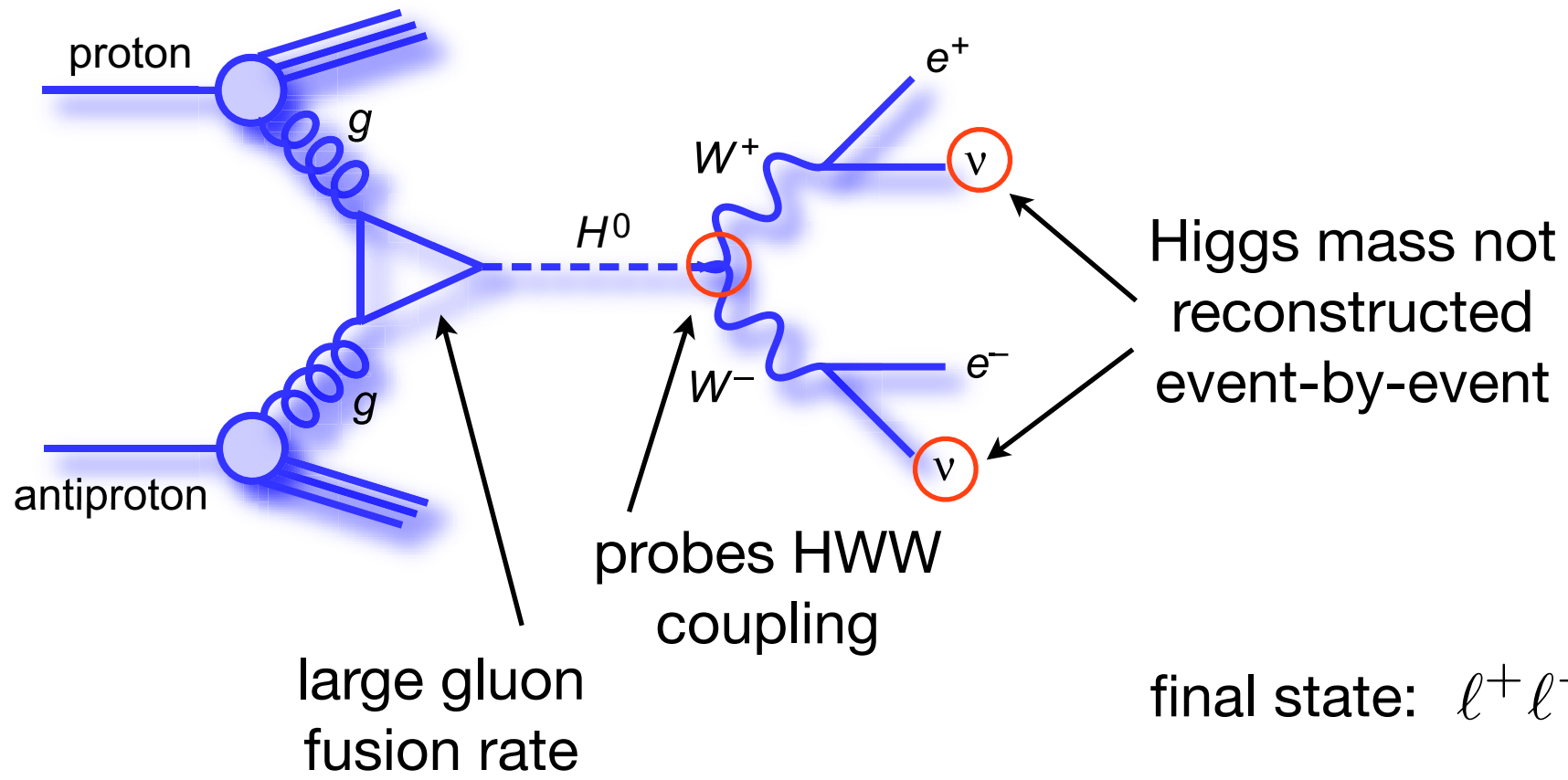
0-jet cross section



NNLO Higgs MC

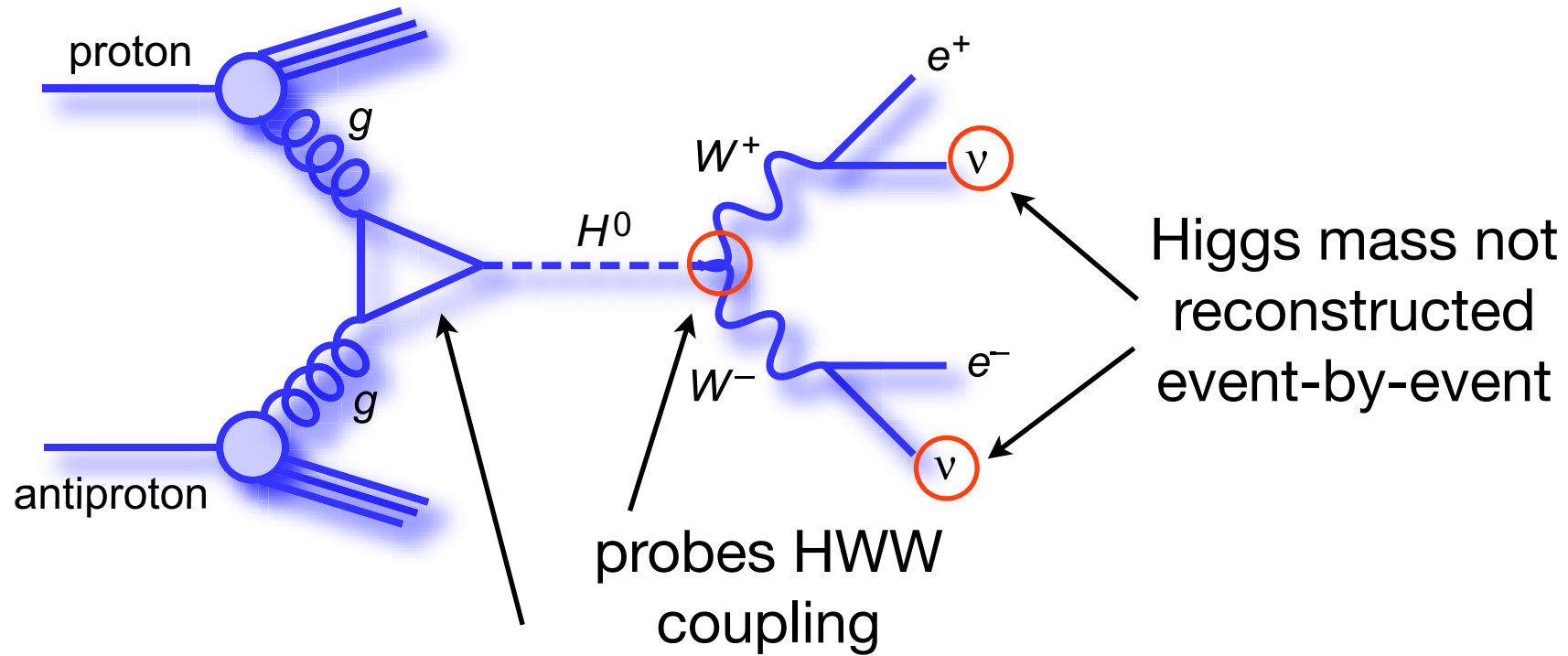


H → WW channel



final state: $l^+ l^- + \text{MET} + \text{jets}$

H → WW channel



large gluon fusion rate

probes HWW coupling

Higgs mass not reconstructed event-by-event

final state: $\ell^+ \ell^- + \text{MET} + \text{jets}$

several backgrounds:

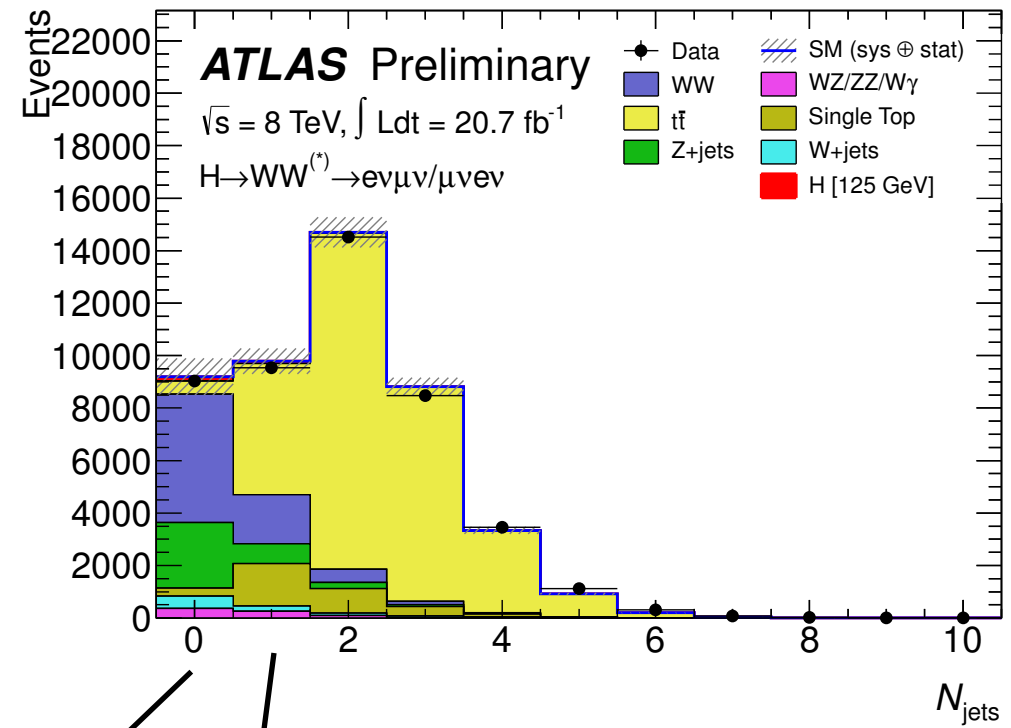
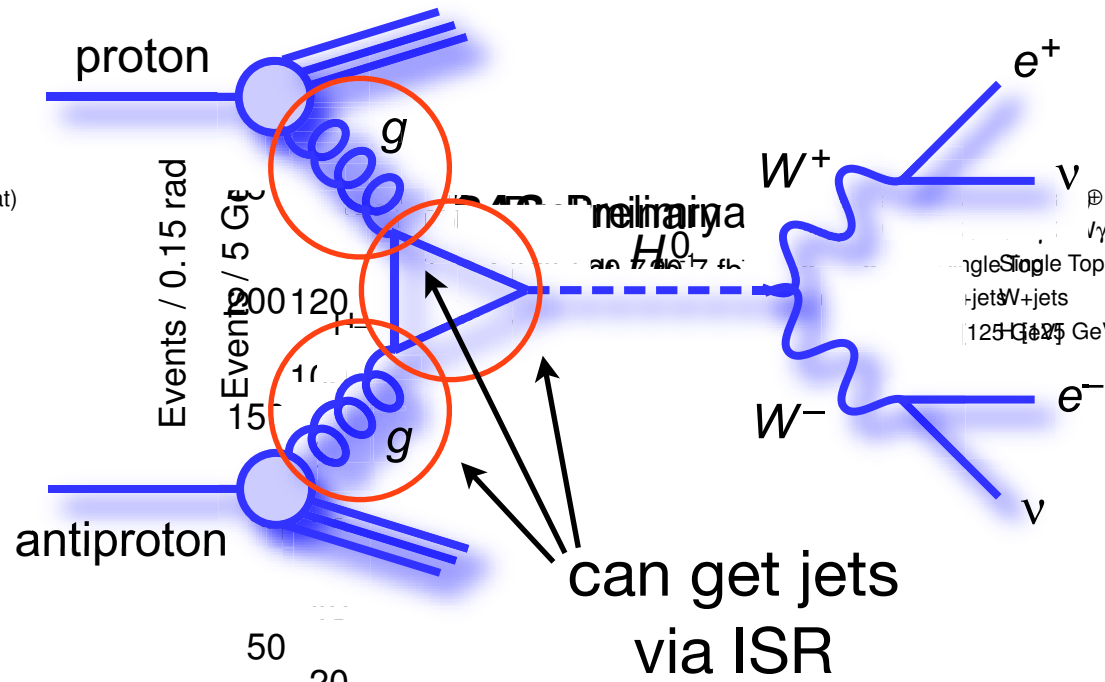
WW , $Z + \text{jets}$, $t\bar{t}$
diboson, single top

reduced with cuts on leptonic final state:

$p_T^{\ell\ell}$, $m_{\ell\ell}$, $\Delta\phi_{\ell\ell}$, $\Delta\phi_{\ell\ell, \text{MET}}$

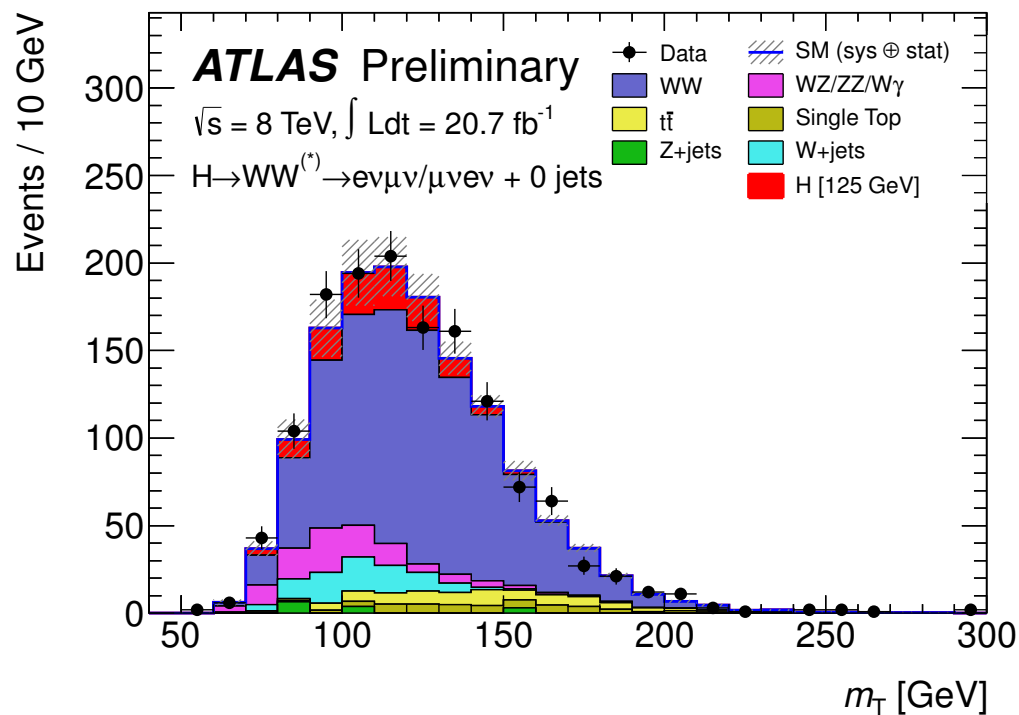
cuts specific to each jet bin

H → WW channel

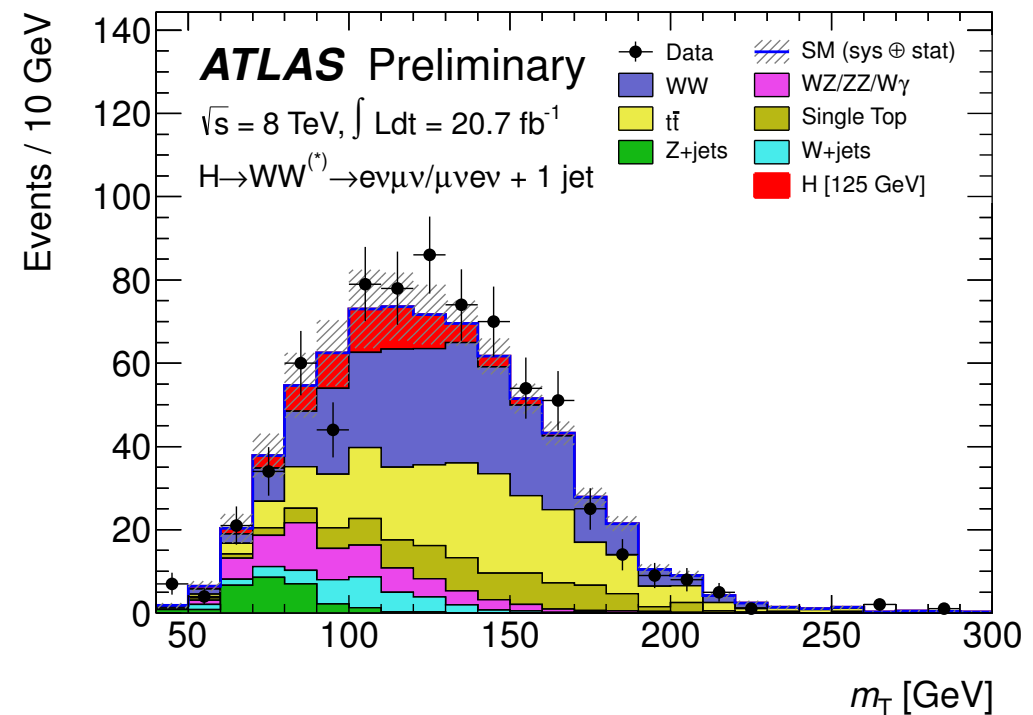


full selection cuts

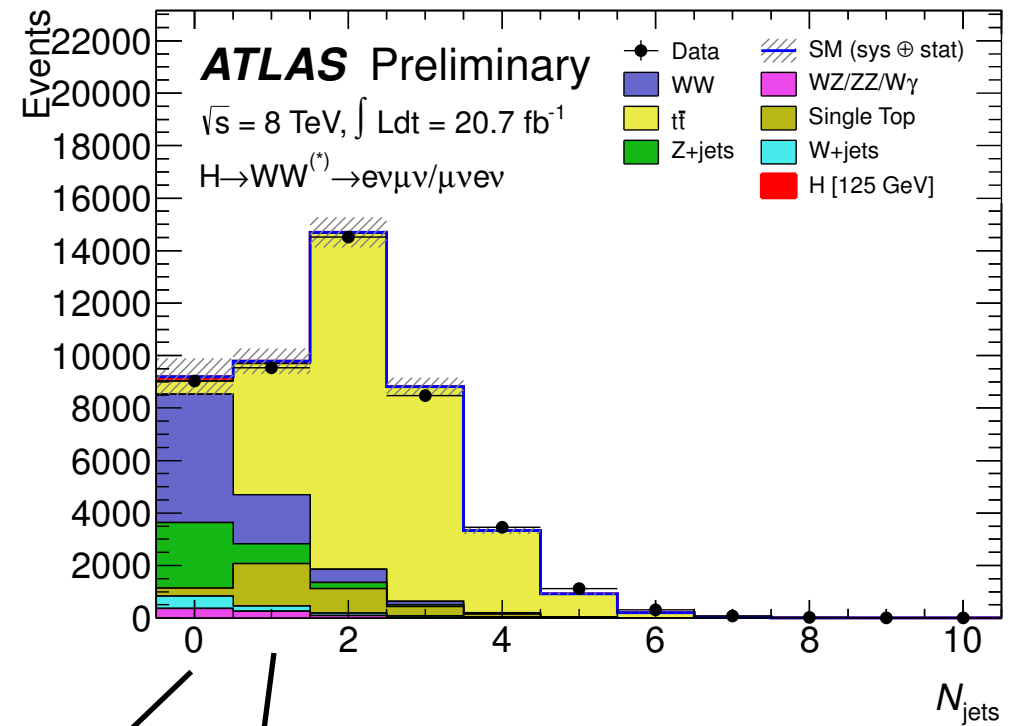
0-jet $e\mu/\mu e$ channel



1-jet $e\mu/\mu e$ channel



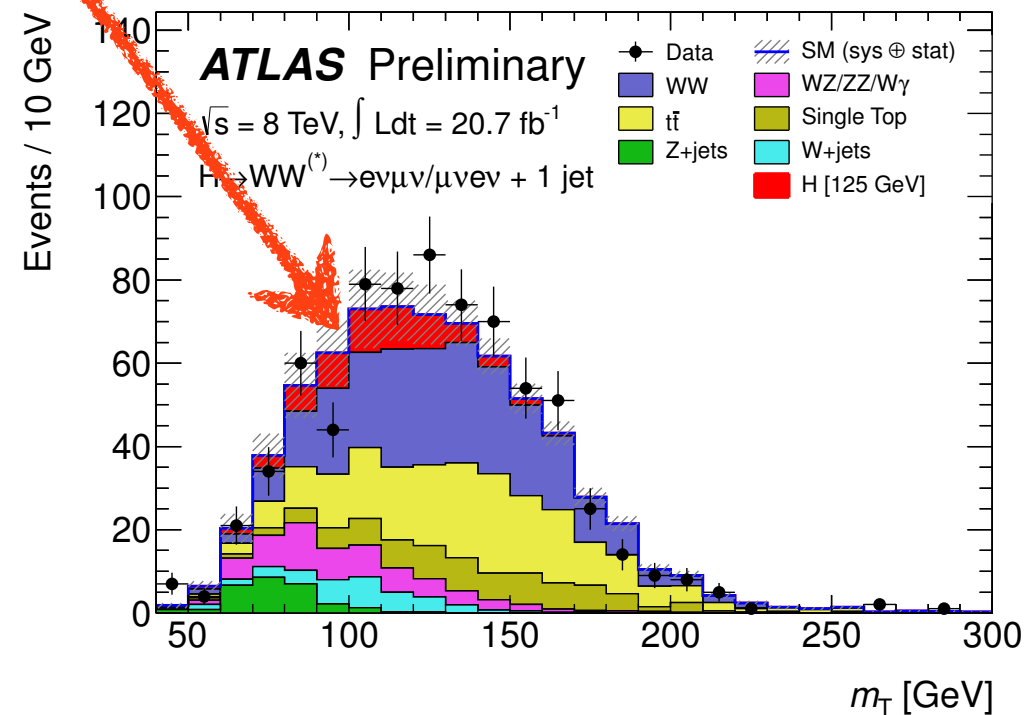
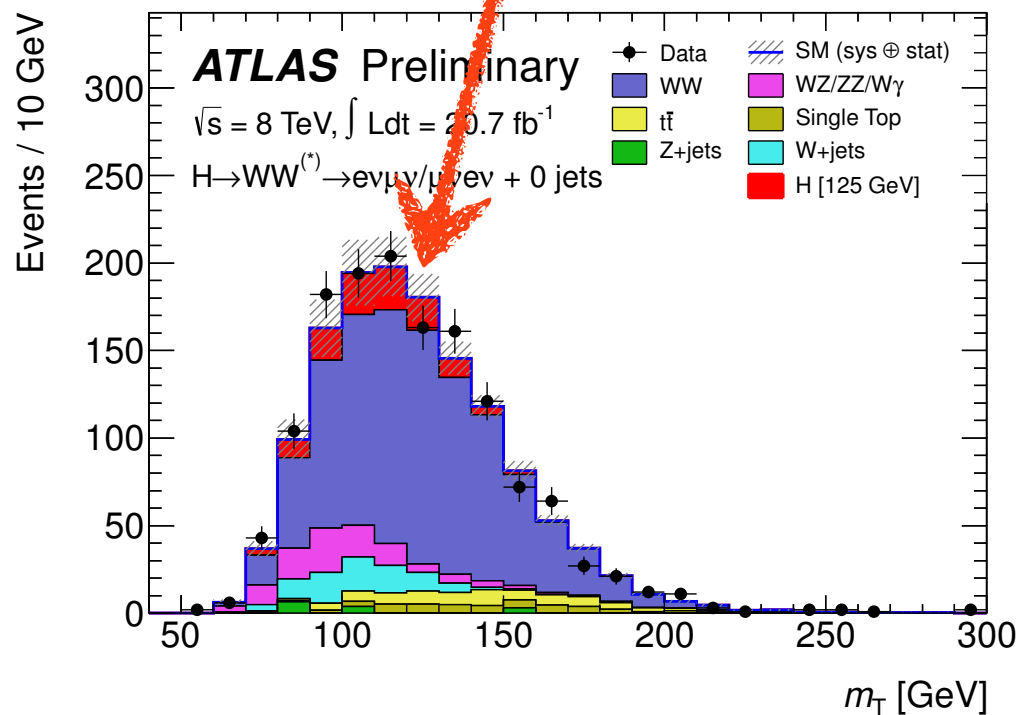
no Higgs mass peak:
the signal strength must be
extracted by comparing to
theory predictions



full selection cuts

0-jet $e\mu/\mu e$ channel

1-jet $e\mu/\mu e$ channel



systematic uncertainties for jet bins

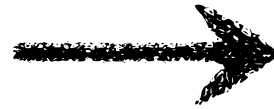
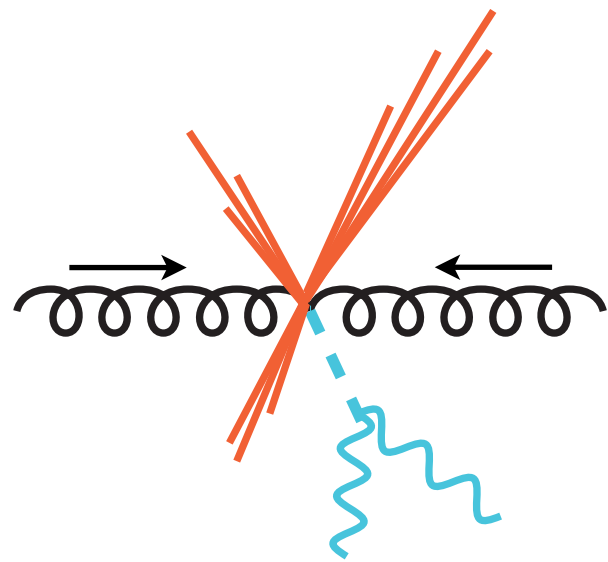
Source	Signal processes (%)			Background processes (%)		
	$N_{\text{jet}} = 0$	$N_{\text{jet}} = 1$	$N_{\text{jet}} \geq 2$	$N_{\text{jet}} = 0$	$N_{\text{jet}} = 1$	$N_{\text{jet}} \geq 2$
Theoretical uncertainties						
NNLO → QCD scale for ggF signal for $N_{\text{jet}} \geq 0$	13	-	-	-	-	-
NLO → QCD scale for ggF signal for $N_{\text{jet}} \geq 1$	10	27	-	-	-	-
LO → QCD scale for ggF signal for $N_{\text{jet}} \geq 2$	-	15	4	-	-	-
LO → QCD scale for ggF signal for $N_{\text{jet}} \geq 3$	-	-	4	-	-	-
Parton shower and UE model (signal only)	3	10	5	-	-	-
PDF model	8	7	3	1	1	1
$H \rightarrow WW$ branching ratio	4	4	4	-	-	-
QCD scale (acceptance)	4	4	3	-	-	-
WW normalisation	-	-	-	1	2	4
Experimental uncertainties						
Jet energy scale and resolution	5	2	6	2	3	7
b -tagging efficiency	-	-	-	-	7	2
f_{recoil} efficiency	1	1	-	4	2	-

ATLAS-CONF-2013-030

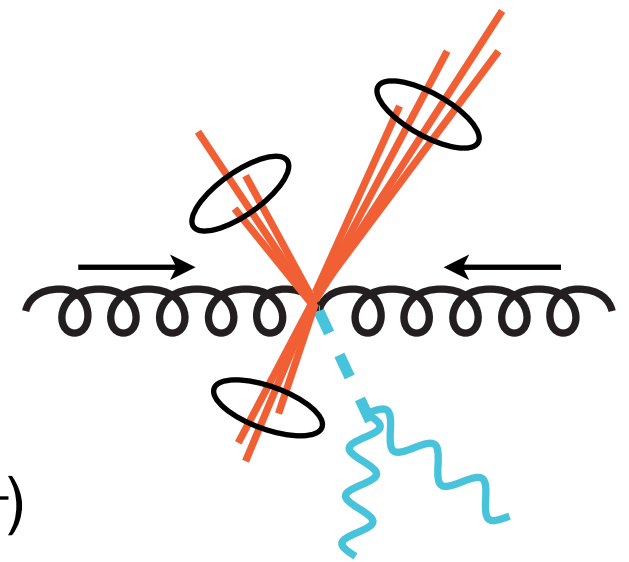
17% 30%

resummation will help control these uncertainties

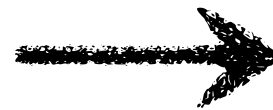
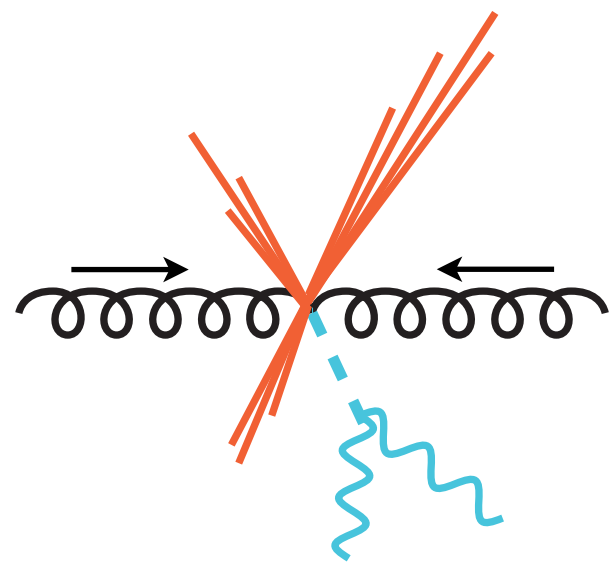
jet clustering and jet vetoes



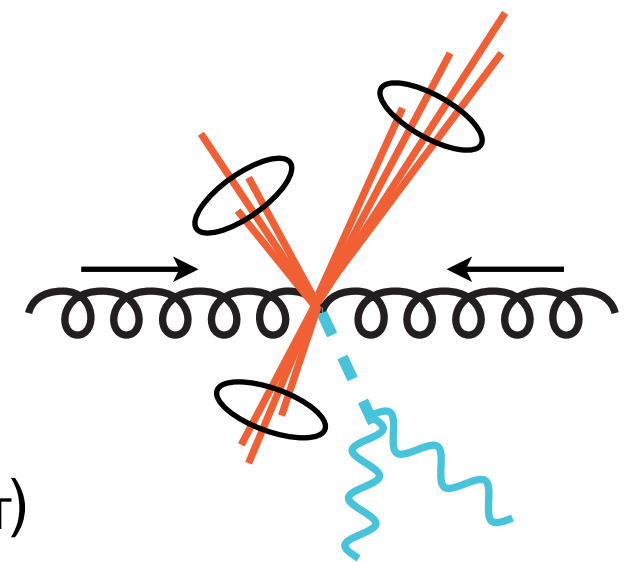
cluster final state into jets
uses an algorithm (e.g. anti- k_T)



jet clustering and jet vetoes



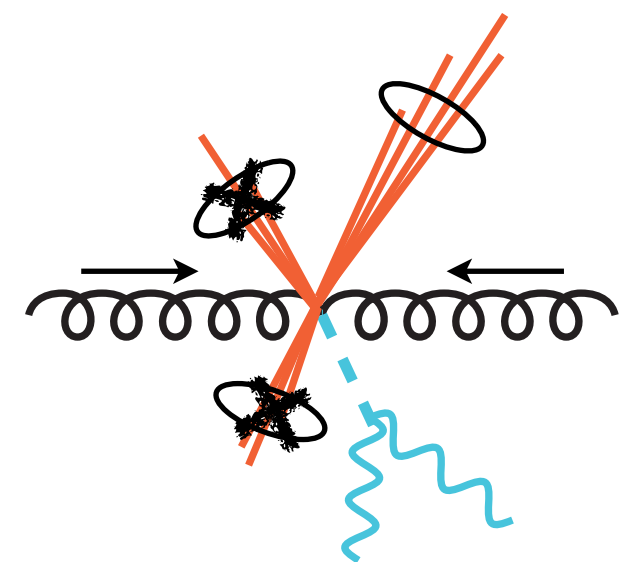
cluster final state into jets
uses an algorithm (e.g. anti- k_T)



veto on soft jets
(usually by p_T)

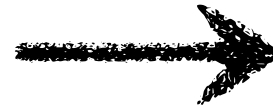
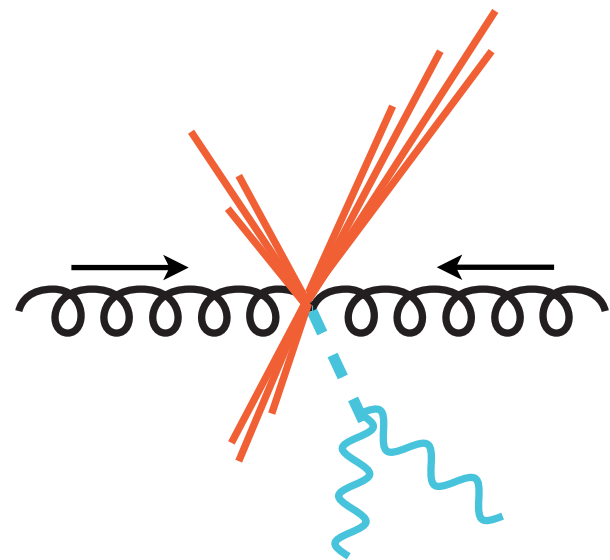


only jets with
 $p_T > p_T^{\text{cut}}$
are counted

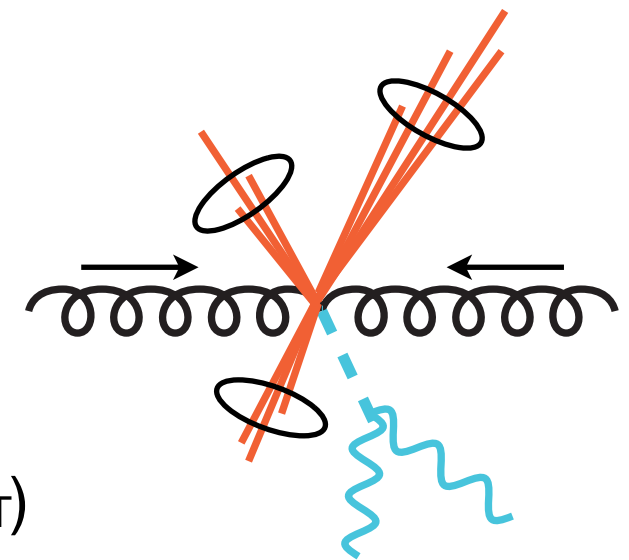


1-jet event

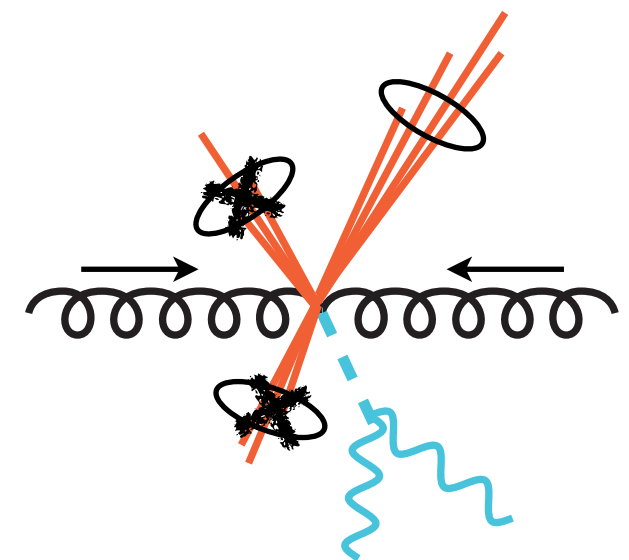
jet clustering and jet vetoes



cluster final state into jets
uses an algorithm (e.g. anti- k_T)



veto on soft jets
(usually by p_T)



1-jet event

IR safety

- collinear safety
- soft safety

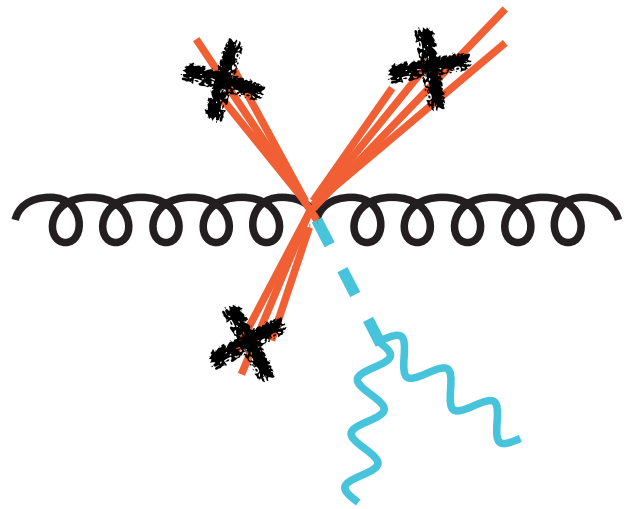
p_T veto scale set by:

1. soft jets poorly measured
 2. high p_T veto less effective
- scale usually $\sim 25-30$ GeV

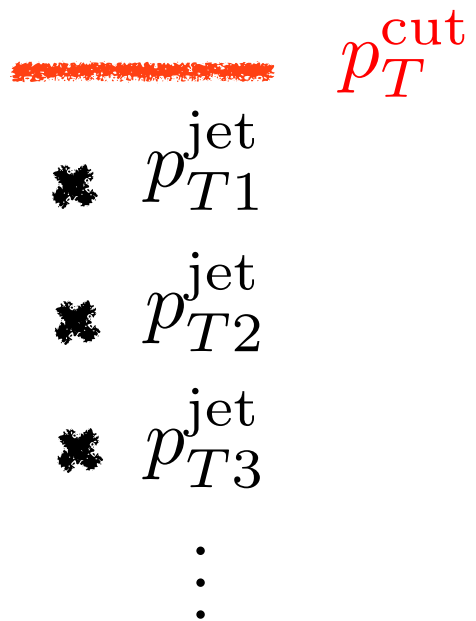
only jets with
 $p_T > p_T^{\text{cut}}$
are counted

jet binning

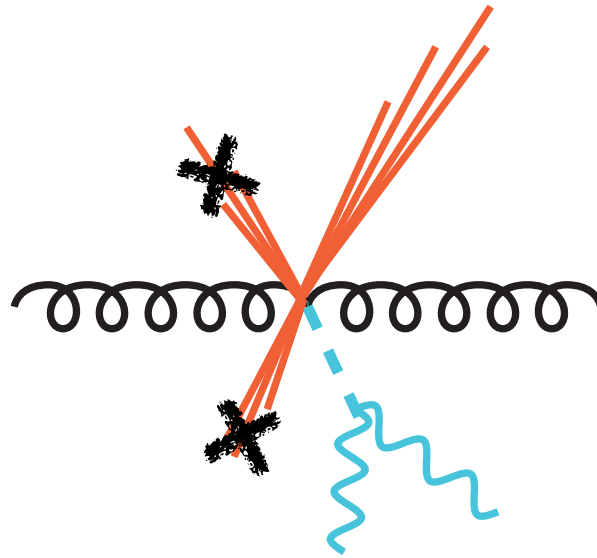
0-jet events



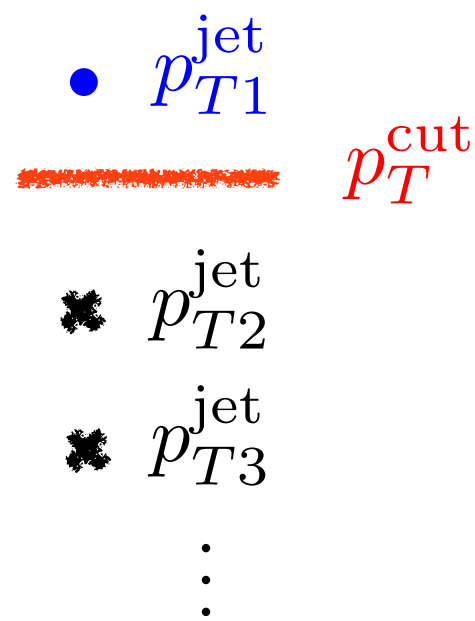
jet p_T



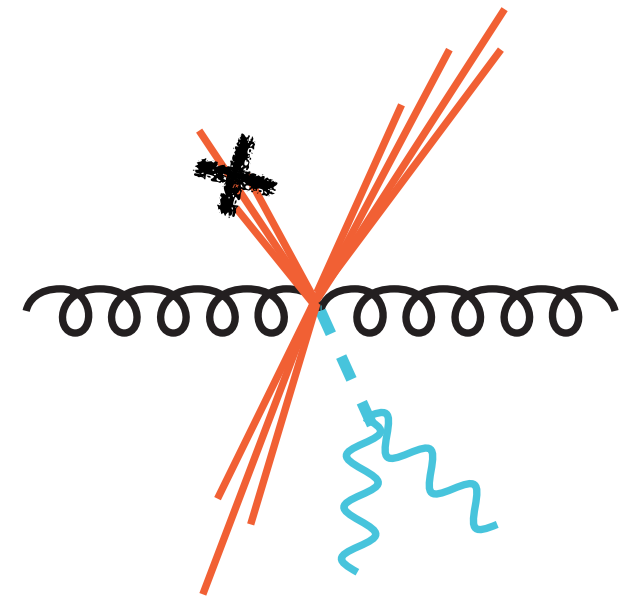
1-jet events



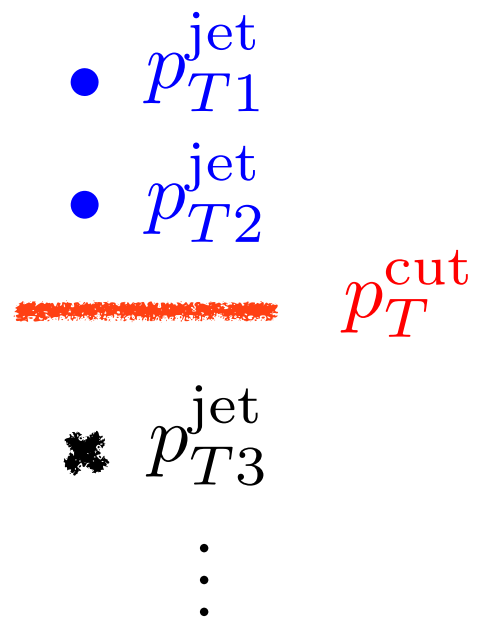
jet p_T



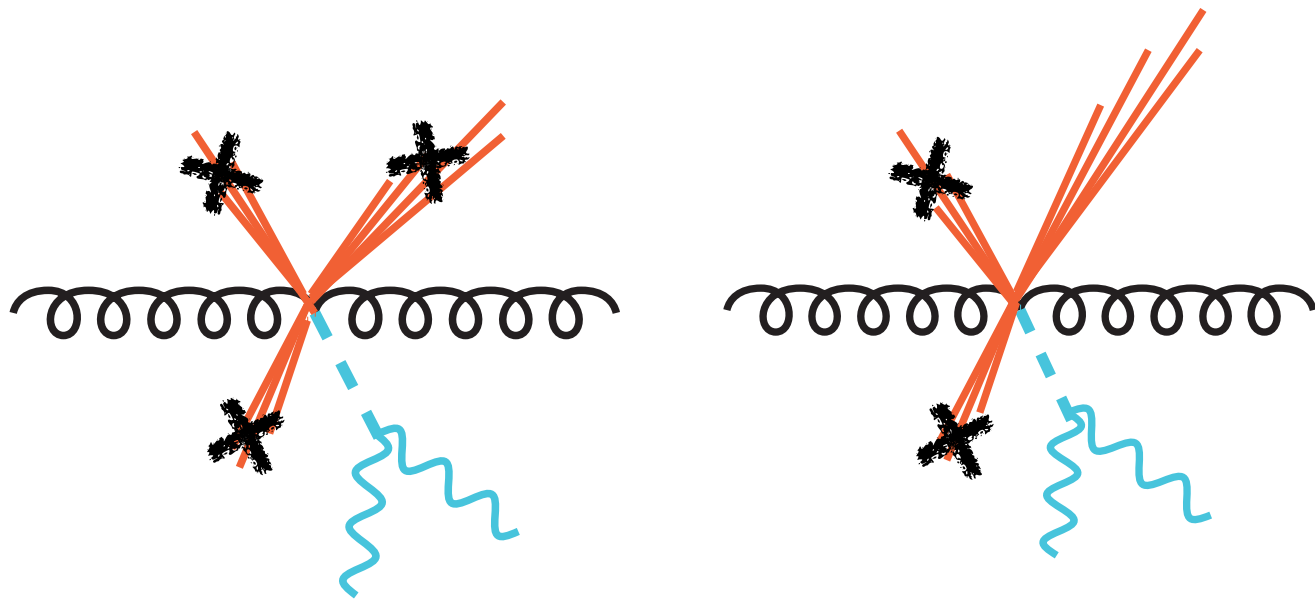
2-jet events



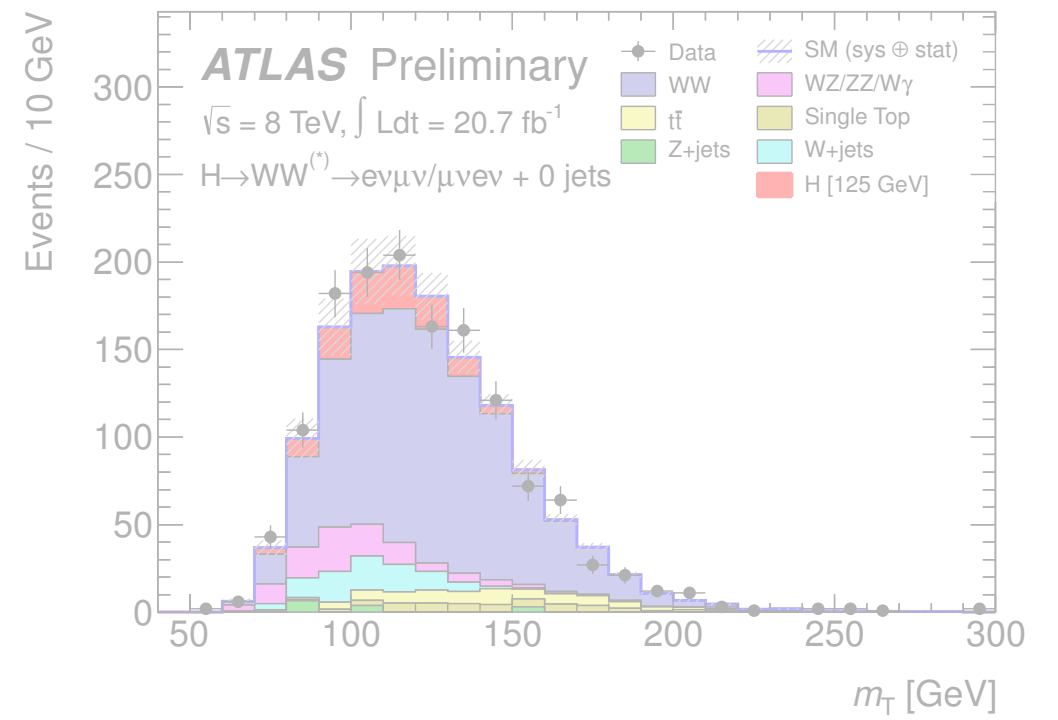
jet p_T



The precision frontier and the Higgs

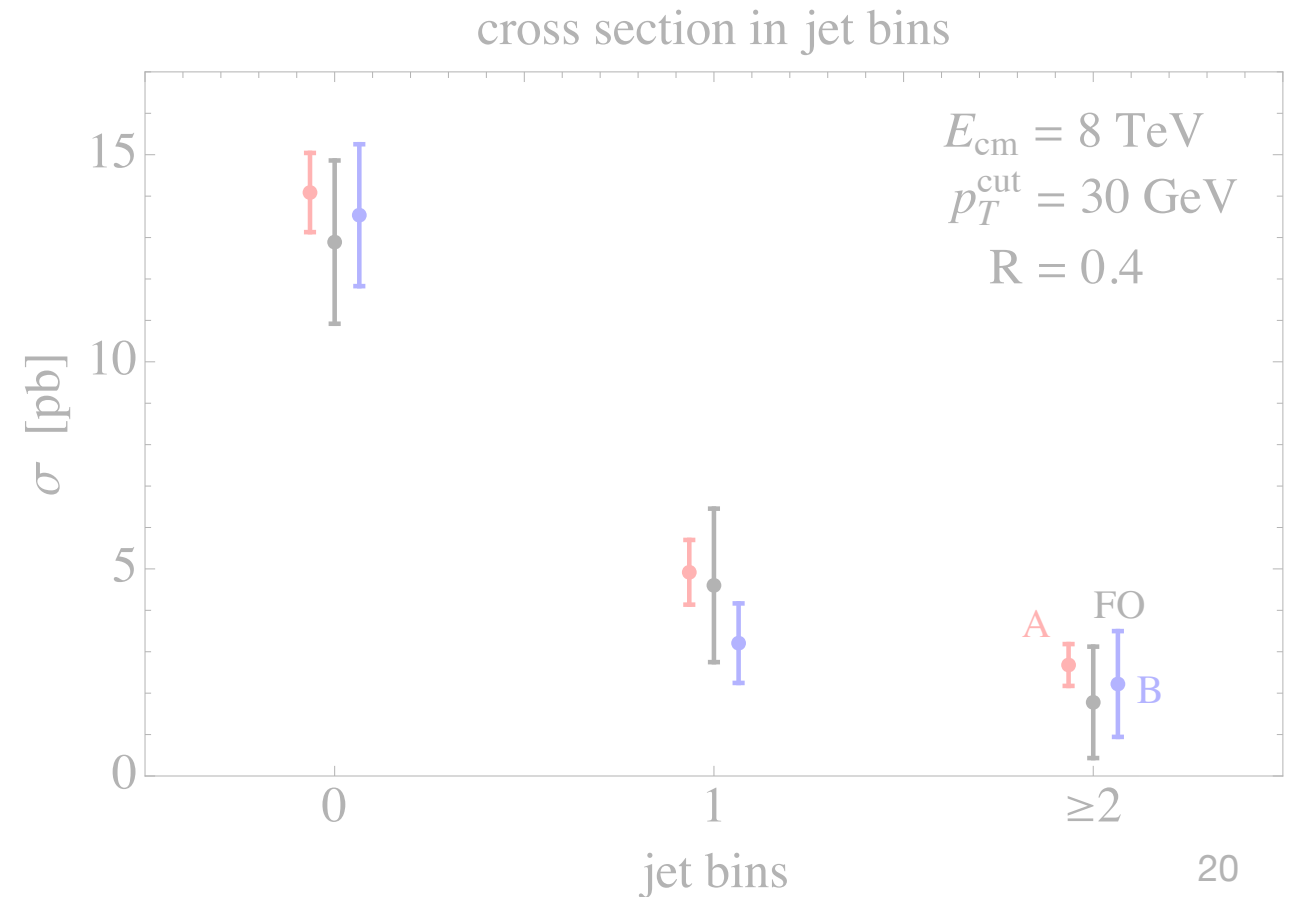


Implementation and future work



Exclusive jet cross sections

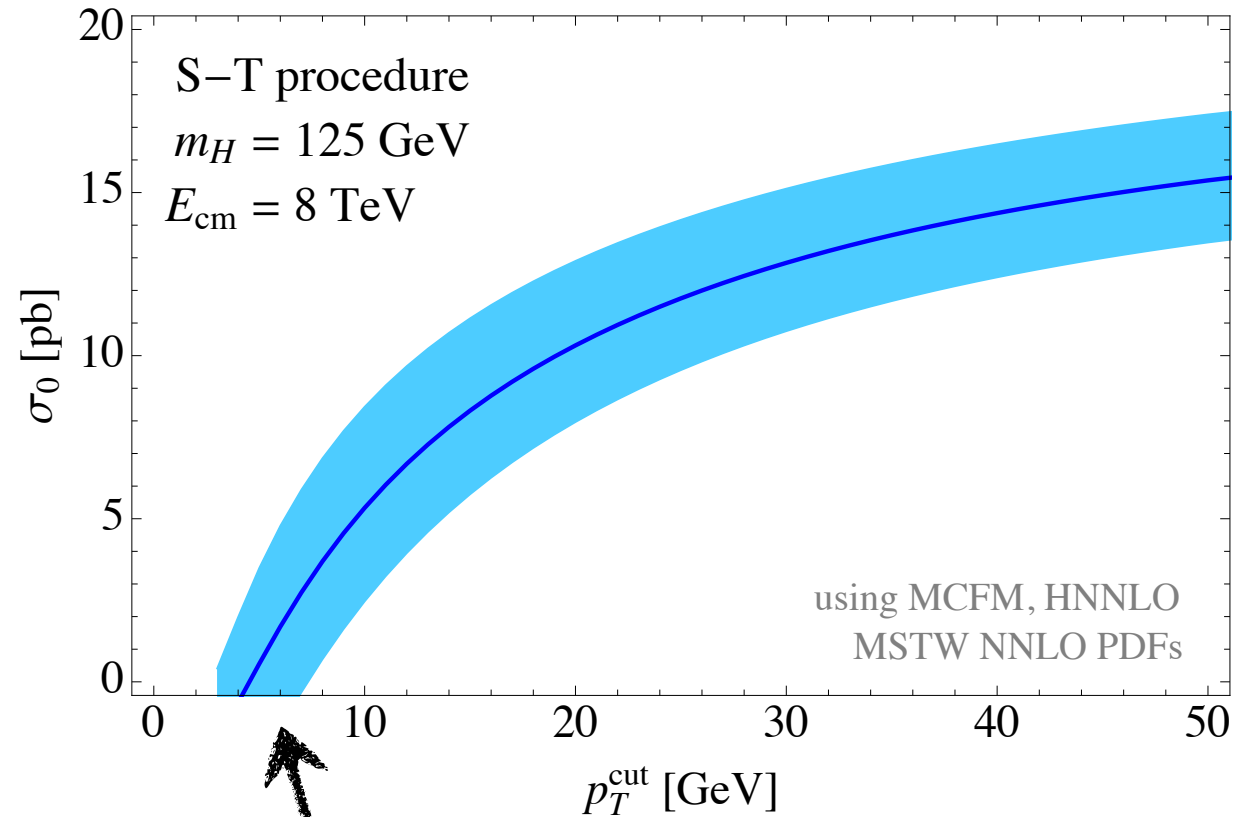
Stewart, Tackmann, JW, Zuberi, 1307.1808
 Boughezal, Liu, Petriello, Tackmann, JW, 1312.4535



0-jet cross section resummation vs. fixed order

0-jet cross section

$gg \rightarrow H$ at NNLO



fixed order dips negative:
breakdown of perturbation theory,
resummation needed

$$\sigma_0(p_T^{\text{cut}}) = \sigma_0^{\text{sing}}(p_T^{\text{cut}}) + \sigma_1^{\text{nons}}(p_T^{\text{cut}})$$

singular
(resummed)
nonsingular
(added at FO)

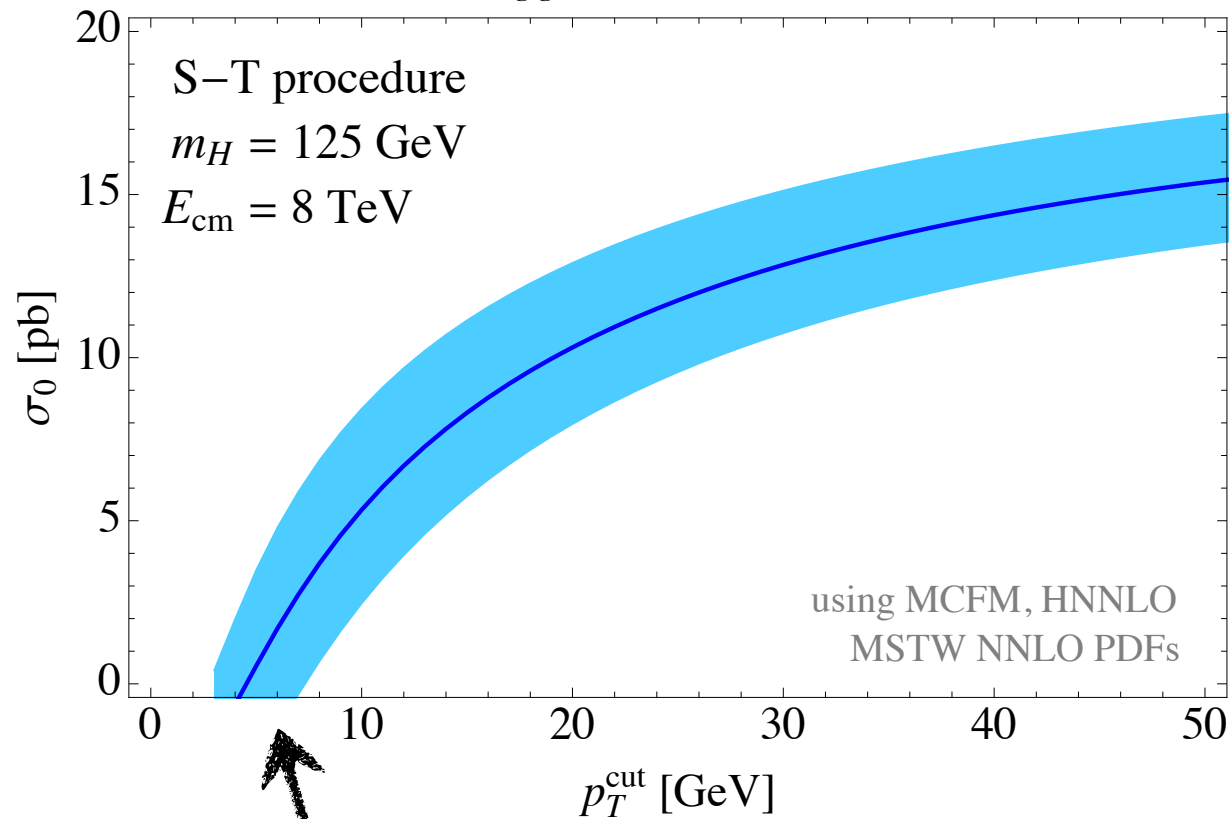
$$\alpha_s^n \ln^k \frac{m_H}{p_T^{\text{cut}}}, \quad k \leq 2n$$

finite as
 $p_T^{\text{cut}} \rightarrow 0$

0-jet cross section resummation vs. fixed order

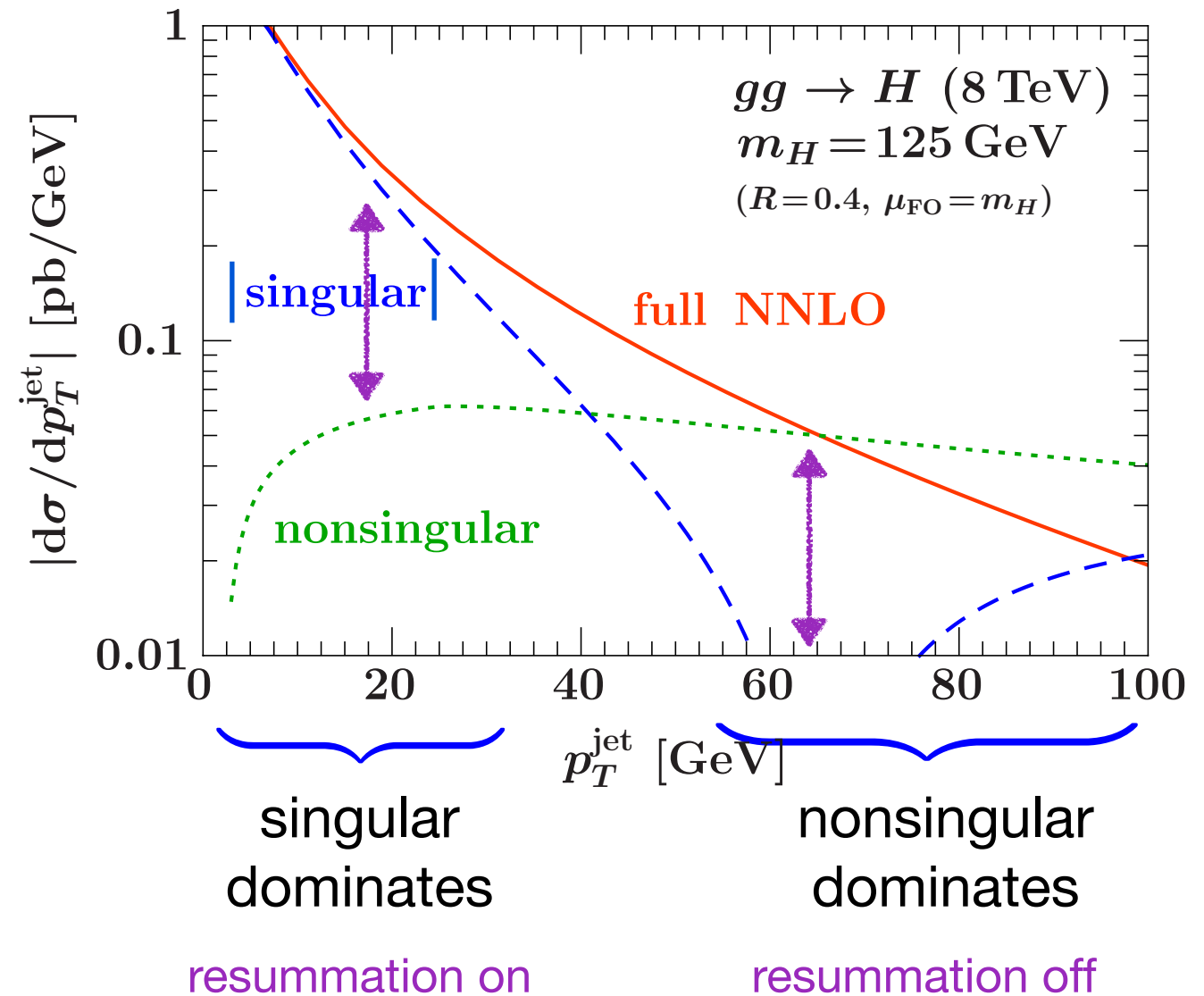
0-jet cross section

$gg \rightarrow H$ at NNLO



fixed order dips negative:
breakdown of perturbation theory,
resummation needed

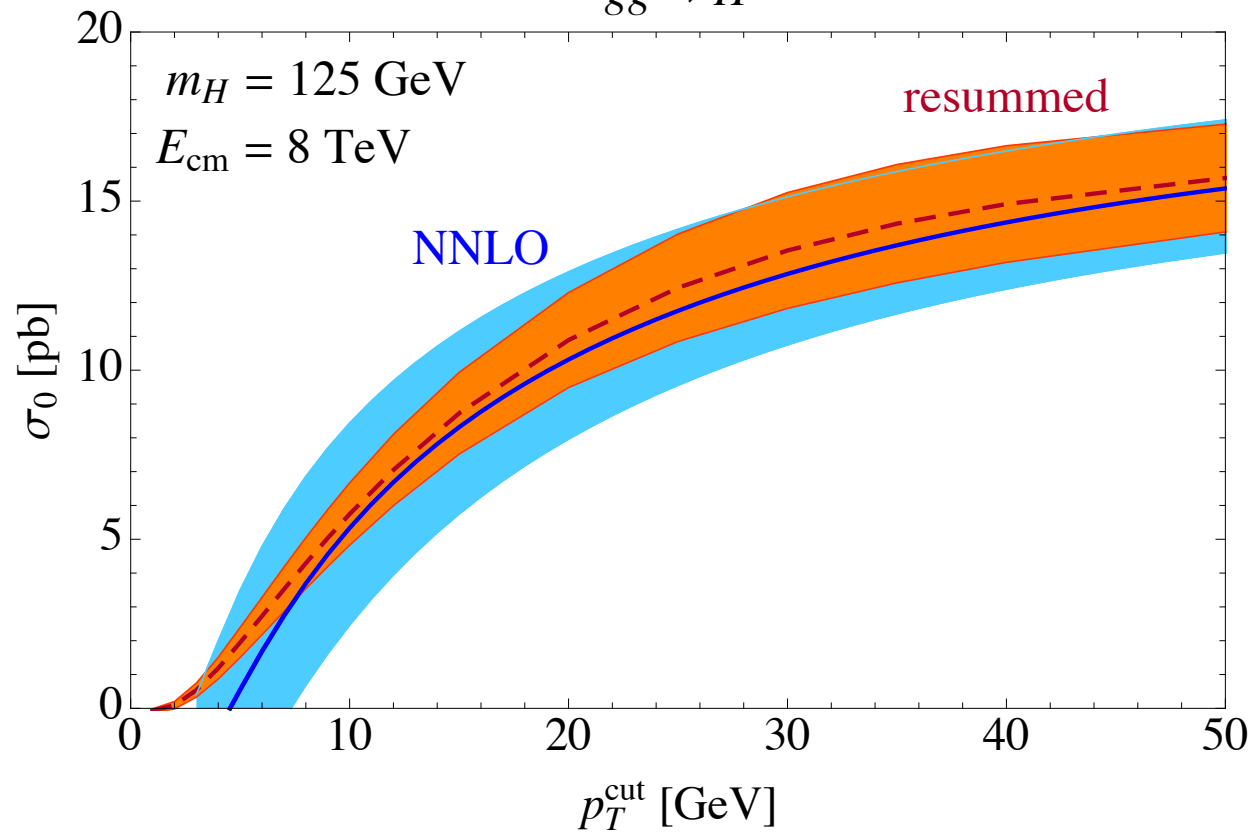
leading jet p_T spectrum at NNLO



0-jet cross section resummation vs. fixed order

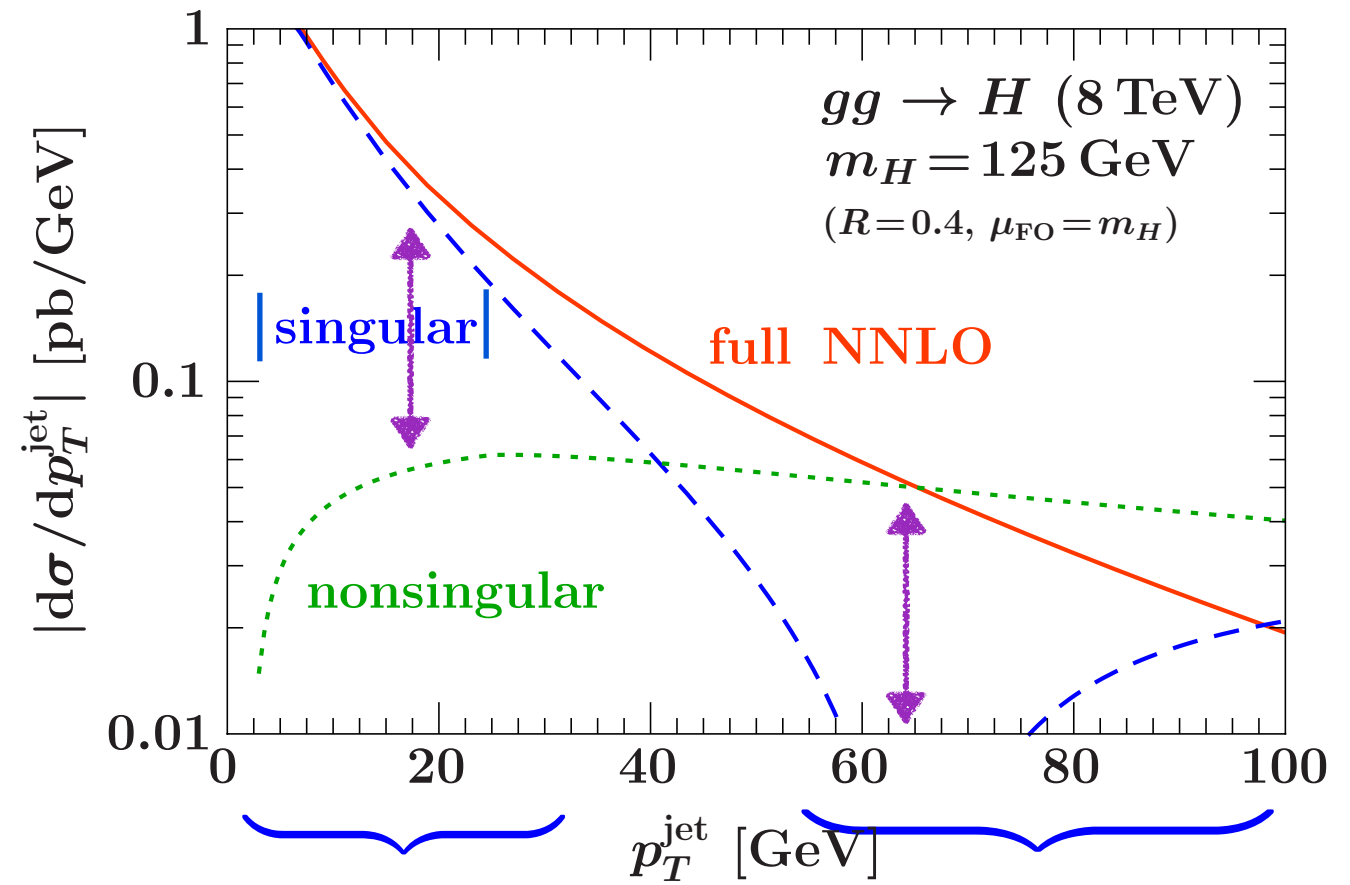
0-jet cross section

$gg \rightarrow H$



resummation can improve
precision and accuracy of
fixed order perturbation theory

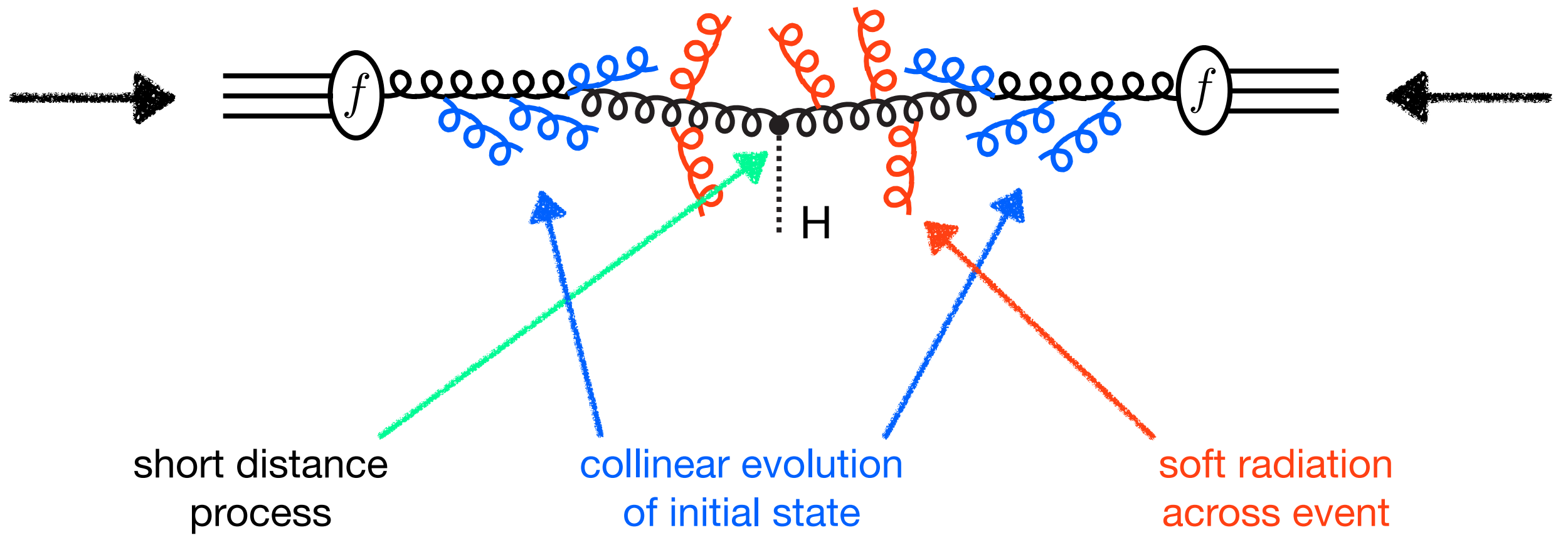
leading jet p_T spectrum at NNLO



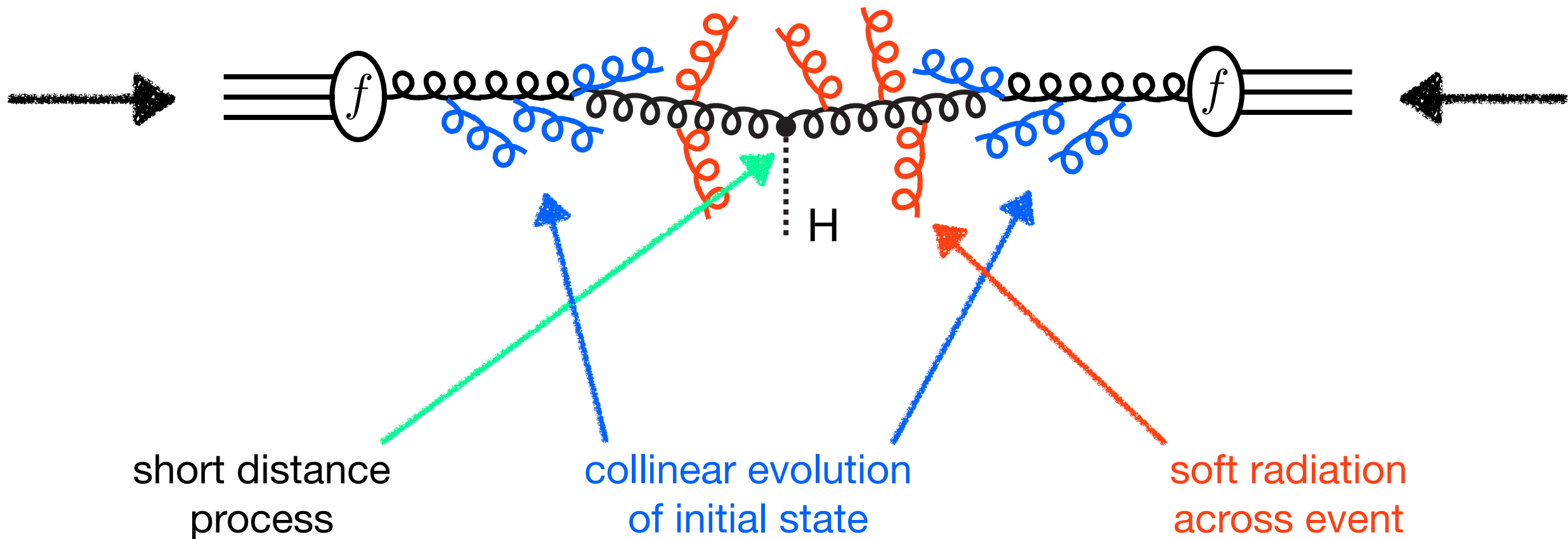
singular
dominates
resummation on

nonsingular
dominates
resummation off

0-jet factorization theorem



0-jet factorization theorem

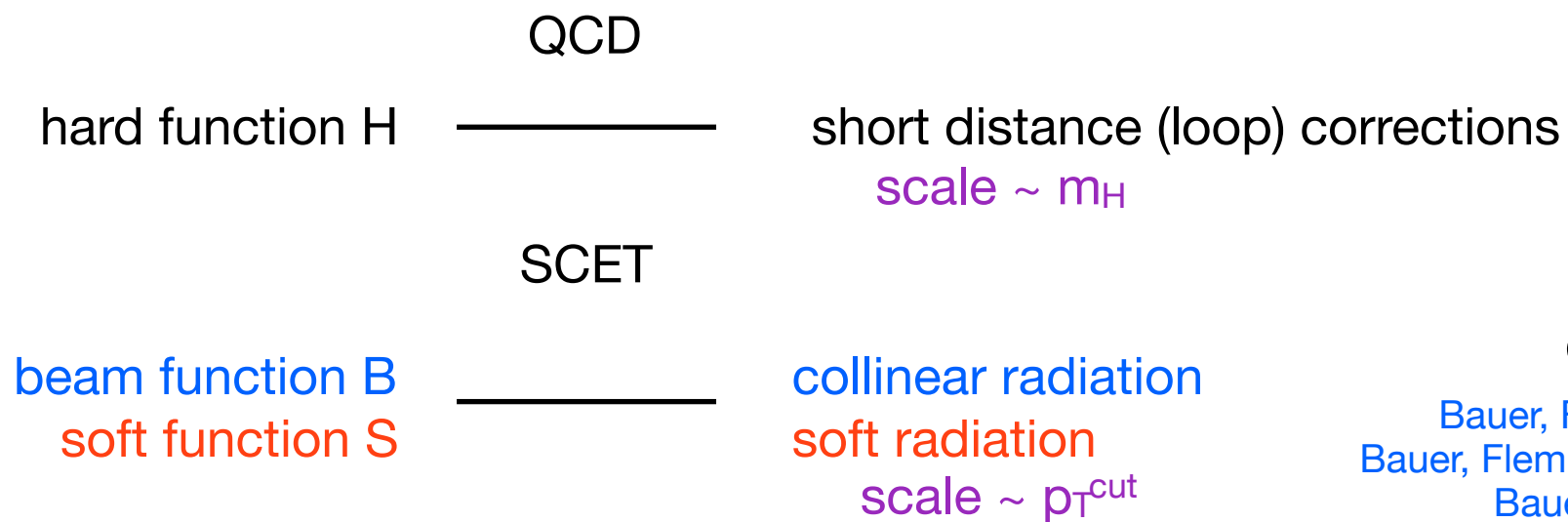


short distance process

collinear evolution of initial state

soft radiation across event

increasing scale

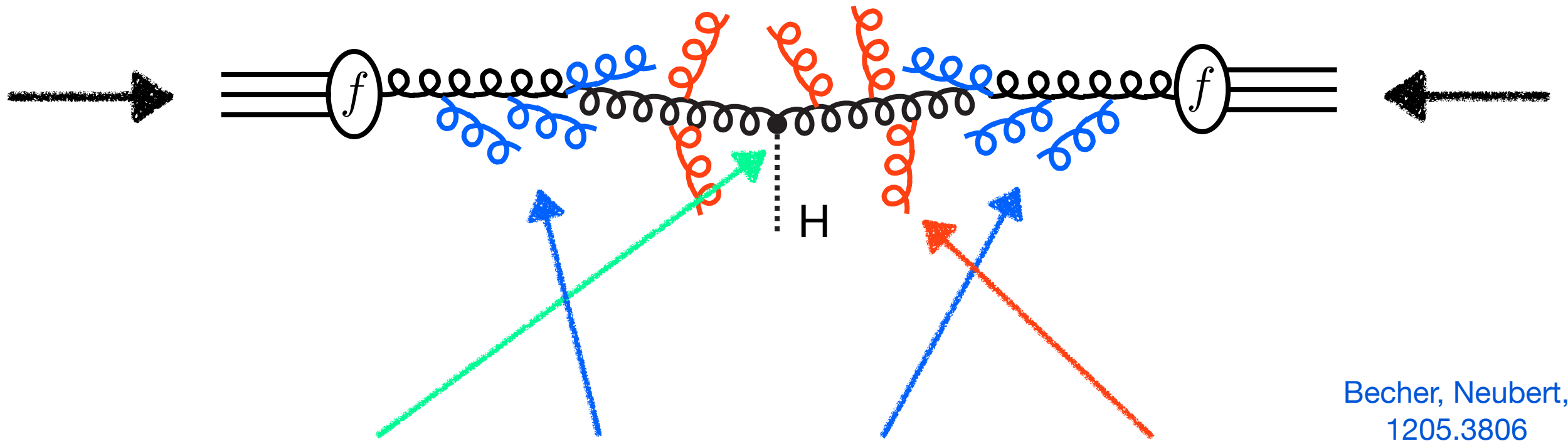


soft-collinear effective theory

- Bauer, Fleming, Luke, hep-ph/0005275
- Bauer, Fleming, Pirjol, Stewart, hep-ph/0011336
- Bauer, Stewart, hep-ph/0107001
- Bauer, Pirjol, Stewart, hep-ph/0109045
- Bauer, Fleming, Pirjol, Rothstein, Stewart, hep-ph/0202088

renormalization group evolution in SCET
sums logarithms of m_H / p_T^{cut}

0-jet factorization theorem



Becher, Neubert,
1205.3806

$$\sigma(p_T^{\text{cut}}) \sim H_{gg}(\mu) [B_a(p_T^{\text{cut}}, \mu, \nu) \times B_b(p_T^{\text{cut}}, \mu, \nu) \times S(p_T^{\text{cut}}, \mu, \nu)] + \sigma_{ns}(\mu)$$

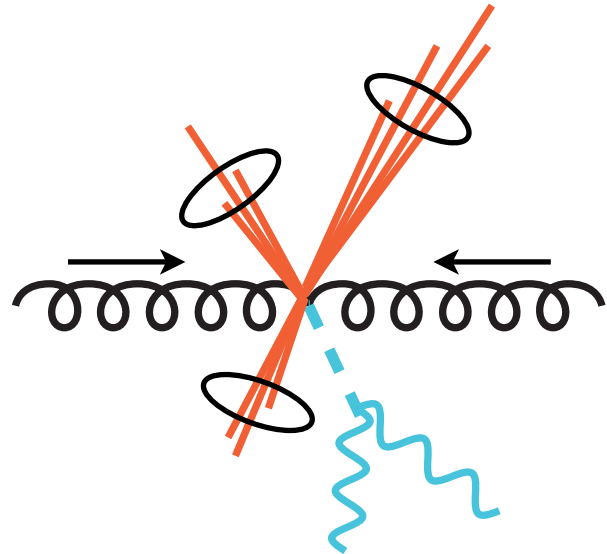
virtualls known to NNLO
we add π^2 resummation,
which increases total rate

Fully calculated to
NNLO by us

Fit to NNLO from
MCFM/HNNLO by us

Logarithms known to NNLO through RGE
Finite $\log(R)$ dependence calculated by us
(finite means p_T^{cut} independent)
Remaining finite terms fit via MCFM

technical and conceptual complications



veto is on final state jets

we need to include the jet algorithm in the theoretical framework for resummation

clustering effects arise
at each order
(start at NNLO)

$$\left(\frac{\alpha_s C_A}{\pi}\right)^n \left[C_n(R) \ln \frac{m_H}{p_T^{\text{cut}}} + D_n(R) \right]$$

Tackmann, JW, Zuberi,
1206.4312

leading terms

$$\left(\frac{\alpha_s C_A}{\pi}\right)^2 C_2^{(1)} \ln \frac{m_H}{p_T^{\text{cut}}} \ln R^2 \sim 0.14$$

NNLO effects (only LO in the algorithm) are large
need to ensure uncertainties are under control

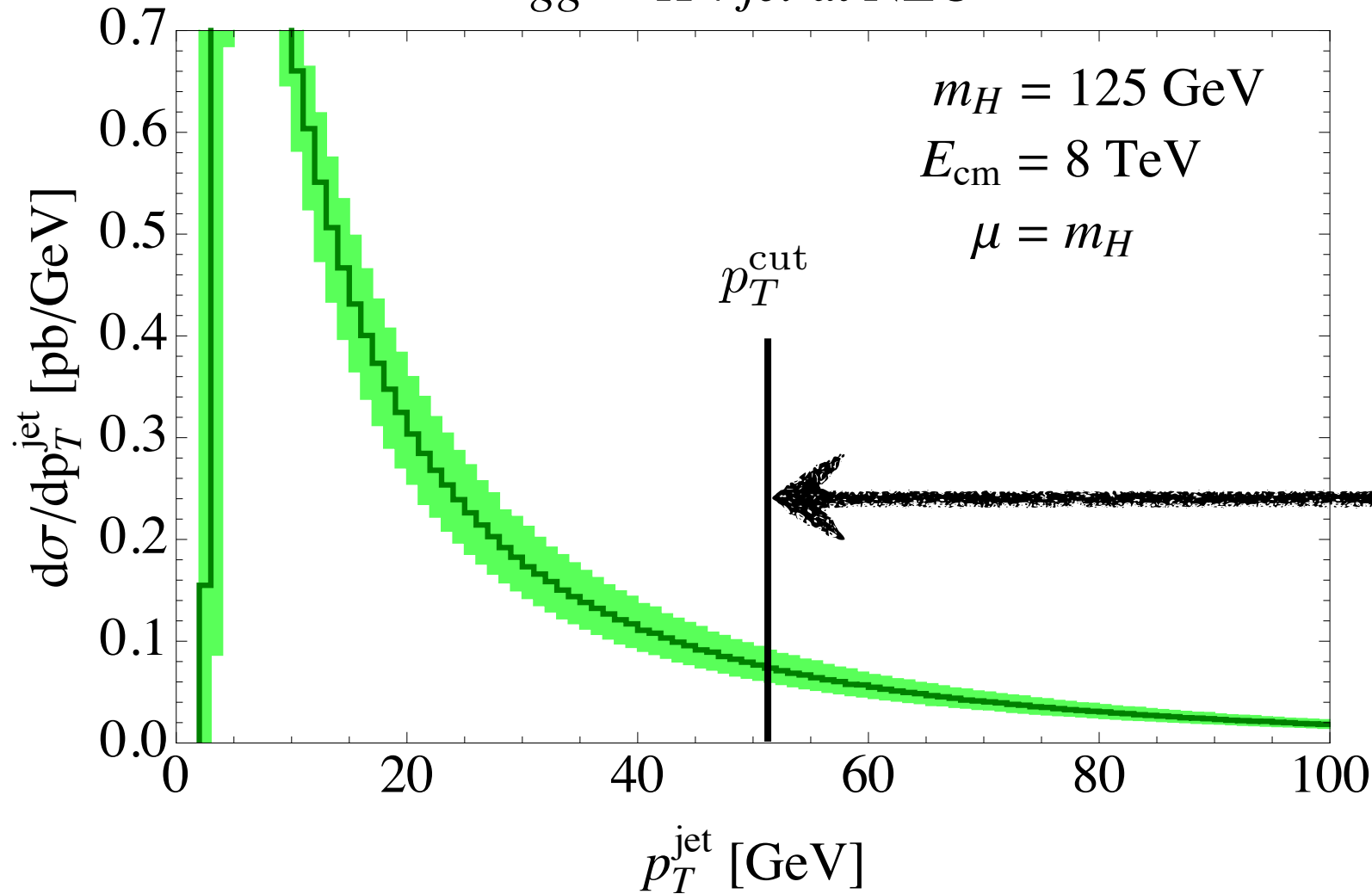
$$\left(\frac{\alpha_s C_A}{\pi}\right)^3 C_3^{(2)} \ln \frac{m_H}{p_T^{\text{cut}}} \ln^2 R^2 \sim -5 \cdot 10^{-3}$$

we have calculated the N³LO leading contributions
JW, Alioli, 1311.5234

nonsingular terms

fixed order code gives
leading jet p_T spectrum

$gg \rightarrow H + jet$ at NLO



0-jet cross section

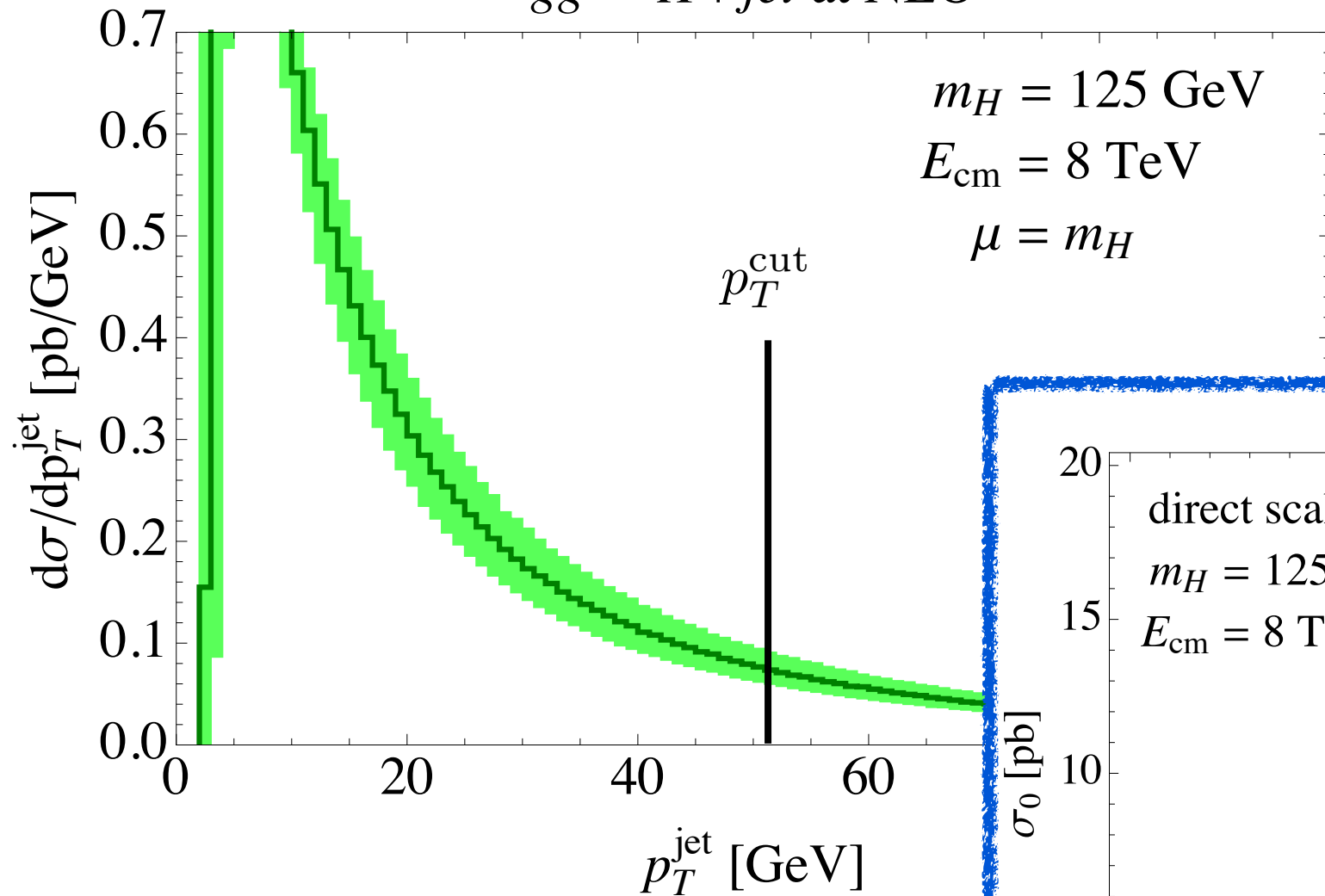
$$\sigma_0(p_T^{\text{cut}}) = \sigma_{\text{tot}} - \int_{p_T^{\text{cut}}}^{\infty} dp_T^{\text{jet}} \frac{d\sigma}{dp_T^{\text{jet}}}$$

inclusive rate
(boundary condition)

nonsingular terms

fixed order code gives
leading jet p_T spectrum

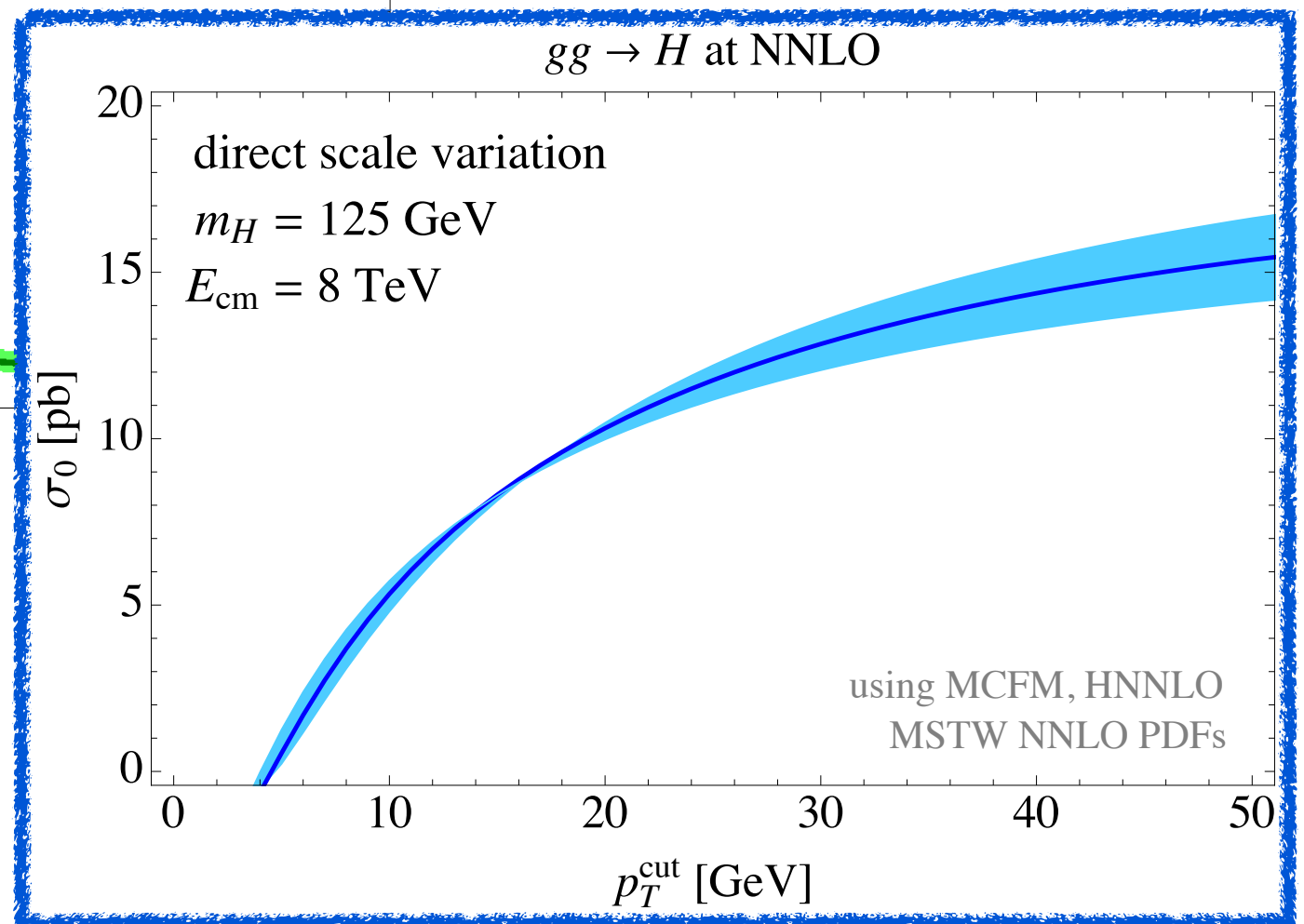
$gg \rightarrow H + jet$ at NLO



0-jet cross section

$$\sigma_0(p_T^{\text{cut}}) = \sigma_{\text{tot}} - \int_{p_T^{\text{cut}}}^{\infty} dp_T^{\text{jet}} \frac{d\sigma}{dp_T^{\text{jet}}}$$

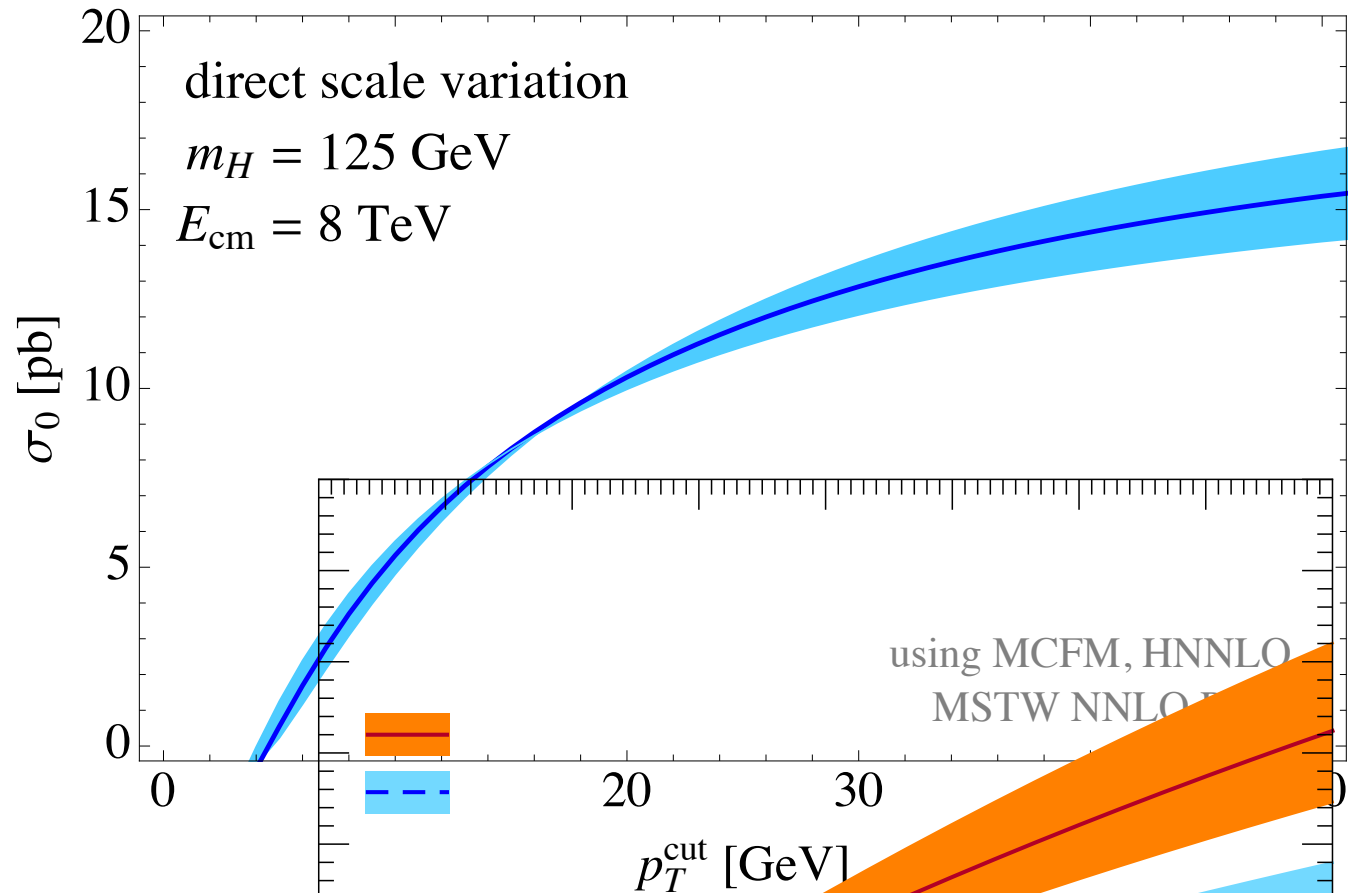
gives the NNLO
0-jet cross section



nonsingular terms

fixed order 0-jet cross section

$gg \rightarrow H$ at NNLO

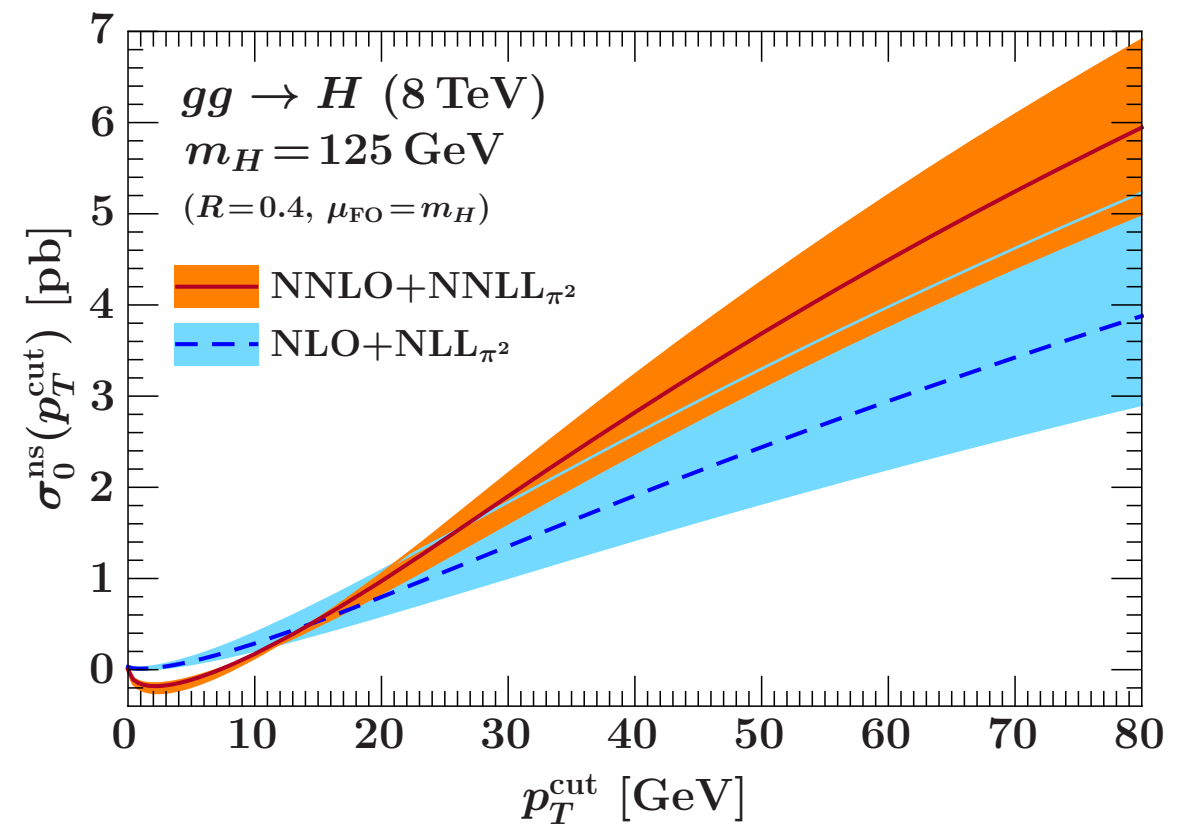


lets us also fit unknown
singular constants
in $p_T^{\text{cut}} \rightarrow 0$ limit

nonsingular terms

$$\sigma_0^{\text{ns}}(p_T^{\text{cut}}) = \sigma_0^{\text{FO}}(p_T^{\text{cut}}) - \sigma_0^{\text{sing}}(p_T^{\text{cut}})$$

given by difference
between FO, singular



resummation and profile scales

$$\sigma(p_T^{\text{cut}}) \sim H_{gg}(\mu) [B_a(p_T^{\text{cut}}, \mu, \nu) B_b(p_T^{\text{cut}}, \mu, \nu) S(p_T^{\text{cut}}, \mu, \nu)] + \sigma_{ns}(\mu)$$



renormalization group evolution

$$\sim \underbrace{U_0(\{\mu_F\}, \{\nu_F\})}_{\text{evolution factor}} H_{gg}(\mu_H) [B_a(p_T^{\text{cut}}, \mu_B, \nu_B) B_b(p_T^{\text{cut}}, \mu_B, \nu_B) S(p_T^{\text{cut}}, \mu_S, \nu_S)] + \sigma_{ns}(\mu)$$

evolution factor

factorization scales

$$\begin{aligned} \mu_H &\sim \nu_B \sim m_H \\ \mu_B &\sim \mu_S \sim \nu_S \sim p_T^{\text{cut}} \end{aligned}$$

resummation and profile scales

$$\sigma(p_T^{\text{cut}}) \sim H_{gg}(\mu) [B_a(p_T^{\text{cut}}, \mu, \nu) B_b(p_T^{\text{cut}}, \mu, \nu) S(p_T^{\text{cut}}, \mu, \nu)] + \sigma_{ns}(\mu)$$

renormalization group evolution

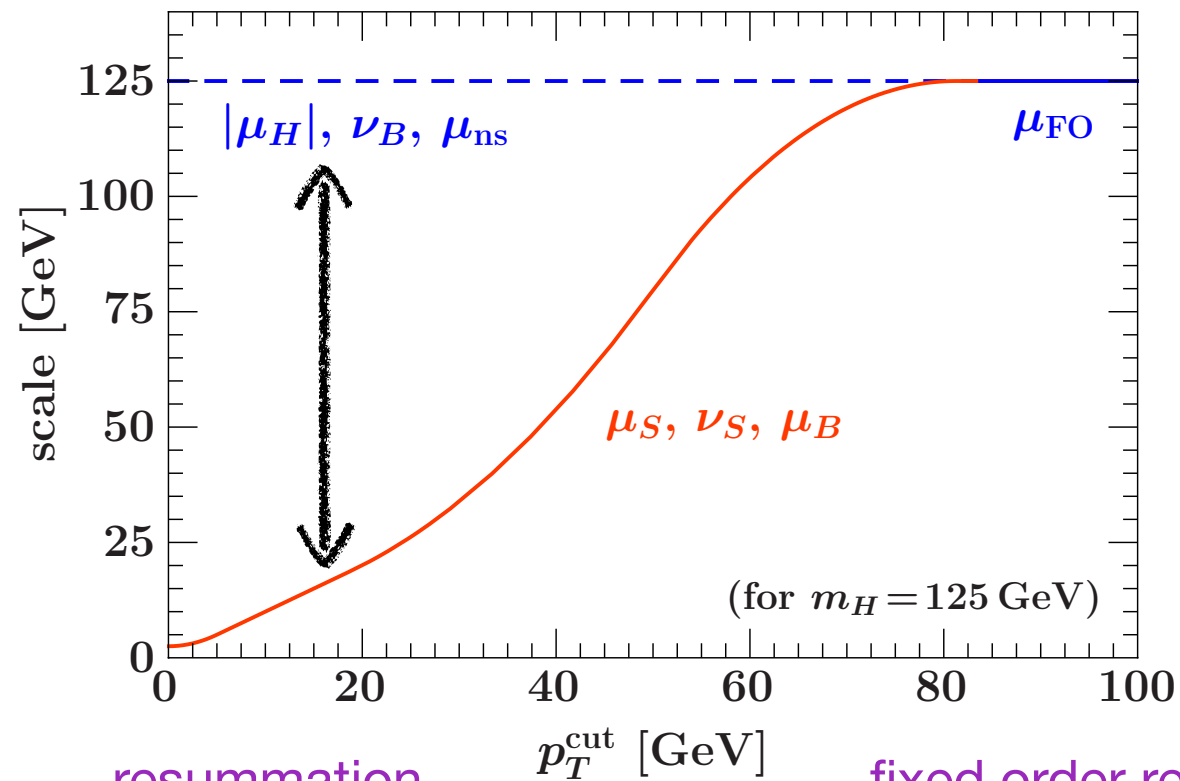
$$\sim \underbrace{U_0(\{\mu_F\}, \{\nu_F\})}_{\text{evolution factor}} H_{gg}(\mu_H) [B_a(p_T^{\text{cut}}, \mu_B, \nu_B) B_b(p_T^{\text{cut}}, \mu_B, \nu_B) S(p_T^{\text{cut}}, \mu_S, \nu_S)] + \sigma_{ns}(\mu)$$

evolution factor

factorization scales

$$\begin{aligned} \mu_H &\sim \nu_B \sim m_H \\ \mu_B &\sim \mu_S \sim \nu_S \sim p_T^{\text{cut}} \end{aligned}$$

profile scales



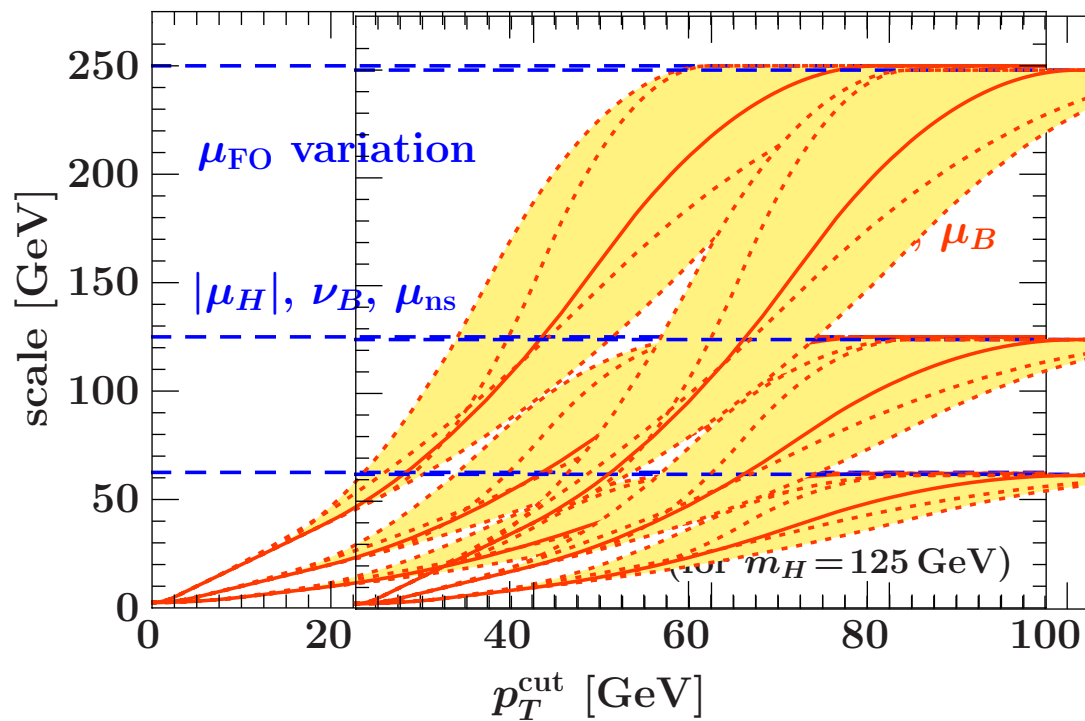
resummation regime

fixed order regime
(all scales equal)

profile scales implement
resummation *and* matching

uncertainties

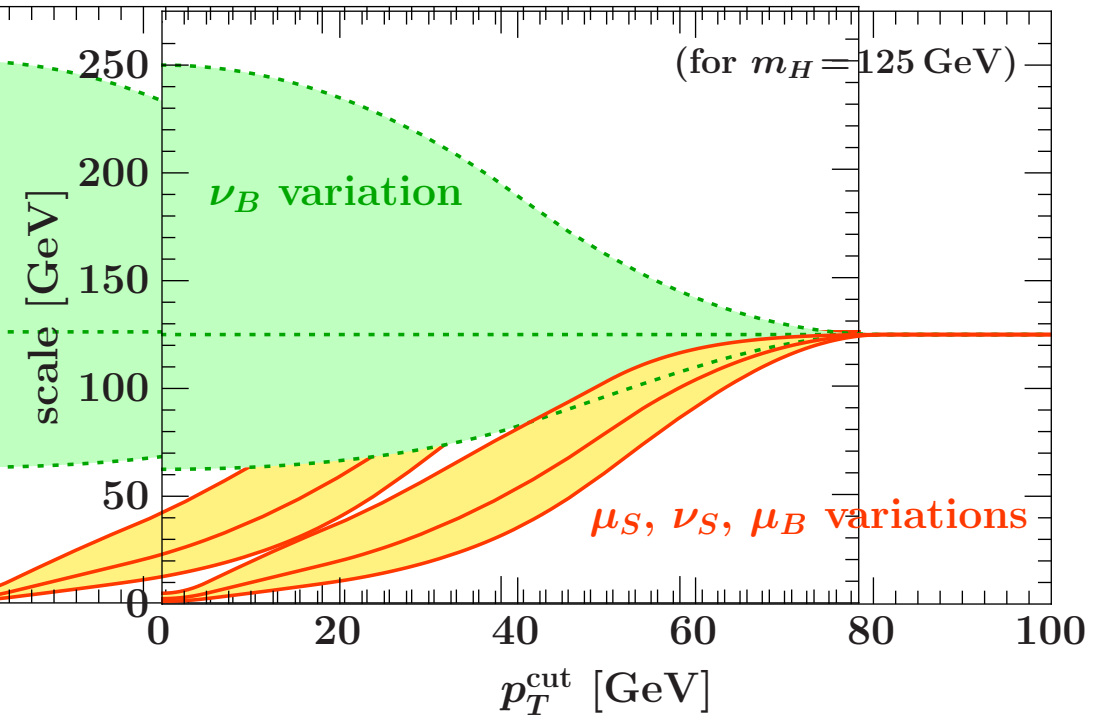
uncertainties estimated via profile scale variations



collective variation of all scales
and profile shape variations

envelope: $\Delta_{\mu 0}(p_T^{\text{cut}})$

yield uncertainty
on the 0-jet rate



variation of beam, soft factorization
scales in physical combinations

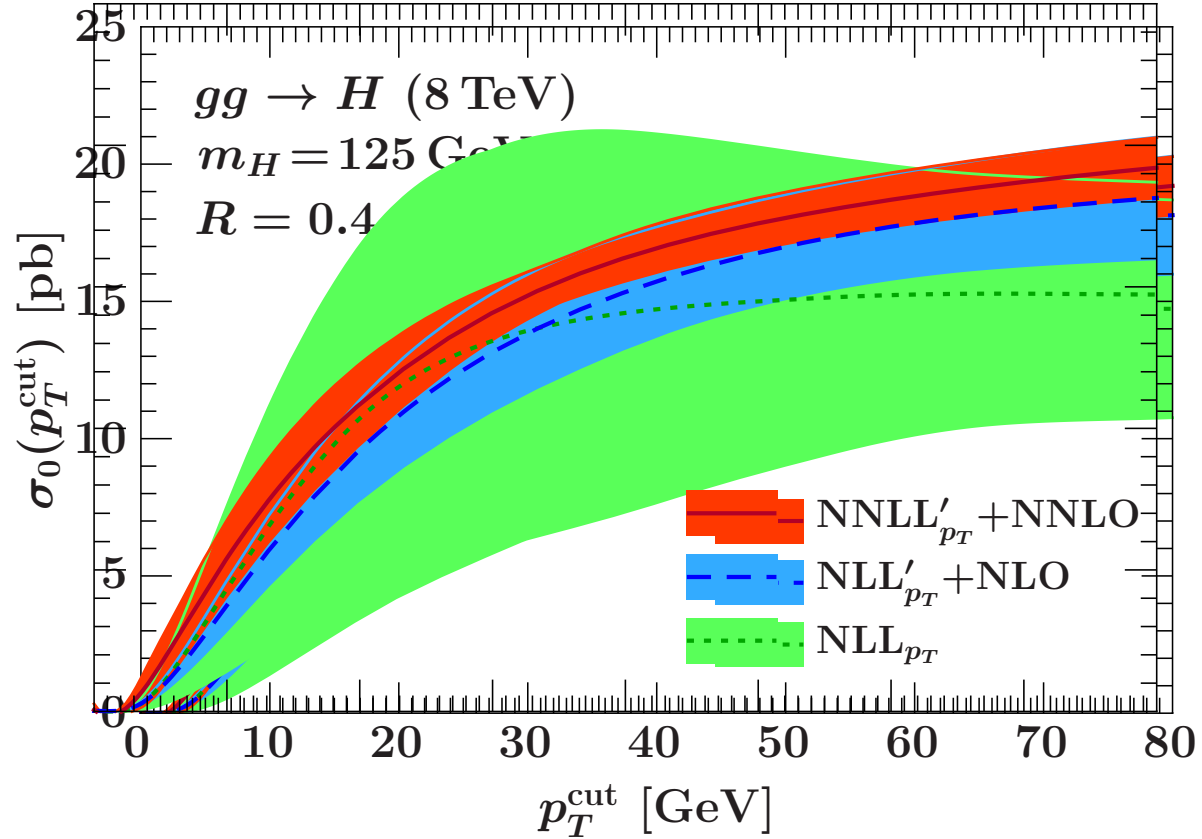
envelope: $\Delta_{\text{resum}}(p_T^{\text{cut}})$

migration uncertainty between the
0-jet and inclusive 1-jet bins

$$\text{total 0-jet uncertainty: } \Delta_{\text{tot}}^2(p_T^{\text{cut}}) = \Delta_{\mu 0}^2(p_T^{\text{cut}}) + \Delta_{\text{resum}}^2(p_T^{\text{cut}})$$

H + 0-jet results

0-jet cross section: resummed convergence



rates with uncertainties:

R = 0.4:

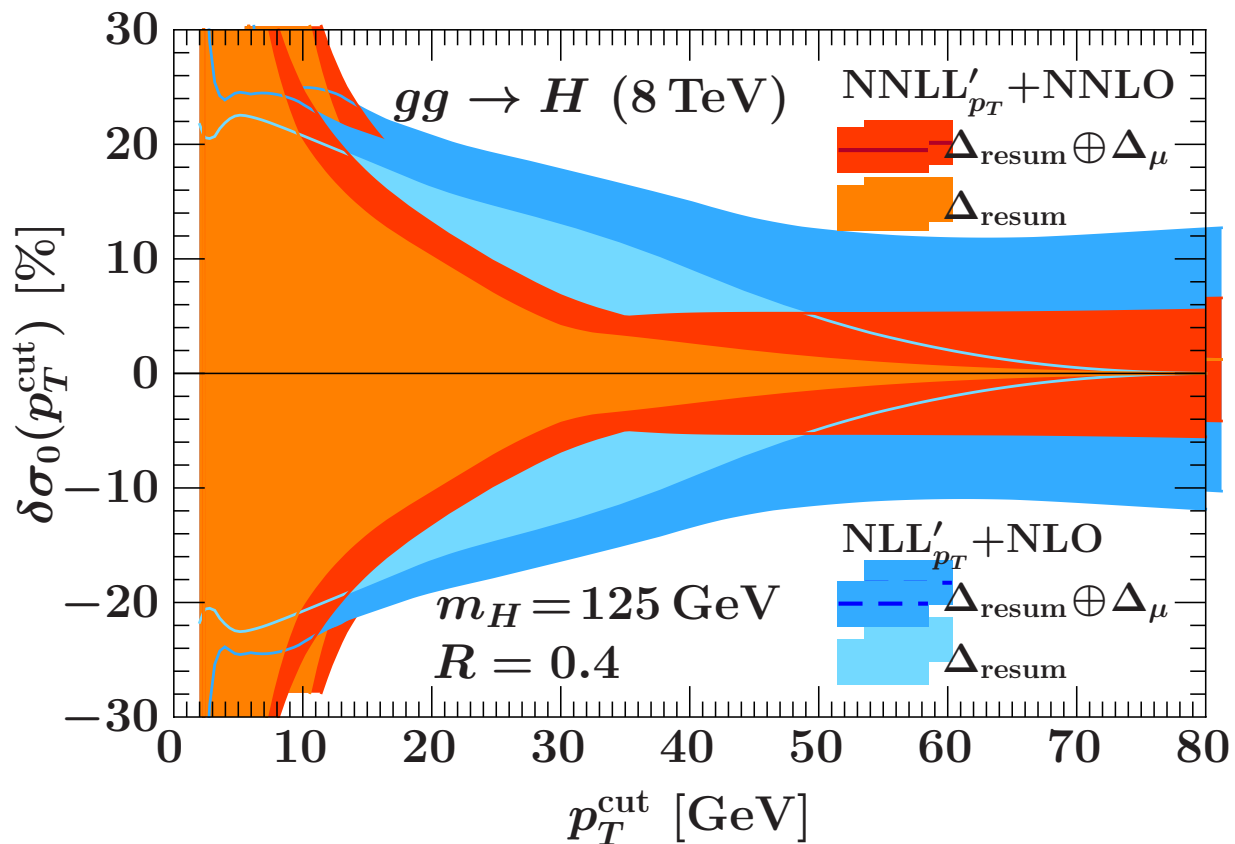
$$p_T^{\text{cut}} = 25 \text{ GeV} : \sigma_0 = 12.67 \pm 1.22 (9.6\%)$$

$$p_T^{\text{cut}} = 30 \text{ GeV} : \sigma_0 = 14.09 \pm 0.96 (6.8\%)$$

R = 0.5:

$$p_T^{\text{cut}} = 25 \text{ GeV} : \sigma_0 = 12.40 \pm 1.12 (9.0\%)$$

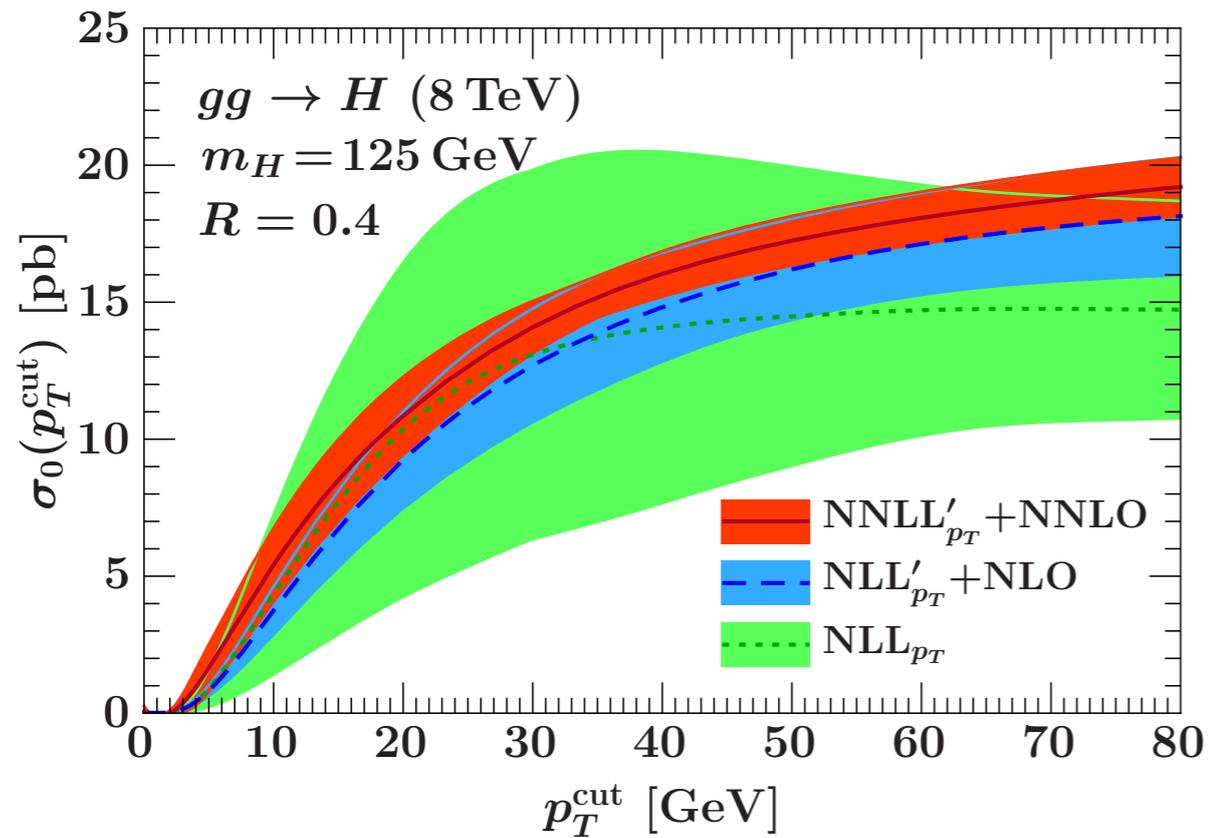
$$p_T^{\text{cut}} = 30 \text{ GeV} : \sigma_0 = 13.85 \pm 0.87 (6.3\%)$$



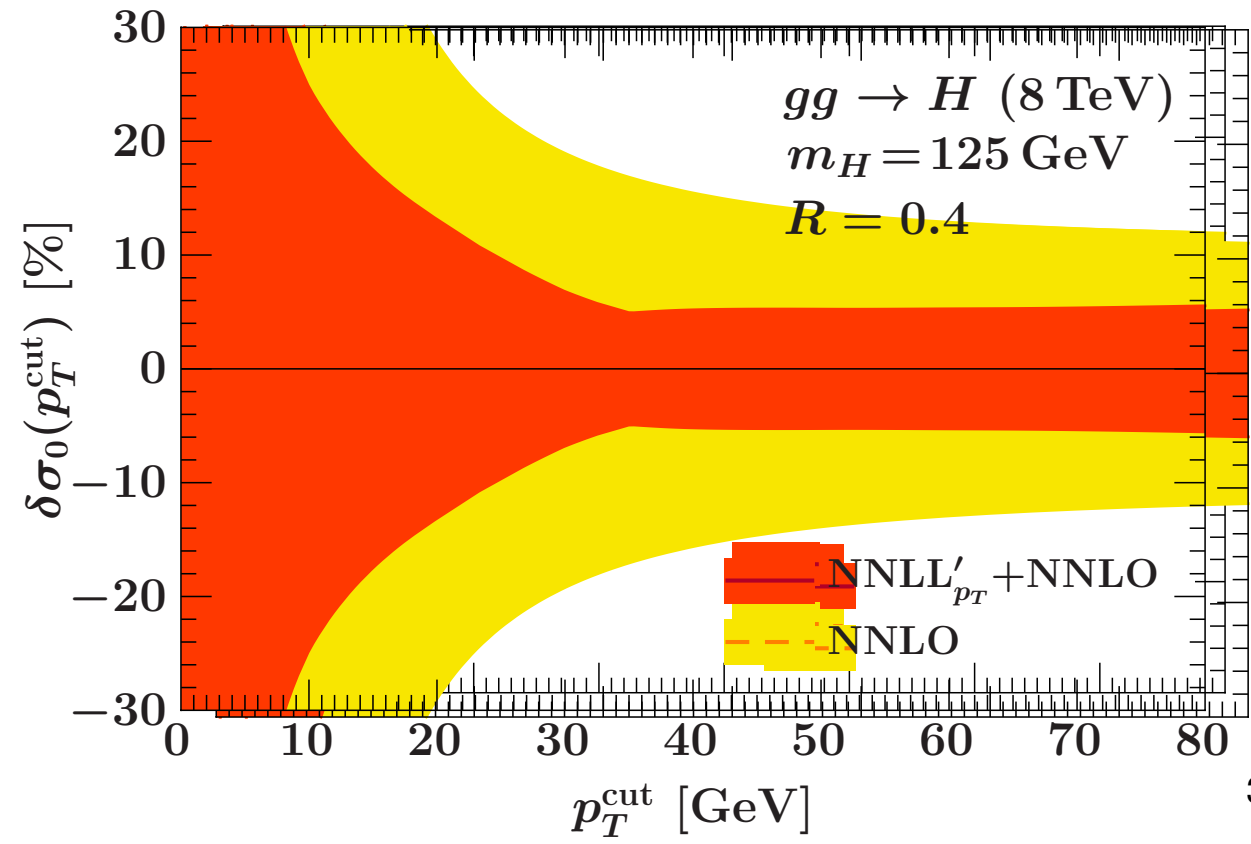
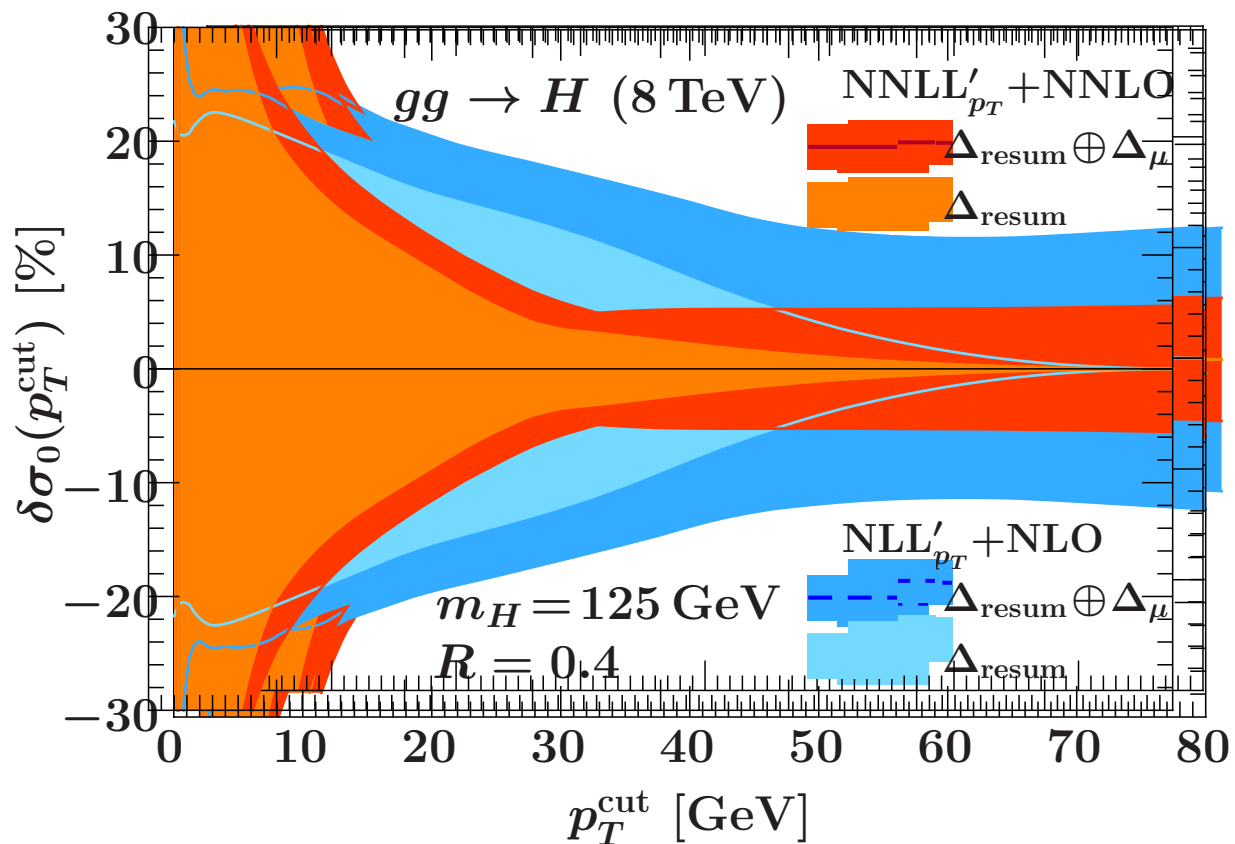
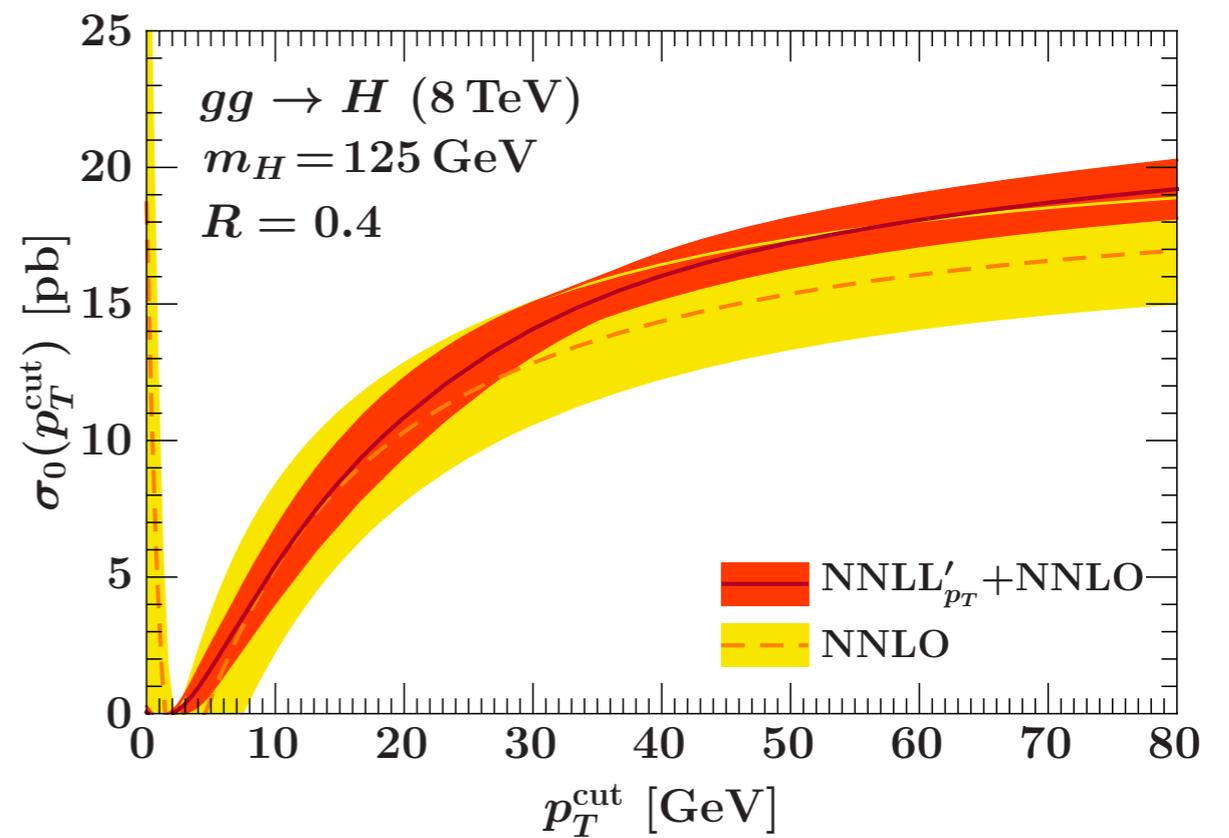
↑
 compare to 17%!

H + 0-jet results

0-jet cross section: resummed convergence

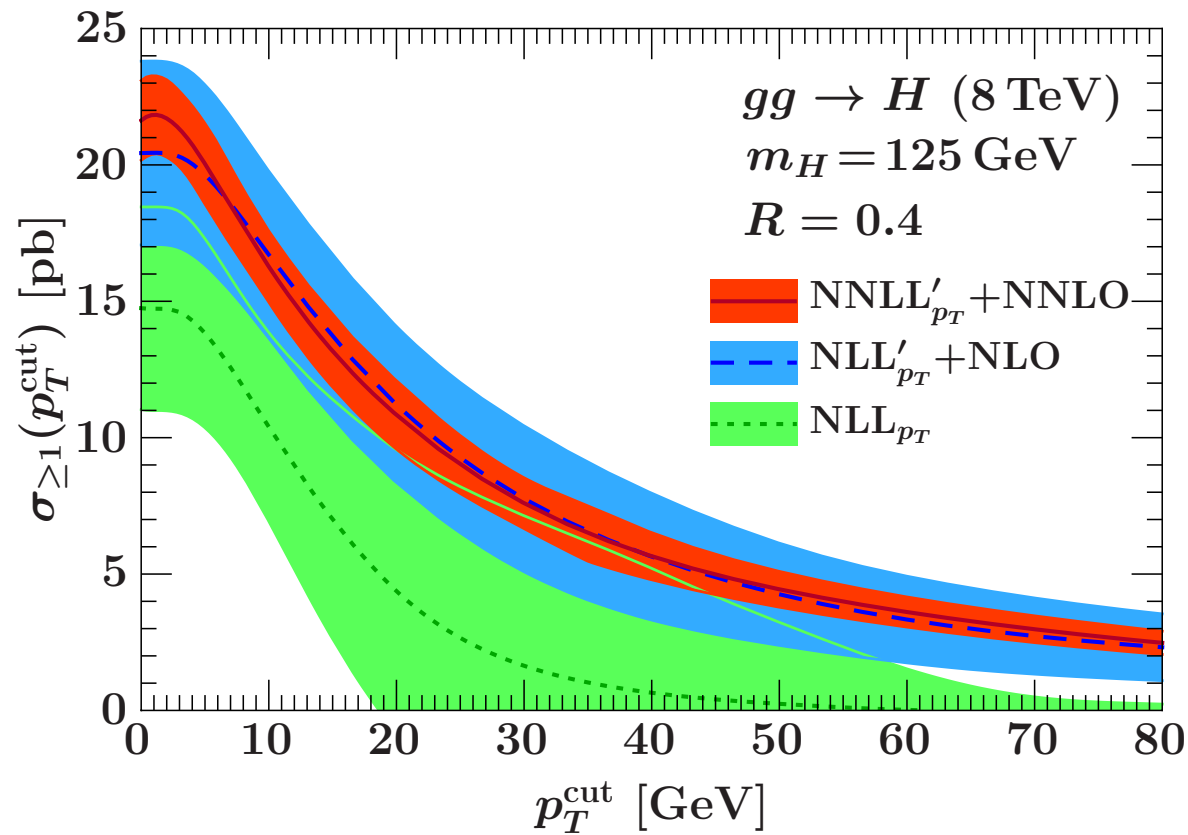


0-jet cross section: comparison to fixed order

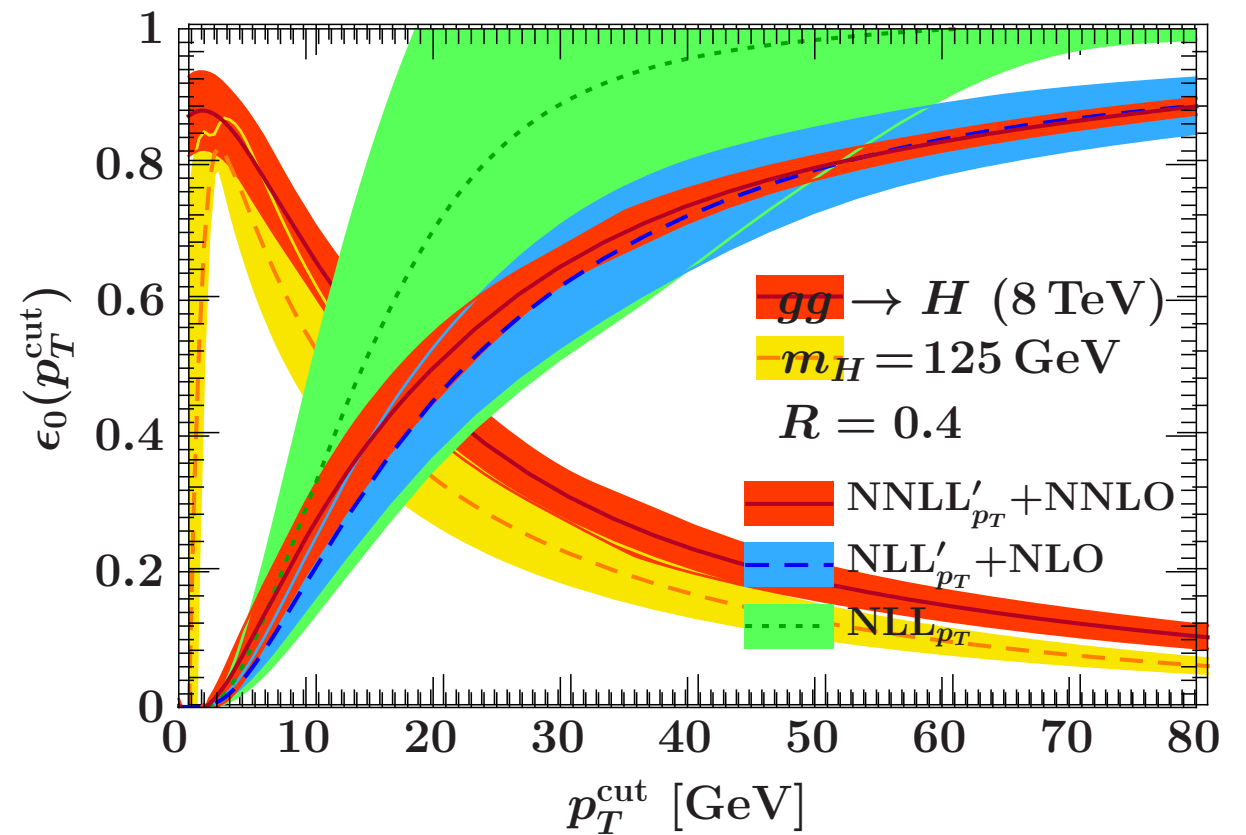


inclusive 1-jet cross section and 0-jet efficiency

inclusive 1-jet cross section



0-jet efficiency



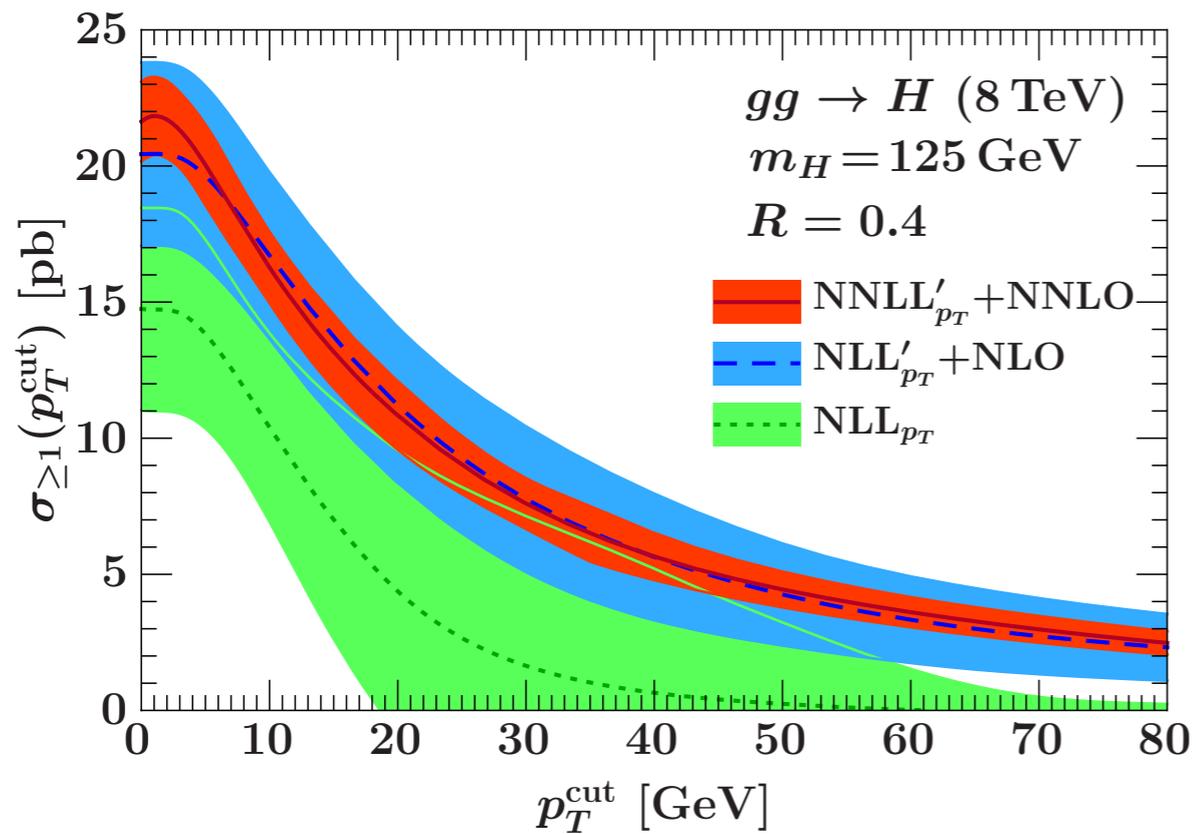
$$\sigma_{\geq 1}(p_T^{\text{cut}}) = \sigma_{\text{tot}} - \sigma_0(p_T^{\text{cut}})$$

$$\epsilon_0(p_T^{\text{cut}}) = \sigma_0(p_T^{\text{cut}}) / \sigma_{\text{tot}}$$

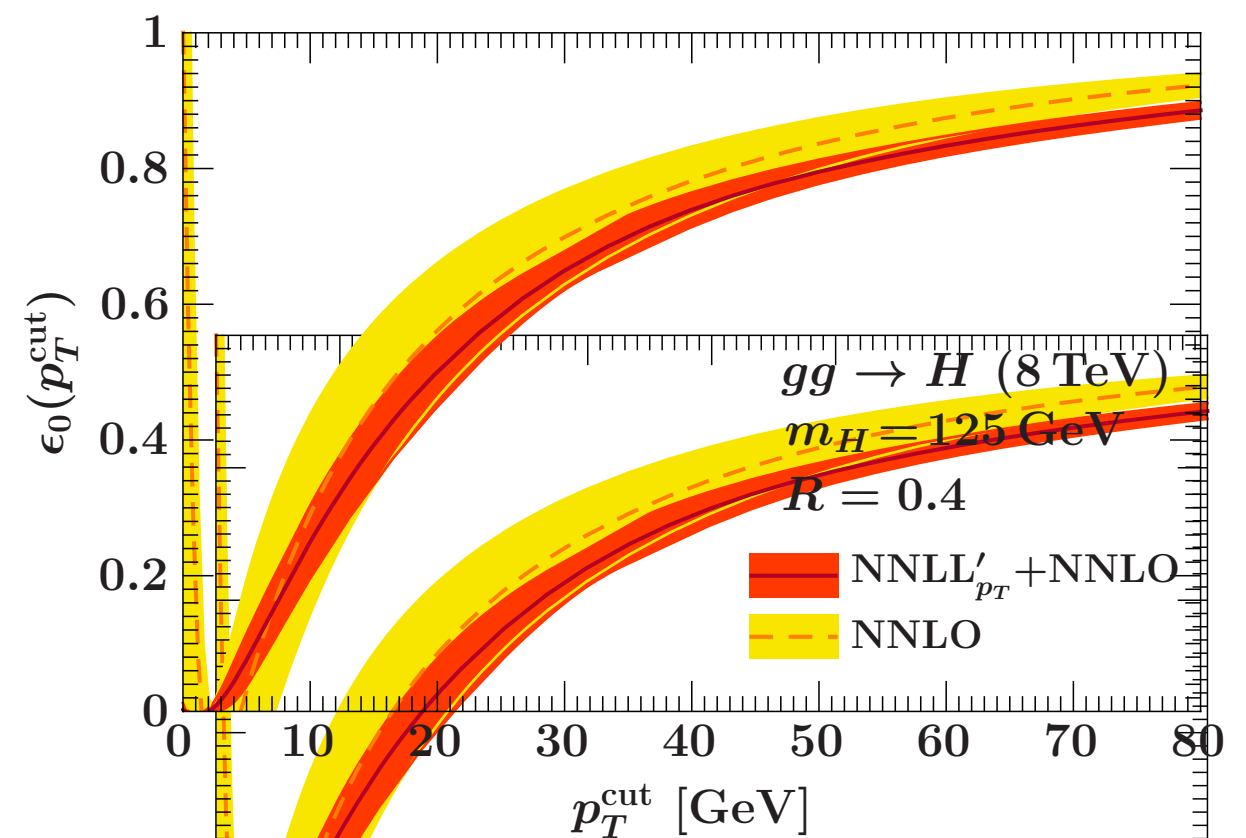
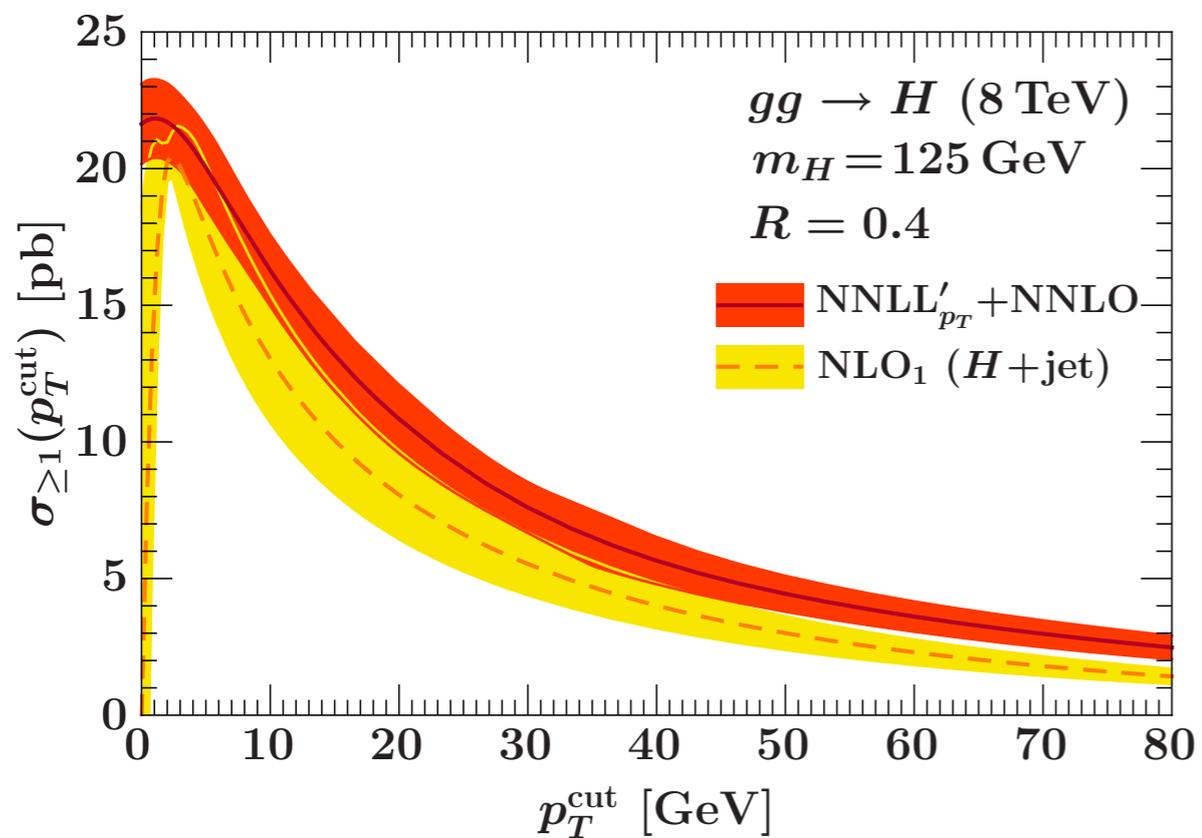
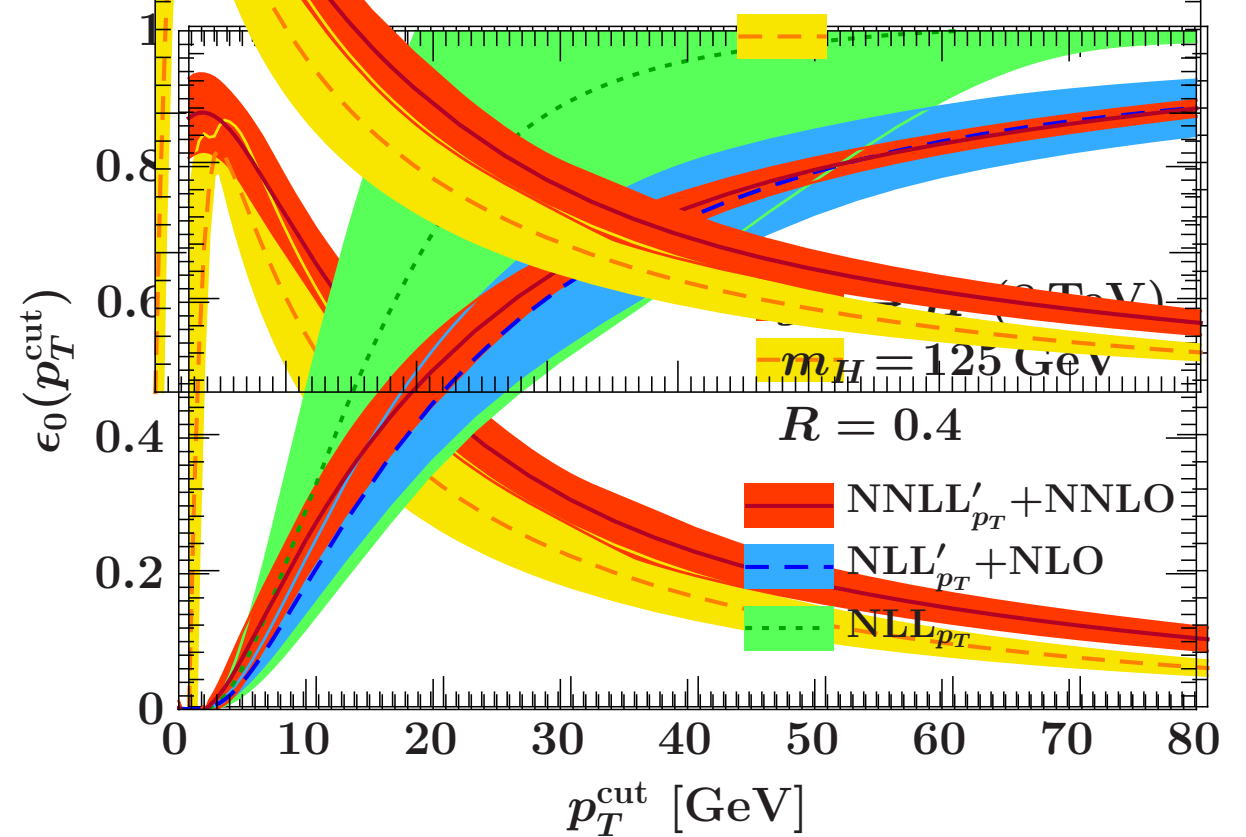
we control correlations between the 0-jet and total cross sections, so we can reliably predict uncertainties

inclusive 1-jet cross section and 0-jet efficiency

inclusive 1-jet cross section

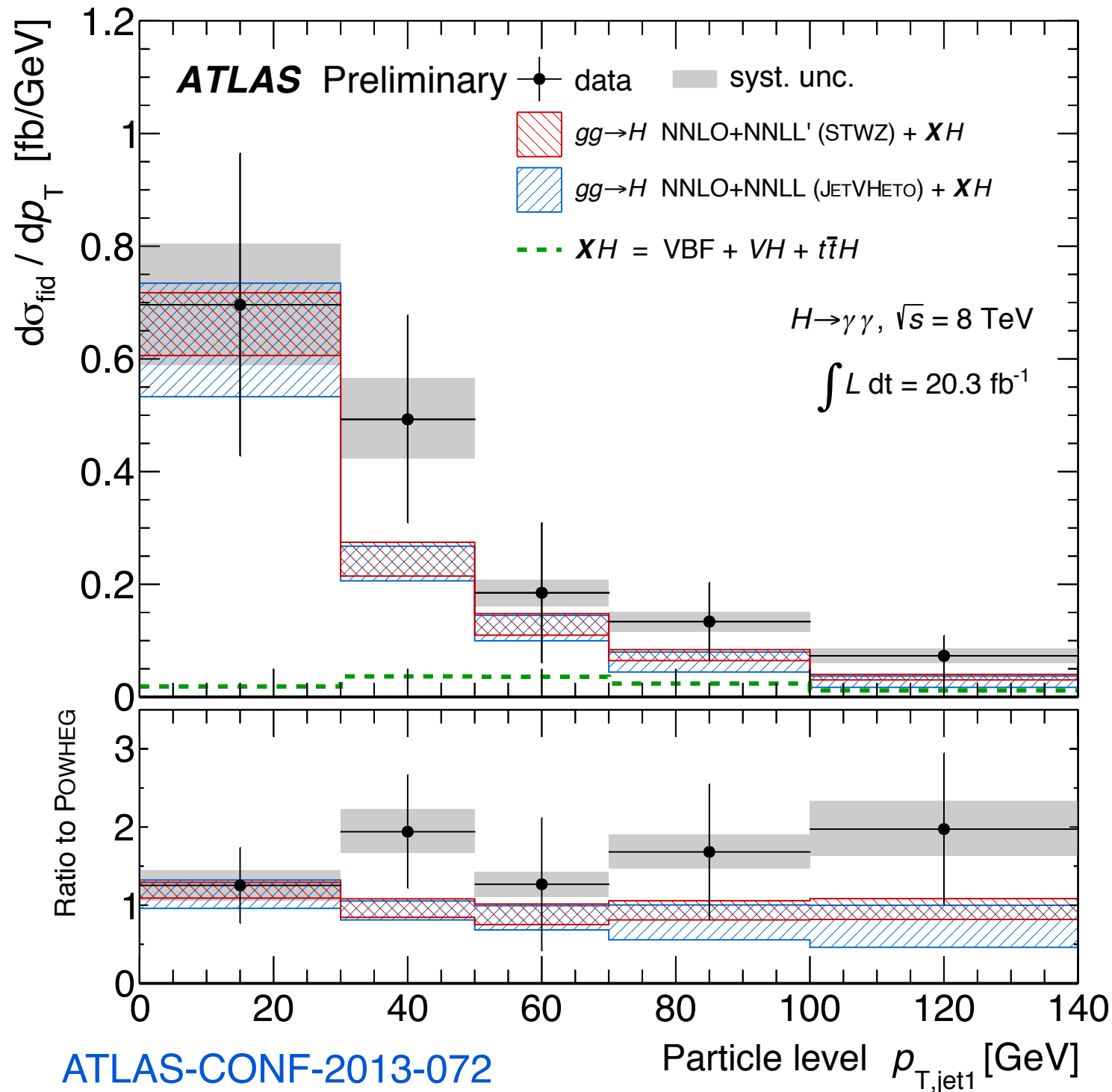


0-jet efficiency



comparison to data

p_T^{jet} spectrum in $\gamma\gamma$



ATLAS-CONF-2013-072

combined binned fit
 (in leading jet p_T)
 to the $\gamma\gamma$ excess

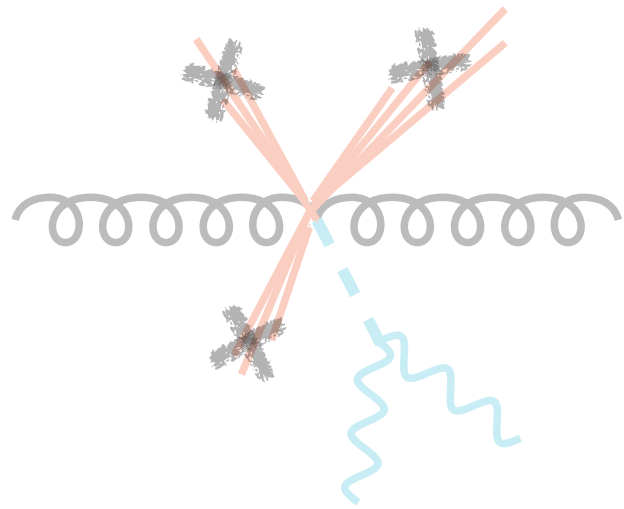
prediction derived from the
 0-jet and inclusive 1-jet results
 good agreement between
 theory/MC predictions

Powheg;
 Stewart, Tackmann, JW, Zuberi;
 Banfi, Monni, Salam, Zanderighi

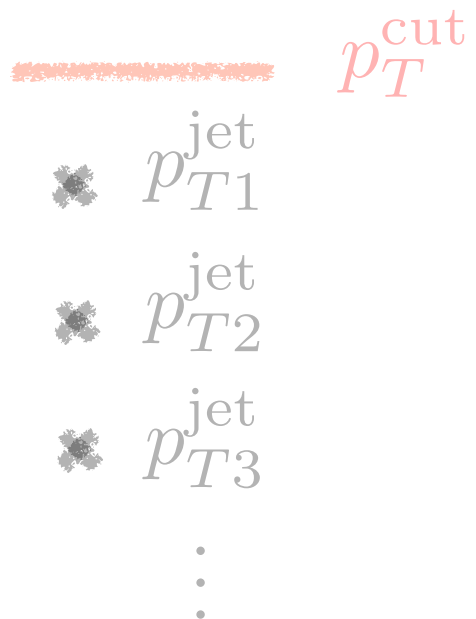
good shape agreement
 outside of the first bin,
 Run 2 comparison will
 be interesting

onto the 1-jet rate!

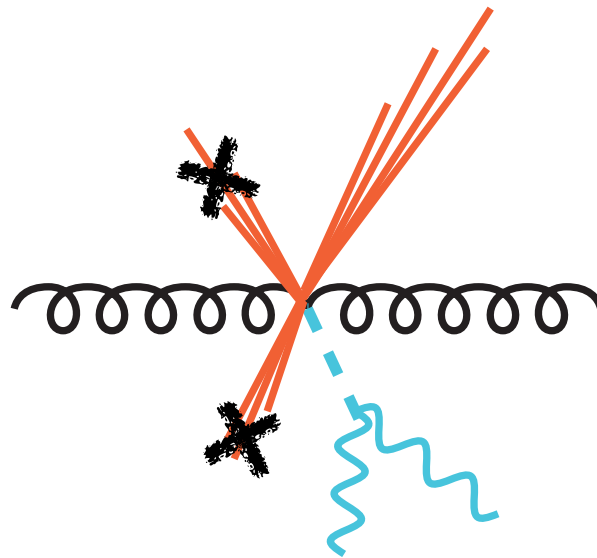
0-jet events



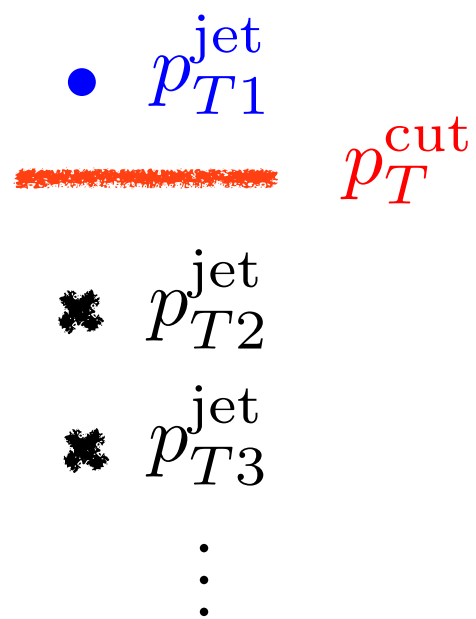
jet p_T



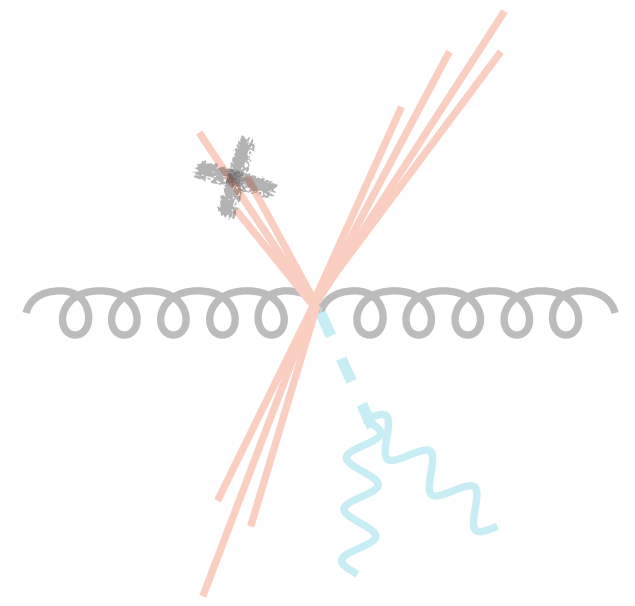
1-jet events



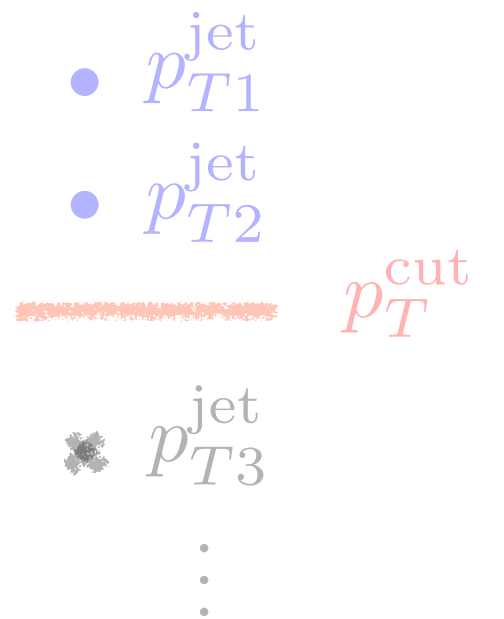
jet p_T



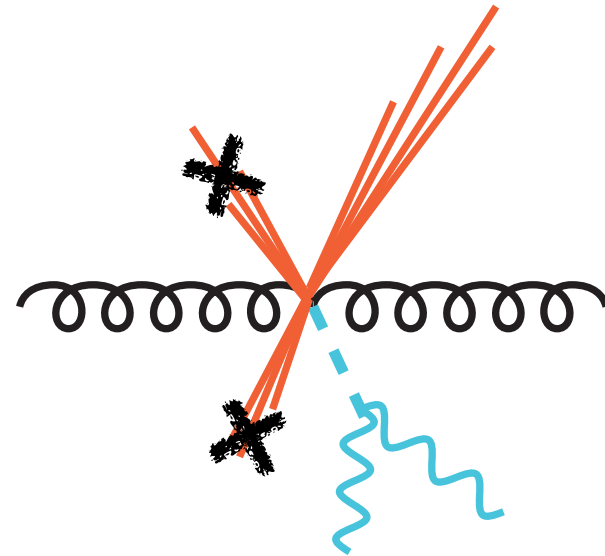
2-jet events



jet p_T



kinematics of the 1-jet cross section



3-scale problem:

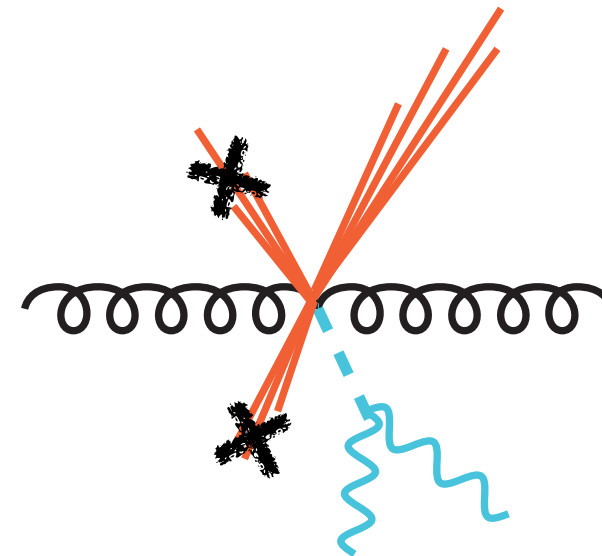
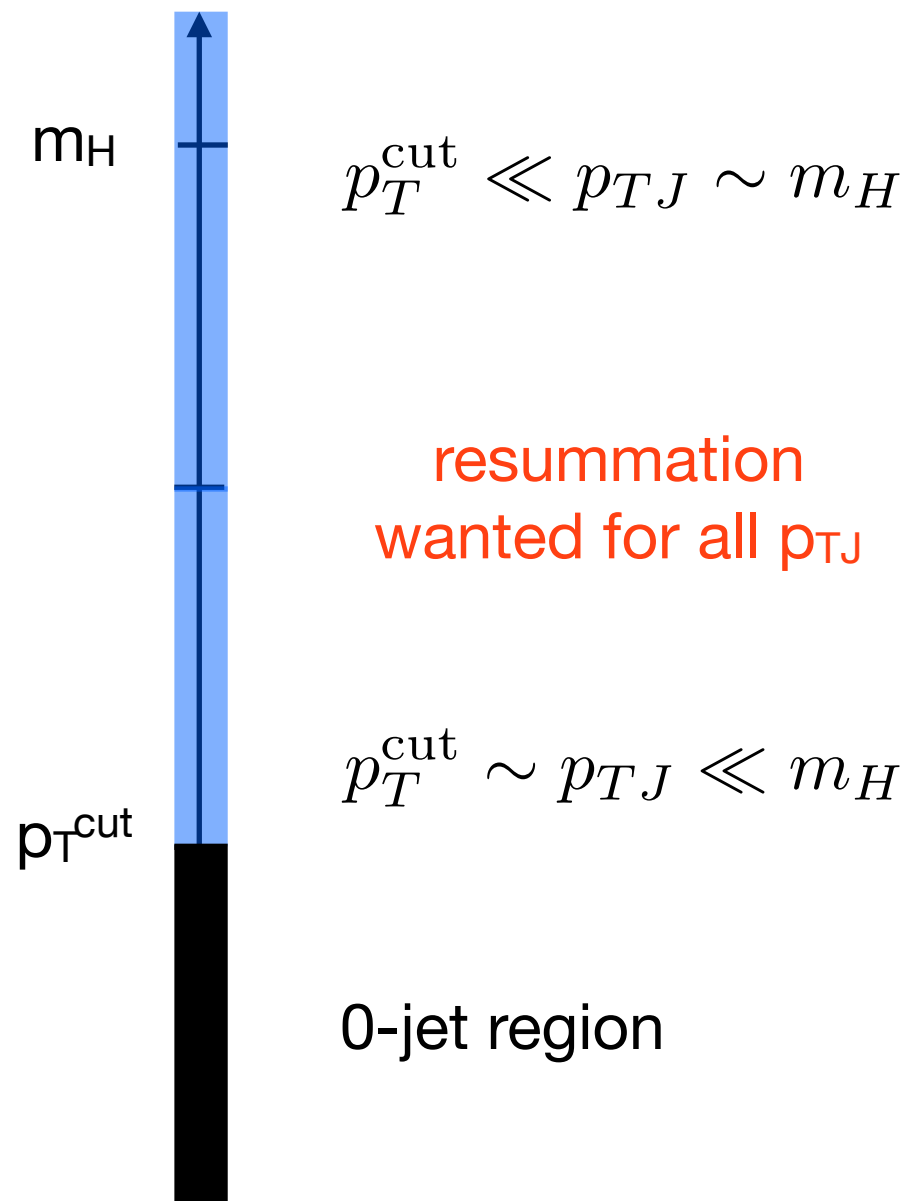
$$p_T^{\text{cut}} \ll m_H$$

what regime is p_{TJ} in?

kinematics of the 1-jet cross section

exclusive 1-jet cross section

p_{TJ} : leading jet p_T



3-scale problem:

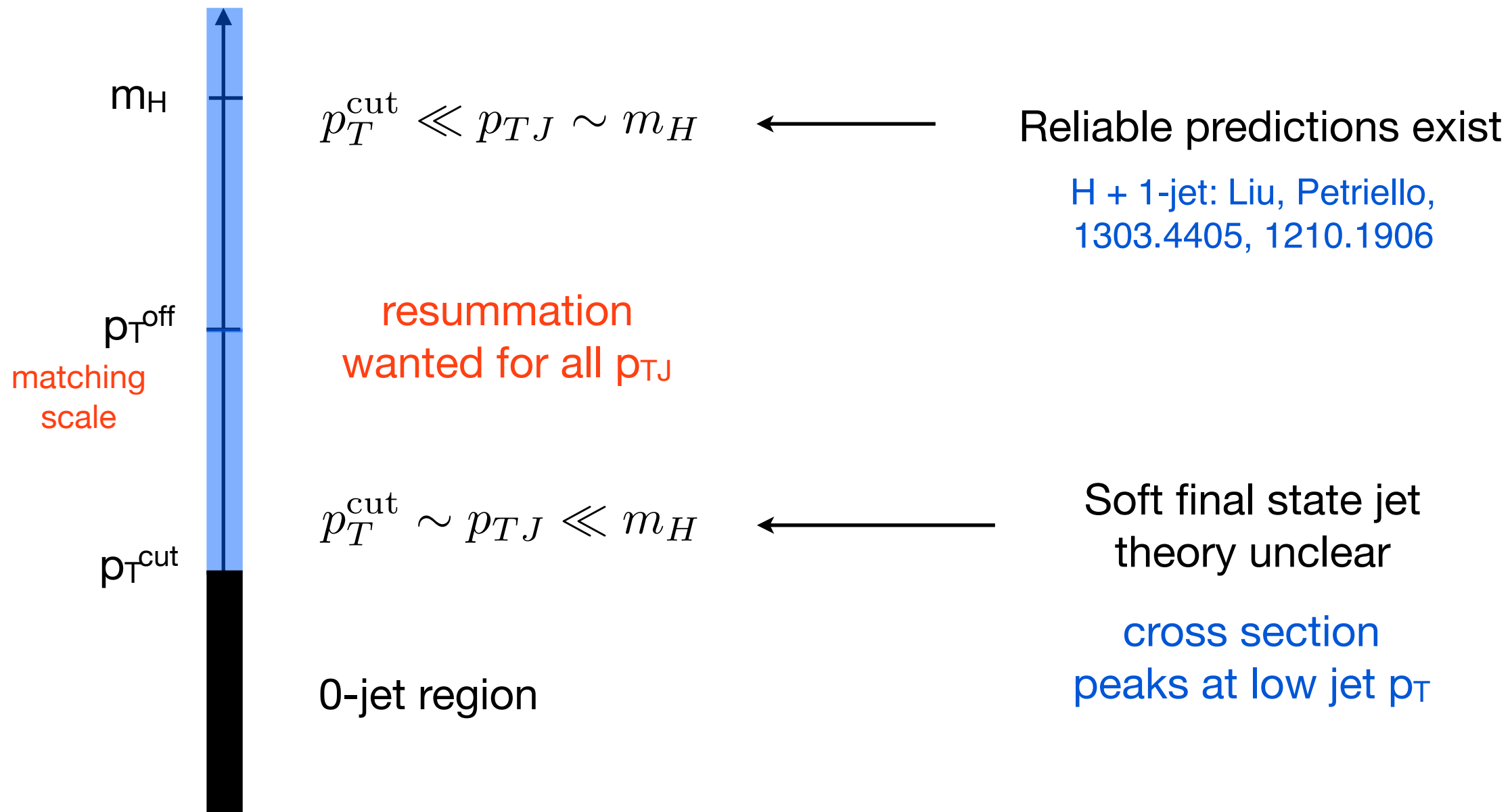
$$p_T^{\text{cut}} \ll m_H$$

what regime is p_{TJ} in?

theory framework for the 1-jet cross section

exclusive 1-jet cross section

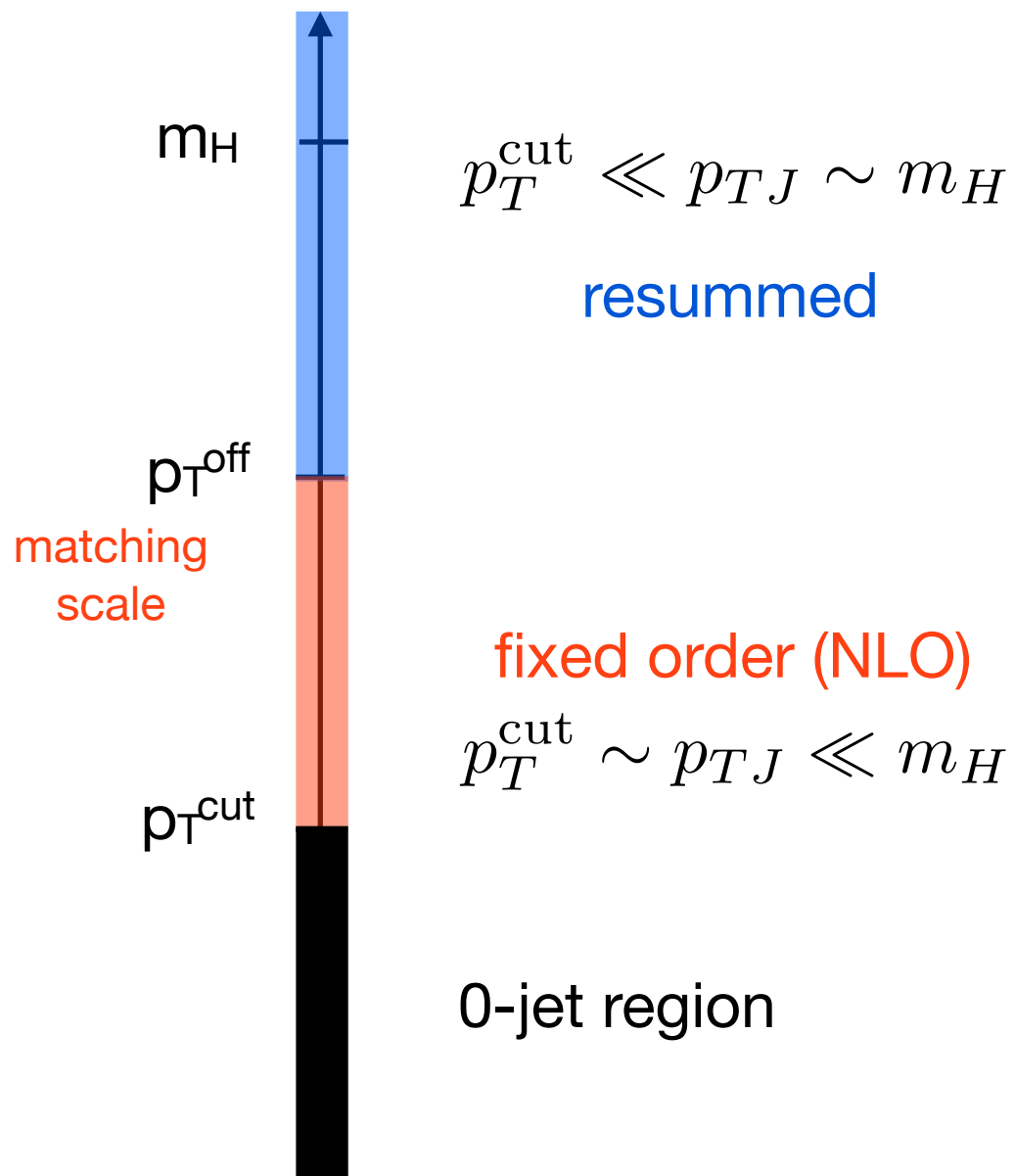
p_{TJ} : leading jet p_T



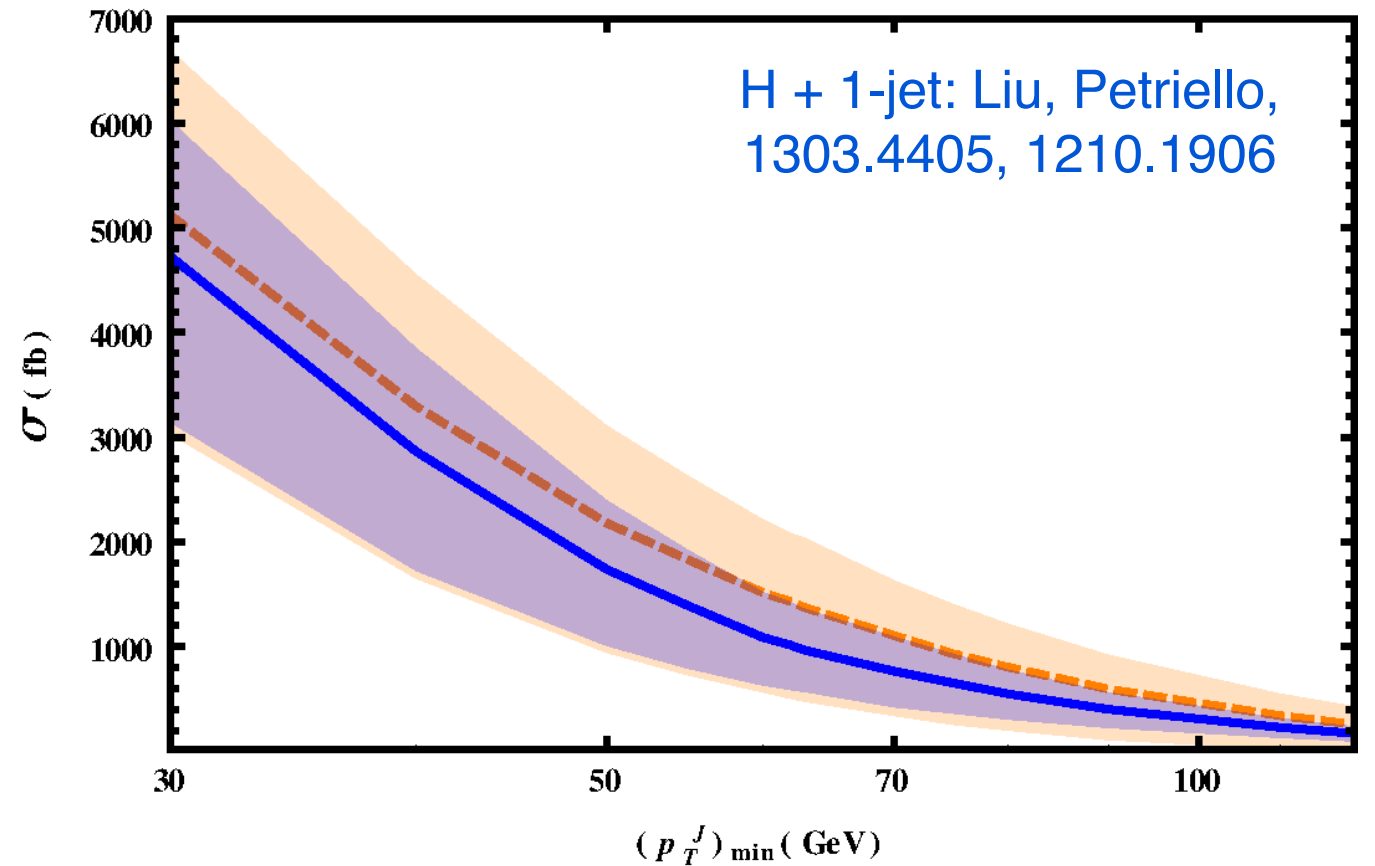
theory framework for the 1-jet cross section

exclusive 1-jet cross section

p_{TJ} : leading jet p_T



direct approach

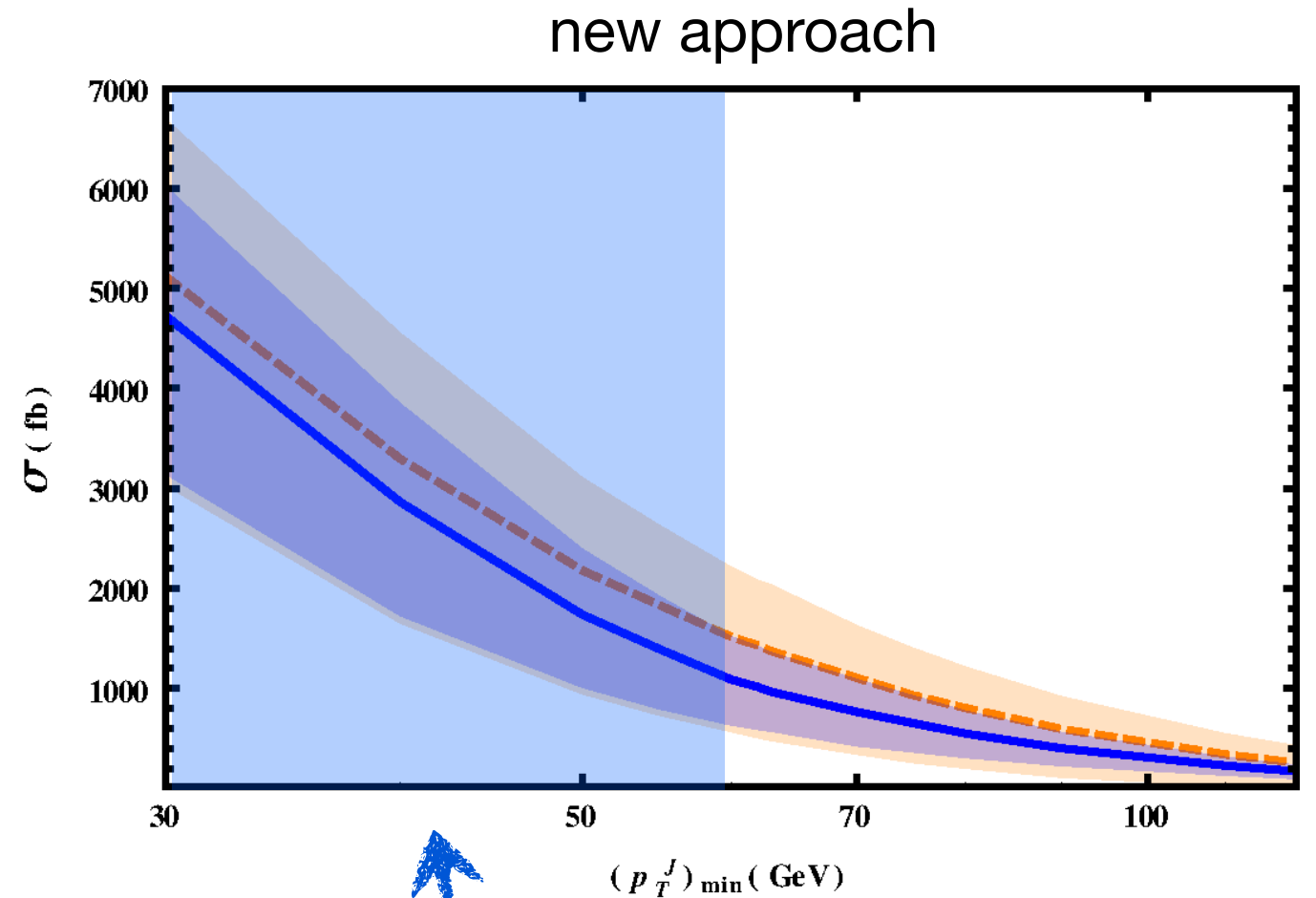
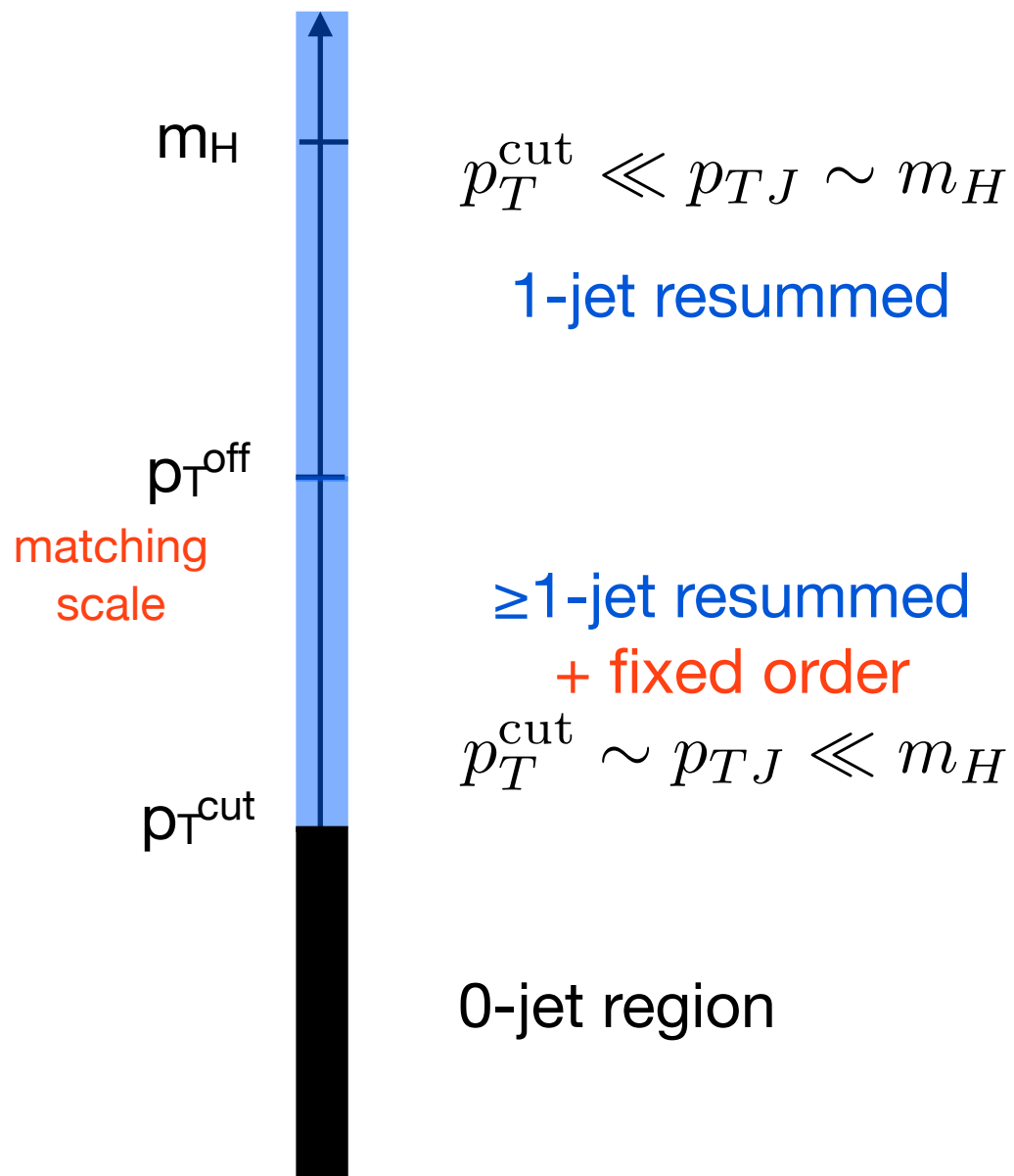


match onto fixed order at low jet p_T
 large logarithms remain

theory framework for the 1-jet cross section

exclusive 1-jet cross section

p_{TJ} : leading jet p_T



use inclusive 1-jet resummation
+ fixed order correction

$$\sigma_1 = \sigma_{\geq 1} - \sigma_{\geq 2}$$

using the inclusive 1-jet cross section

relation for exclusive 1-jet cross section in bin $[p_T^{\text{cut}}, p_T^{\text{off}}]$:

$$\sigma_1([p_T^{\text{cut}}, p_T^{\text{off}}]; p_T^{\text{cut}}) = \underbrace{[\sigma_{\geq 1}(p_T^{\text{cut}}) - \sigma_{\geq 1}(p_T^{\text{off}})]}_{\text{1-jet inclusive terms}} - \underbrace{[\sigma_{\geq 2}(p_T^{\text{cut}}, p_T^{\text{cut}}) - \sigma_{\geq 2}(p_T^{\text{off}}, p_T^{\text{cut}})]}_{\text{2-jet inclusive terms}}$$

↑
inclusive 1-jet resummation

↑
inclusive 2-jet fixed order

indirect contribution: $p_T^{\text{cut}} < p_{TJ} < p_T^{\text{off}}$

1-jet inclusive resummation
+ fixed order correction

direct contribution: $p_T^{\text{off}} < p_{TJ}$

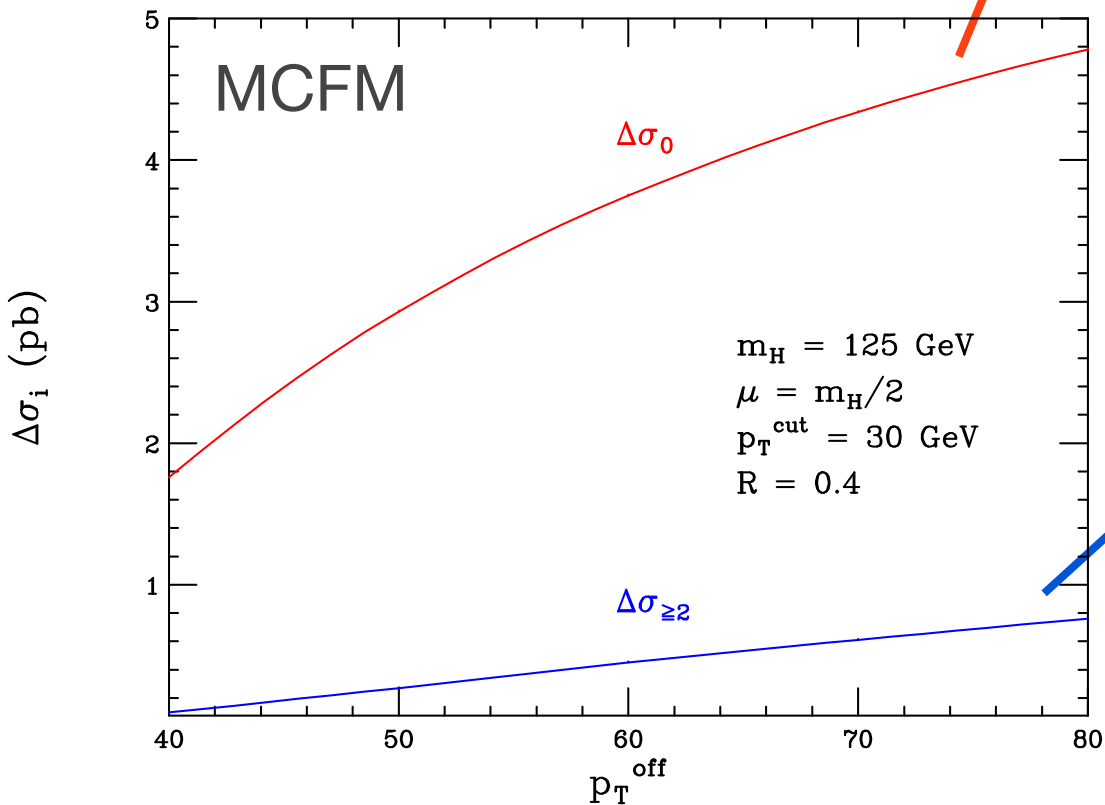
resummed prediction
from Boughezal, Liu, Petriello

using the inclusive 1-jet cross section

relation for exclusive 1-jet cross section in bin $[p_T^{\text{cut}}, p_T^{\text{off}}]$:

$$\sigma_1([p_T^{\text{cut}}, p_T^{\text{off}}]; p_T^{\text{cut}}) = \underbrace{[\sigma_{\geq 1}(p_T^{\text{cut}}) - \sigma_{\geq 1}(p_T^{\text{off}})]}_{\text{1-jet inclusive terms}} - \underbrace{[\sigma_{\geq 2}(p_T^{\text{cut}}, p_T^{\text{cut}}) - \sigma_{\geq 2}(p_T^{\text{off}}, p_T^{\text{cut}})]}_{\text{2-jet inclusive terms}}$$

indirect contribution
fixed order comparison

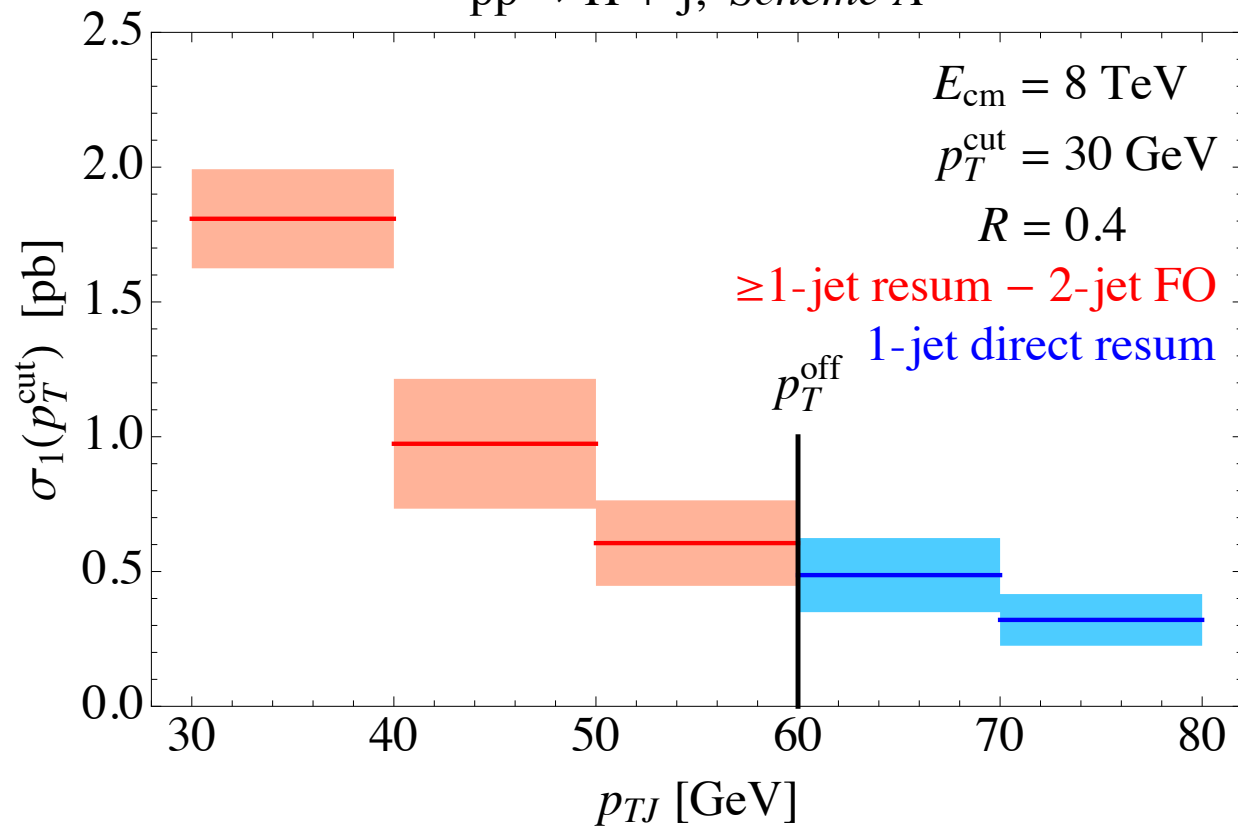


2-jet corrections are small
(LO shown)

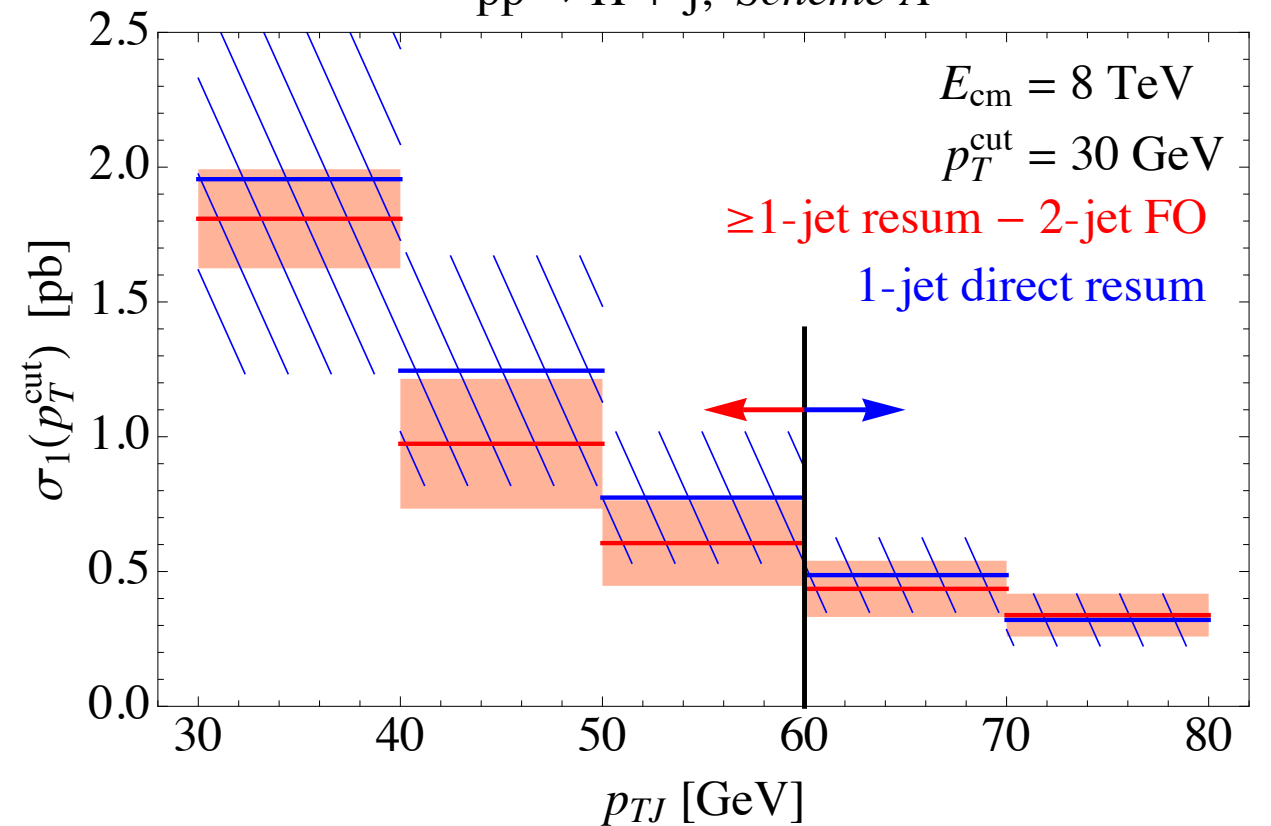
matching the direct and indirect contributions

scheme A: π^2 resummation, H + 1j NNLO virtuals

pp \rightarrow H + j, Scheme A



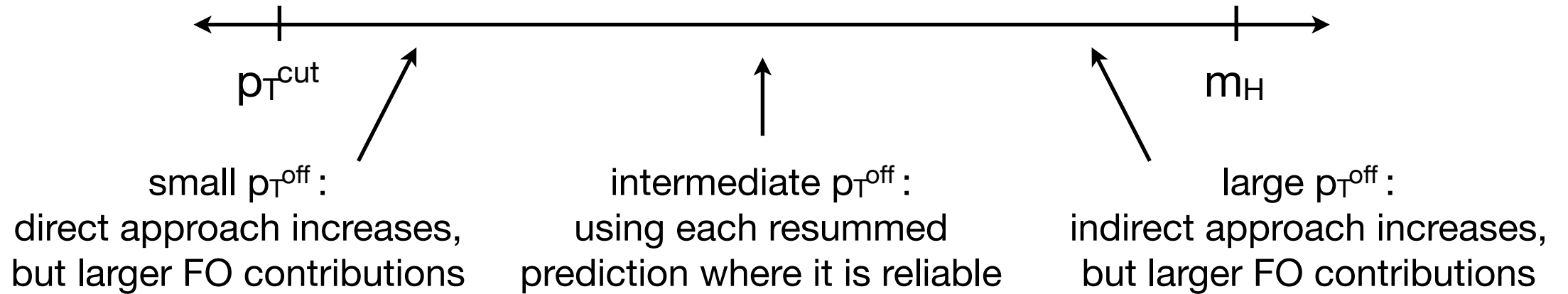
pp \rightarrow H + j, Scheme A



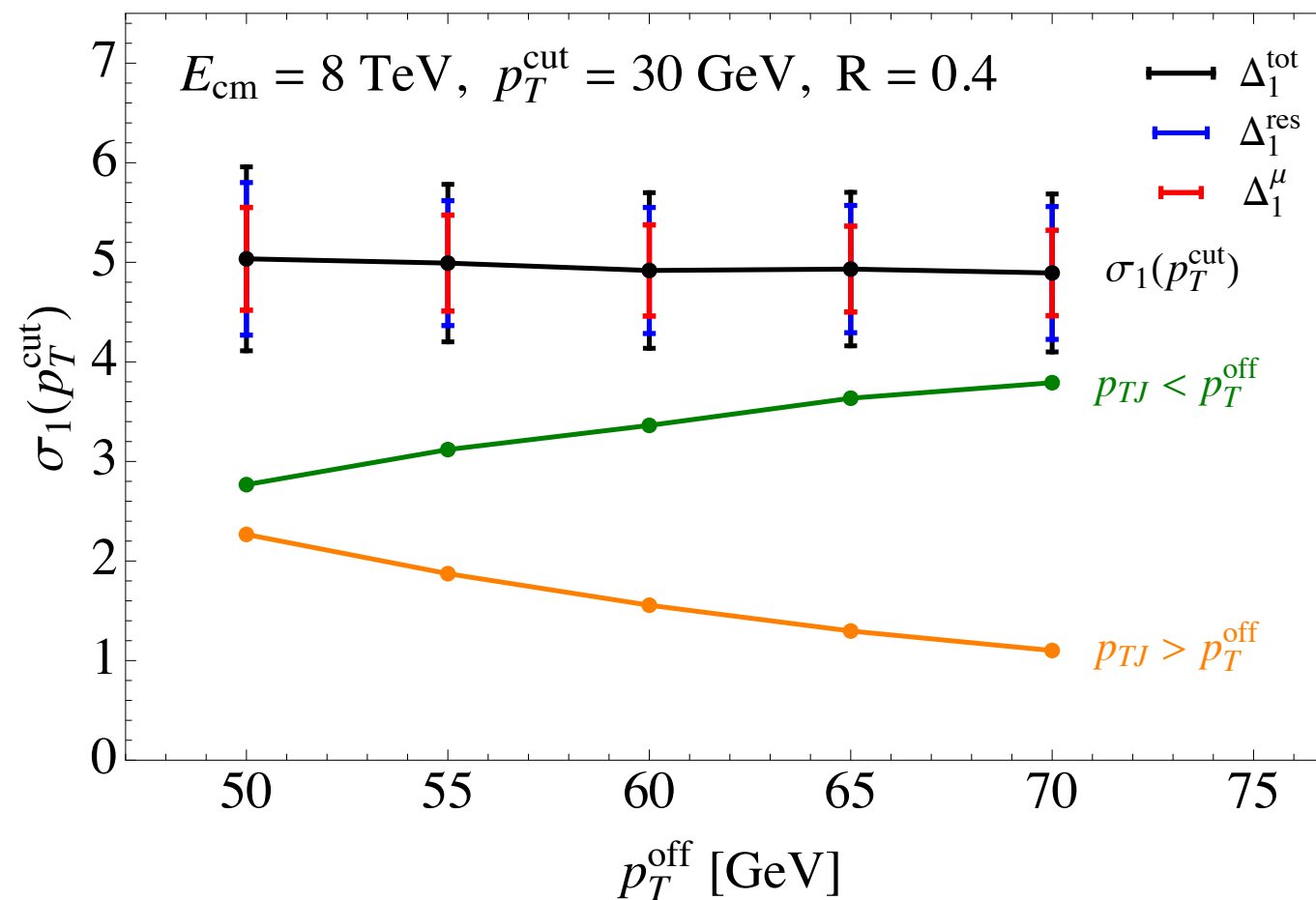
matching of the direct and indirect approaches is smooth across p_T^{cut}

indirect approach lowers the uncertainties in the low p_T regime

testing the matching



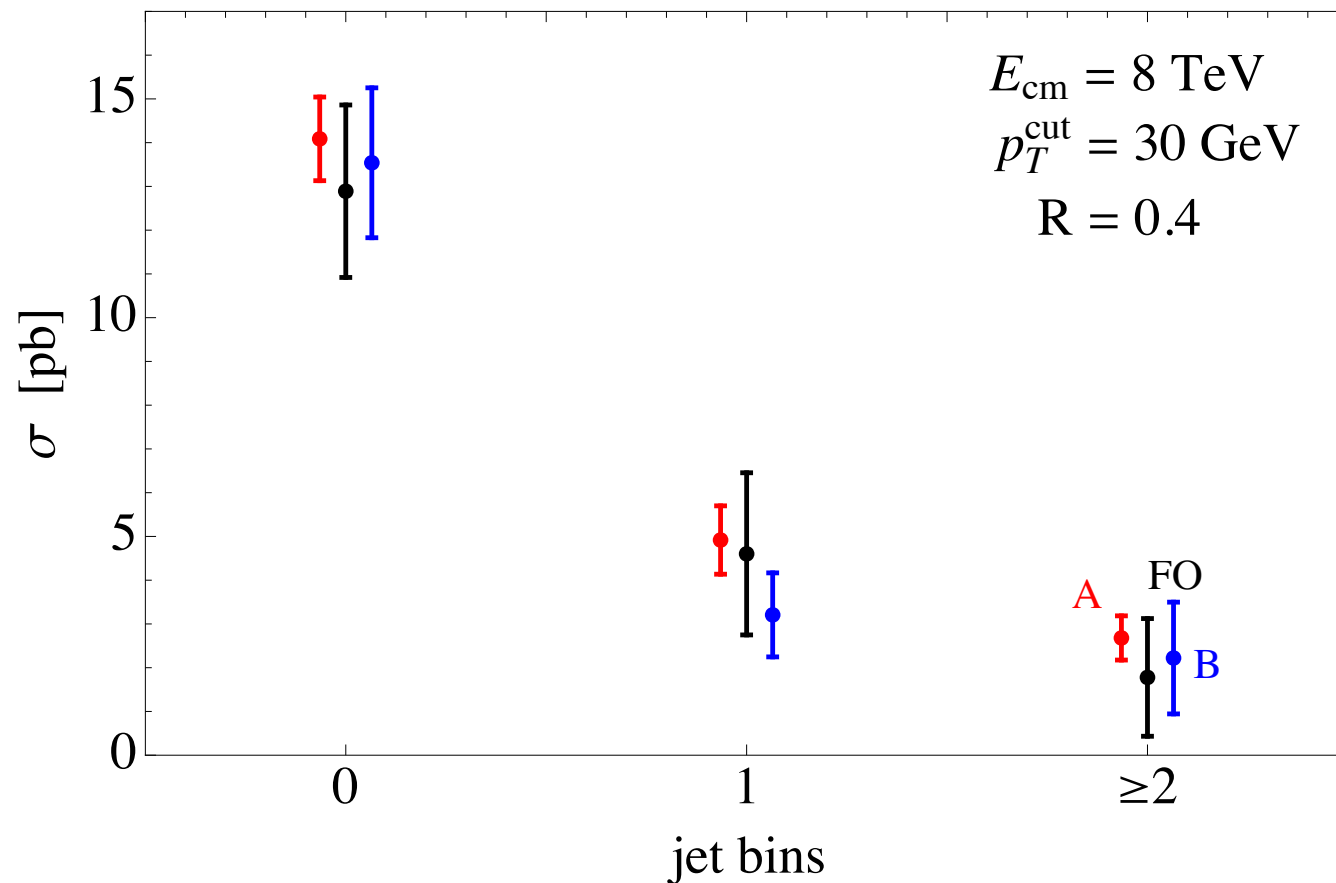
$pp \rightarrow H + j$, *Scheme A*



Matching scale (p_T^{off}) dependence is small

combination of jet bins

cross section in jet bins



bin-by-bin uncertainties reduced
by a factor of 2 over FO

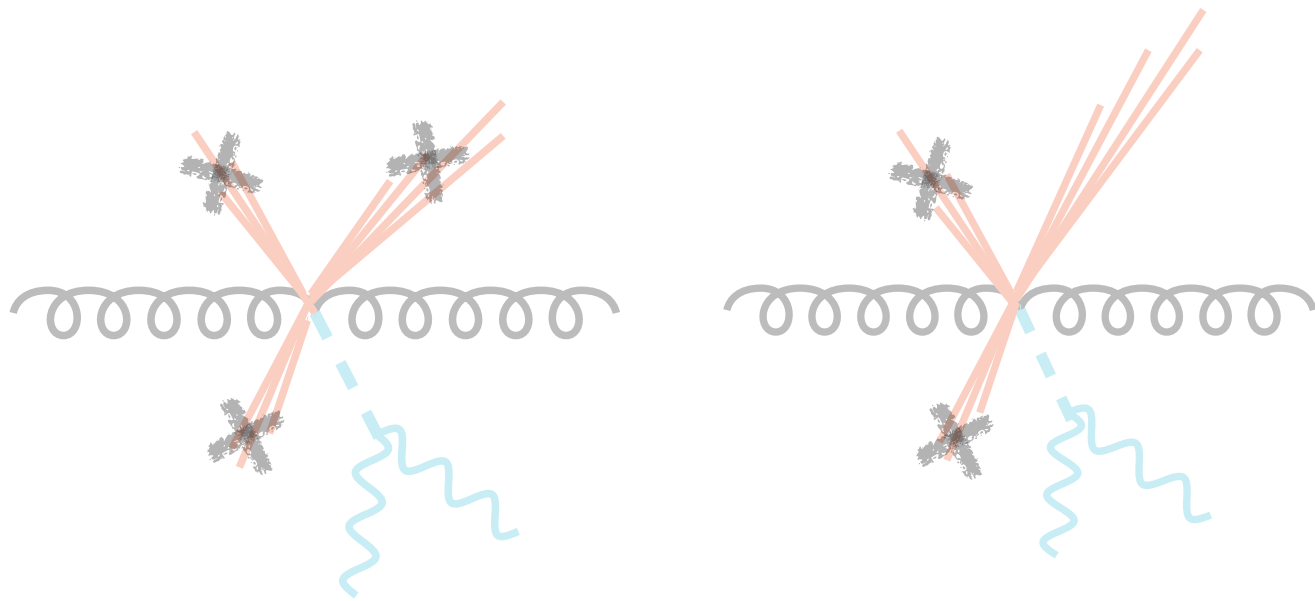
cross section in the WW analysis

$$\sigma_{WW} = \epsilon_0^{\text{acc}} \sigma_0 + \epsilon_1^{\text{acc}} \sigma_1 + \epsilon_{\geq 2}^{\text{acc}} \sigma_{\geq 2}$$

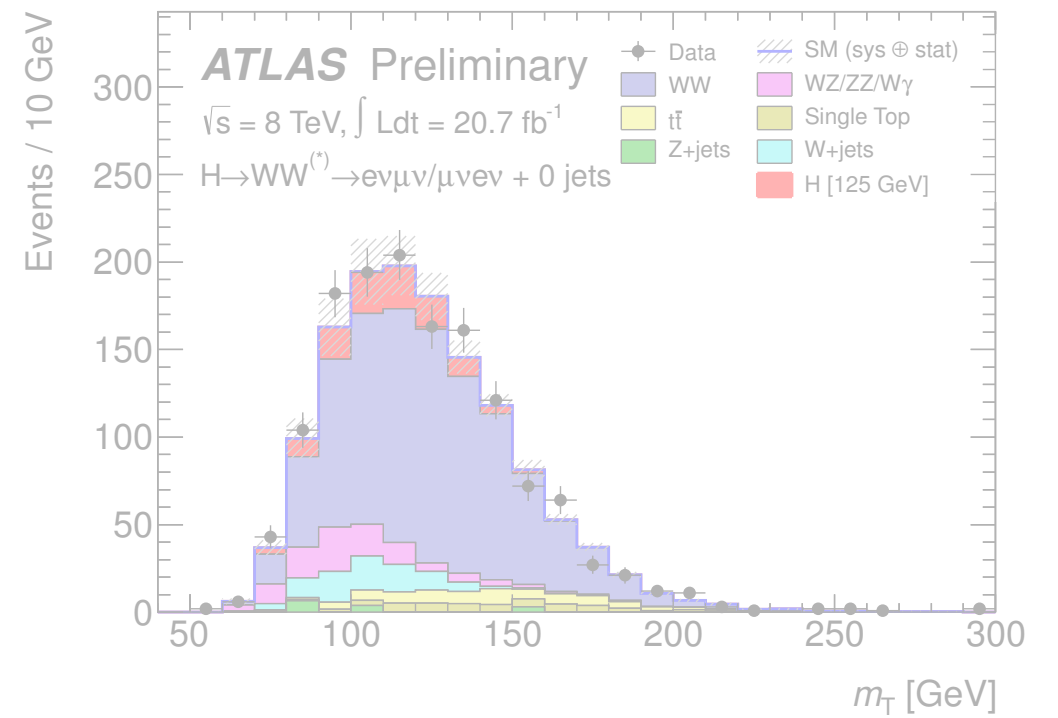
acceptances from analysis cuts
(jet bin cuts, leptonic cuts,
reconstruction efficiencies)

need to determine
the theoretical uncertainty
on this cross section

The precision frontier and the Higgs



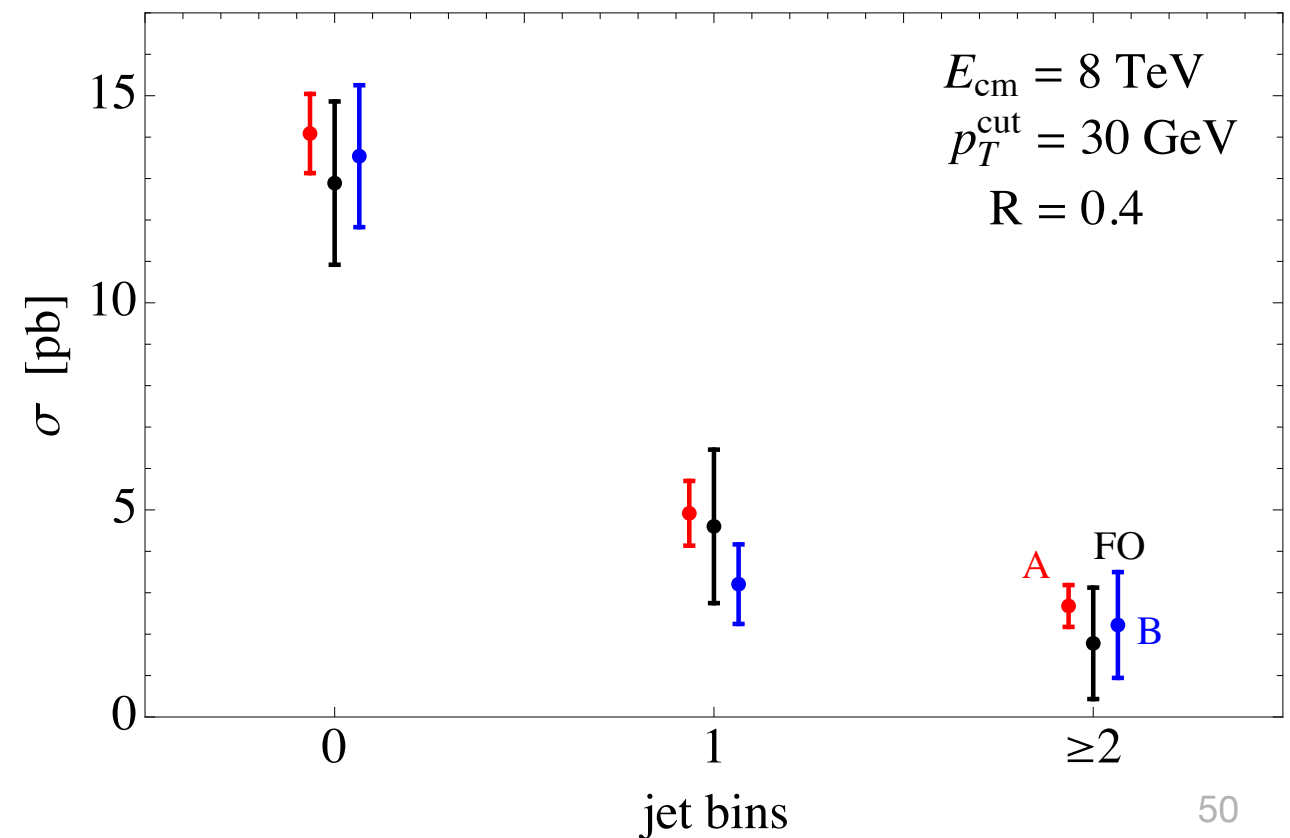
Implementation and future work



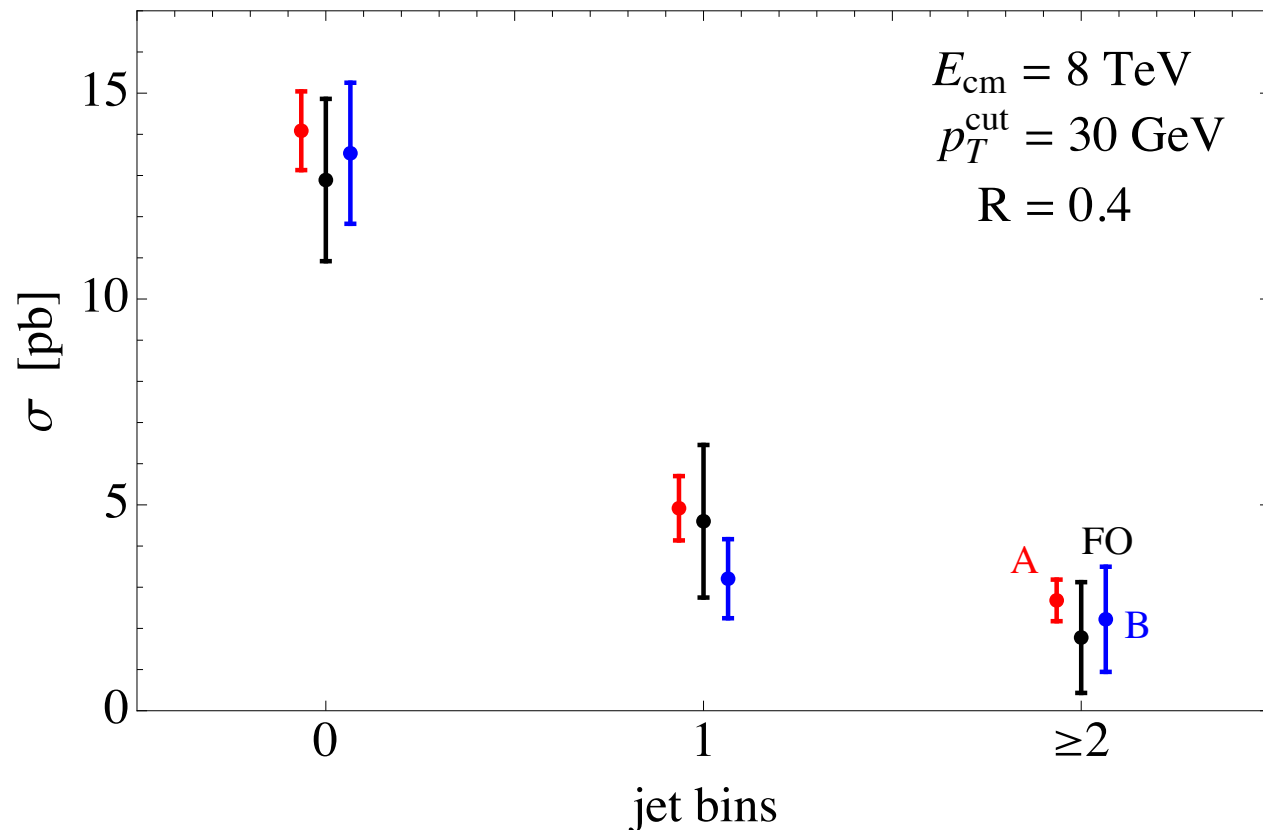
Exclusive jet cross sections

Stewart, Tackmann, JW, Zuberi, 1307.1808
 Boughezal, Liu, Petriello, Tackmann, JW, 1312.4535

cross section in jet bins



cross section in jet bins



how do we implement the resummed results to improve the uncertainties in an analysis?

Considerations:

- Need correlations between jet bins to propagate uncertainties
- A common framework to implement jet bin correlations desirable
- Fixed order results can be implemented in a Monte Carlo framework
 - Allows to propagate jet binning uncertainties through the leptonic cuts to get correlations

correlations between jet bins

We can construct the 0-jet, 1-jet, and 2-jet inclusive covariance matrix

This is part of the goal of making a combined 0-jet / 1-jet prediction

yield and migration components: $C = C_y + C_{\text{cut}}$

fully correlated

$$C_y = \vec{\Delta}_y \vec{\Delta}_y^T$$

yield uncertainty

anti-correlated
2x2 blocks

$$C_{\text{cut}} = \sum_{i,j} \begin{pmatrix} \Delta_{ij \text{ cut}}^2 & -\Delta_{ij \text{ cut}}^2 \\ -\Delta_{ij \text{ cut}}^2 & \Delta_{ij \text{ cut}}^2 \end{pmatrix}_{ij}$$

can directly connect these uncertainty components to nuisance parameters used in the analysis fit

bin migration uncertainty

We determine these covariance matrix entries from 3 sources:

1. Uncertainty components of the 0-jet calculation
2. 0-jet and direct 1-jet uncertainty components in the 1-jet bin
3. Closure relations for the total cross section (e.g., $\Delta_{\text{tot}}^y = \Delta_0^y + \Delta_1^y + \Delta_{\geq 2}^y$)

correlations between jet bins

We can construct the 0-jet, 1-jet, and 2-jet inclusive covariance matrix
 This is part of the goal of making a combined 0-jet / 1-jet prediction

yield and migration components: $C = C_y + C_{\text{cut}}$ can directly connect these uncertainty components to nuisance parameters used in the analysis fit

fully correlated

$$C_y = \vec{\Delta}_y \vec{\Delta}_y^T \quad \text{yield uncertainty}$$

anti-correlated
2x2 blocks

$$C_{\text{cut}} = \sum_{i,j} \begin{pmatrix} \Delta_{ij \text{ cut}}^2 & -\Delta_{ij \text{ cut}}^2 \\ -\Delta_{ij \text{ cut}}^2 & \Delta_{ij \text{ cut}}^2 \end{pmatrix}_{ij}$$

bin migration uncertainty

fixed order vs. resummed uncertainties for ATLAS parameters

$$\left\{ \begin{array}{l} C_{\text{FO}}^{\text{ATLAS}} = \begin{pmatrix} 4.24 & -1.99 & 0 \\ -1.99 & 5.23 & -3.24 \\ 0 & -3.24 & 3.24 \end{pmatrix} \text{ pb}^2 \\ C^{\text{ATLAS}} = \begin{pmatrix} 1.49 & -0.39 & 0.20 \\ -0.39 & 0.88 & -0.04 \\ 0.20 & -0.04 & 0.32 \end{pmatrix} \text{ pb}^2 \end{array} \right.$$

the Higgs signal strength

fixed order vs. resummed uncertainties for ATLAS parameters

$$C_{\text{FO}}^{\text{ATLAS}} = \begin{pmatrix} 4.24 & -1.99 & 0 \\ -1.99 & 5.23 & -3.24 \\ 0 & -3.24 & 3.24 \end{pmatrix} \text{ pb}^2$$

$$C^{\text{ATLAS}} = \begin{pmatrix} 1.49 & -0.39 & 0.20 \\ -0.39 & 0.88 & -0.04 \\ 0.20 & -0.04 & 0.32 \end{pmatrix} \text{ pb}^2$$

signal strength: $\mu = \frac{\sigma_{\text{obs}}}{\sigma_{\text{exp}}}$

$$\sigma_{\text{exp}} = \epsilon_0^{\text{exp}} \sigma_0^{\text{exp}} + \epsilon_1^{\text{exp}} \sigma_1^{\text{exp}} + \epsilon_{\geq 2}^{\text{exp}} \sigma_{\geq 2}^{\text{exp}}$$

Table 13: Leading uncertainties on the signal strength μ for the combined 7 and 8 TeV analysis.

Category	Source	Uncertainty, up (%)	Uncertainty, down (%)
Statistical	Observed data	+21	-21
Theoretical	Signal yield ($\sigma \cdot \mathcal{B}$)	+12	-9
Theoretical	WW normalisation	+12	-12
Experimental	Objects and DY estimation	+9	-8
Theoretical	Signal acceptance	+9	-7
Experimental	MC statistics	+7	-7
Experimental	W+ jets fake factor	+5	-5
Theoretical	Backgrounds, excluding WW	+5	-4
Luminosity	Integrated luminosity	+4	-4
Total		+32	-29

naive estimates suggest the signal strength uncertainty will be nearly halved

implementation of resummed results being studied within Higgs cross section working group

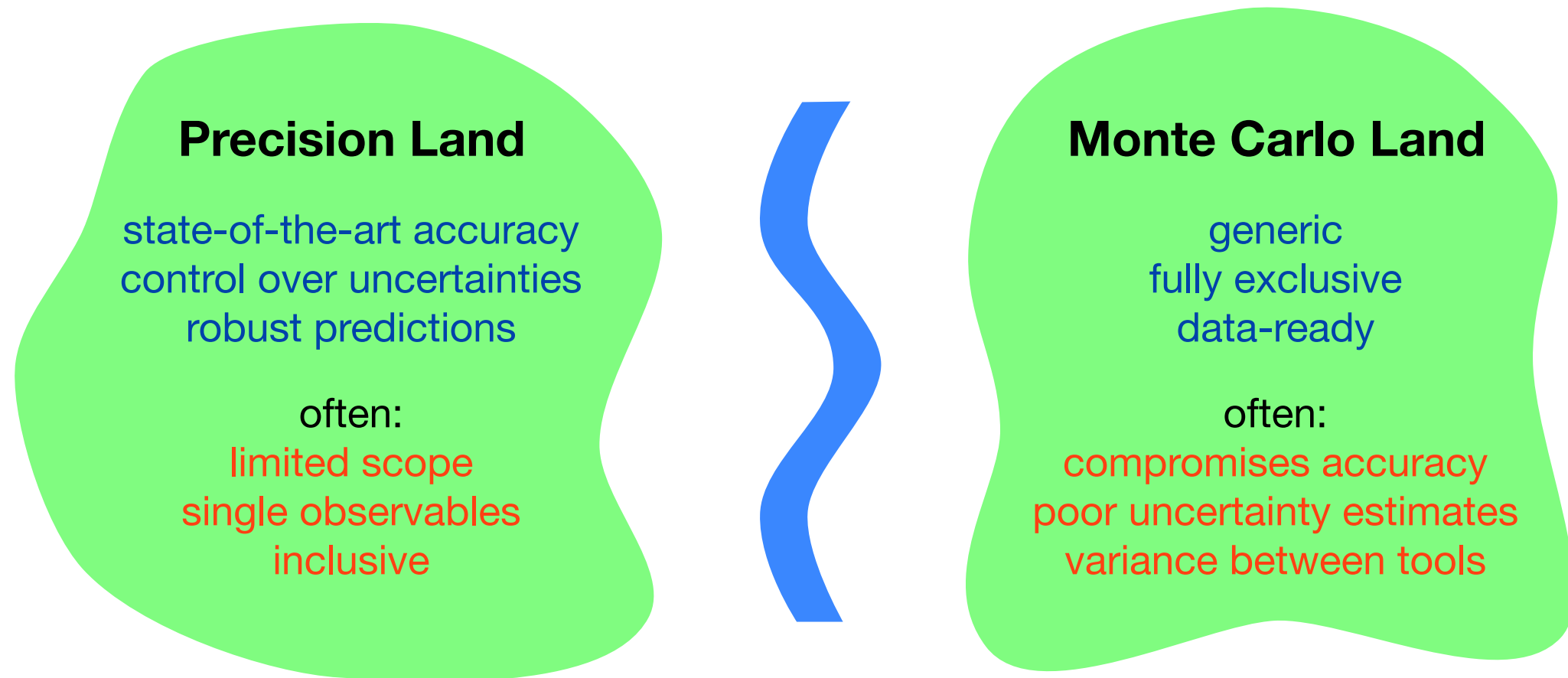
recent work on (p_T) jet vetoes

H + 0 jets	Banfi, Monni, Salam, Zanderighi - 1203.5773, 1206.4996, 1308.4634 (also Z + 0 jets)
	Becher, Neubert, Rothen - 1205.3806, 1307.0025
	Stewart, Tackmann, JW, Zuberi - 1307.1808 (also 1206.4312, TWZ)
H + 1 jet	Liu, Petriello - 1210.1906, 1303.4405
	Boughezal, Liu, Petriello, Tackmann, JW (H + 0/1-jet) 1312.4535
H + 2 jets	Gangal, Tackmann (fixed order uncertainties) - 1302.5437
VH + 0 jets	(Chong Sheng) Li, (Hai Tao) Li, Shao - 1309.5015
	(Ye) Li, Liu - 1401.2149
clustering effects	Alioli, JW - 1311.5234

future directions in jet vetoes

- Many analyses use jet binning, often with novel features:
 - WW - interesting SM measurement, a leading uncertainty in $H \rightarrow WW$ NNLO will be finished soon, offers jump in precision
 - VH with $H \rightarrow bb$ - combines substructure and jet vetoes, would also like to understand $V + \text{jets}$ background
 - $gg \rightarrow H$ in VBF topology - large uncertainties on the contamination, needs good theory development for forward jets
 - $tt + \text{jets}$ - large logarithms and a gluon initiated process, complex phase space
- Interfacing high order resummation into a fully differential Monte Carlo (Geneva)
 - Possibility to produce state-of-the-art predictions with fully exclusive generator
- Additional precision in gluon fusion possible
 - Requires 3-loop calculations, matching with $H + 1\text{-jet}$ at NNLO
Phenomenologically less urgent, but offers many, many interesting theory aspects

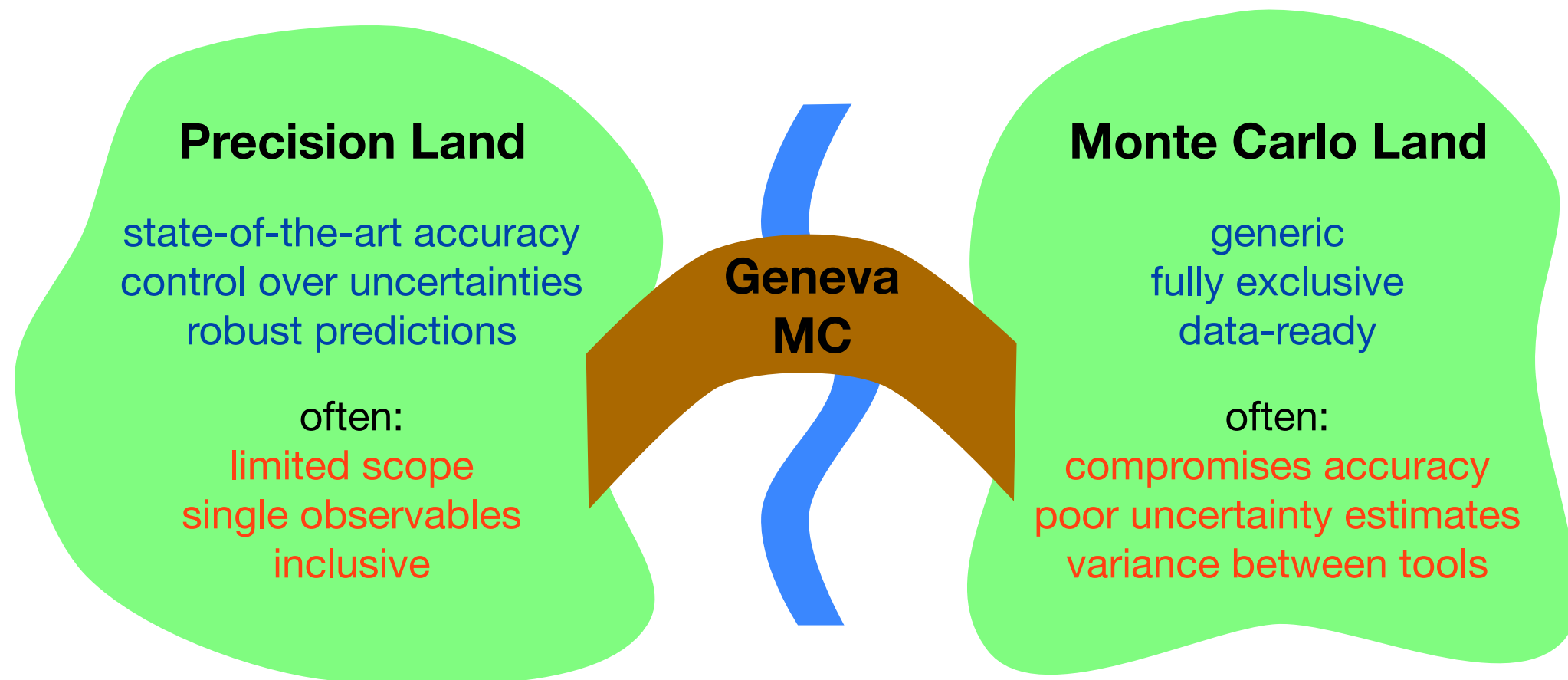
precision Monte Carlo



compromise is necessary in each case,
but progress is being made in merging the two:
Monte Carlo generators with high perturbative/resummed accuracy
that are capable of giving robust uncertainty estimates

this is not a panacea, but is a leap forward for many applications

precision Monte Carlo



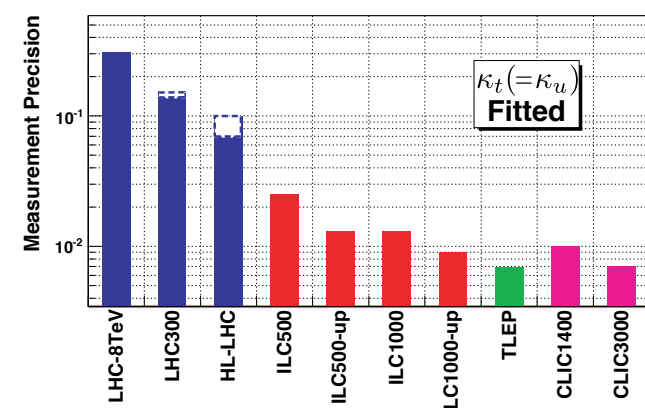
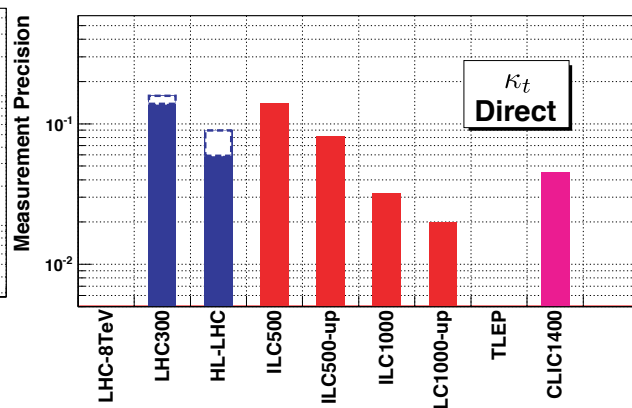
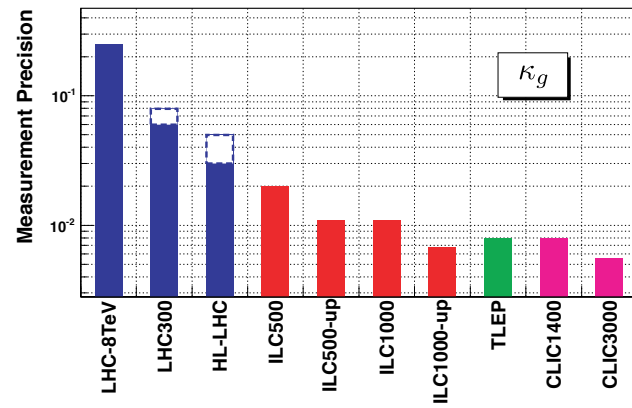
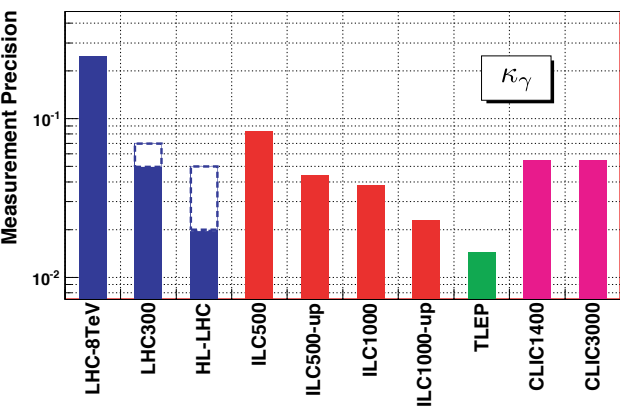
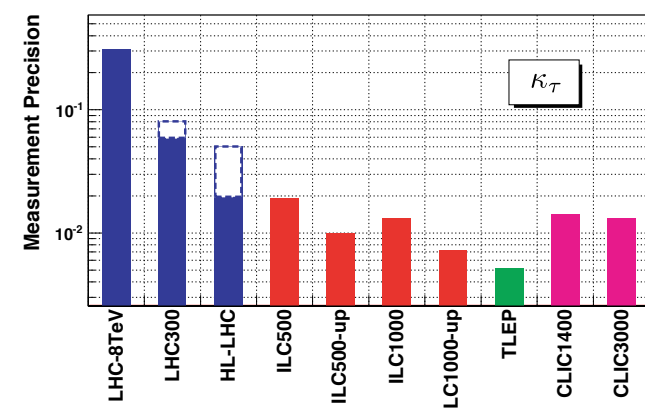
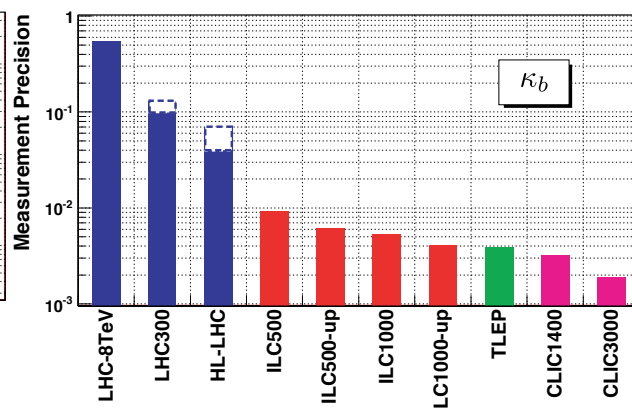
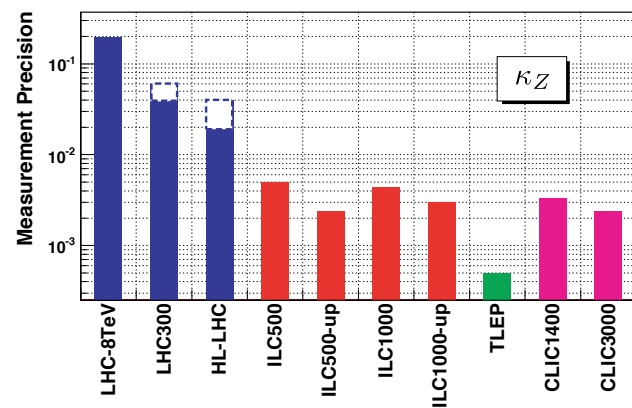
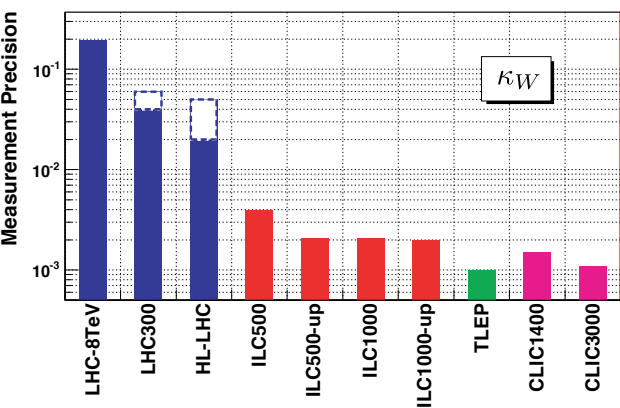
compromise is necessary in each case,
but progress is being made in merging the two:
Monte Carlo generators with high perturbative/resummed accuracy
that are capable of giving robust uncertainty estimates

this is not a panacea, but is a leap forward for many applications

Conclusions

- Precision QCD brings powerful, modern tools to bear on Higgs measurements and beyond
 - Crucial to get the most from the LHC program
 - Broad development of tools impact experimental program
- Resummed results for exclusive H + 0-jet and 1-jet cross sections significantly lower uncertainties over fixed order
 - Expect the use of resummed results by H \rightarrow WW, other analyses
 - Jet vetoes are a broadly interesting, useful area
- Work on jet physics can push the boundaries of precision, discovery

Extra Slides



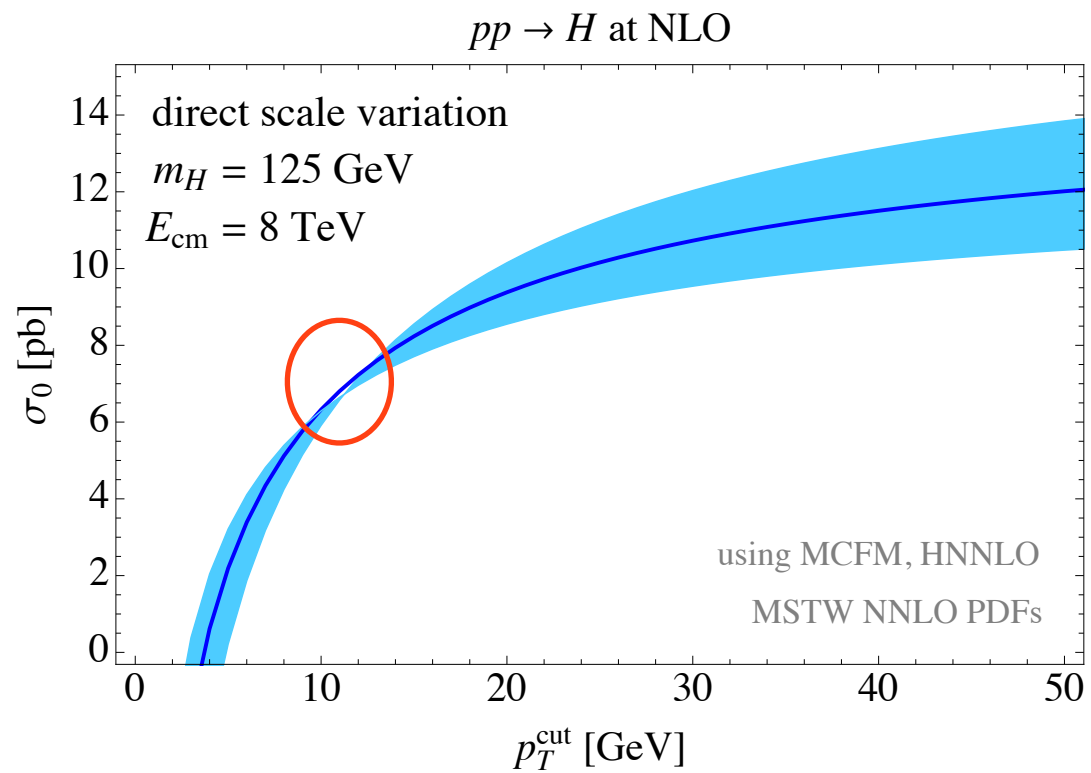
$\int \mathcal{L} dt$ (fb ⁻¹)	Higgs decay final state							
	$\gamma\gamma$	WW^*	ZZ^*	$b\bar{b}$	$\tau\tau$	$\mu\mu$	$Z\gamma$	BR_{inv}
ATLAS								
300	9 – 14%	8 – 13%	6 – 12%	N/A	16 – 22%	38 – 39%	145 – 147%	< 23 – 32%
3000	4 – 10%	5 – 9%	4 – 10%	N/A	12 – 19%	12 – 15%	54 – 57%	< 8 – 16%
CMS								
300	6 – 12%	6 – 11%	7 – 11%	11 – 14%	8 – 14%	40 – 42%	62 – 62%	< 17 – 28%
3000	4 – 8%	4 – 7%	4 – 7%	5 – 7%	5 – 8%	14 – 20%	20 – 24%	< 6 – 17%

Snowmass Higgs report: 1310.8361

ATLAS: range is with/without theory uncertainties

CMS, 2 scenarios:

1. systematics unchanged (from now), taking increased rate into account
2. theory uncertainty halved, others scaled by square root of integrated luminosity



cause of uncertainty pinch:

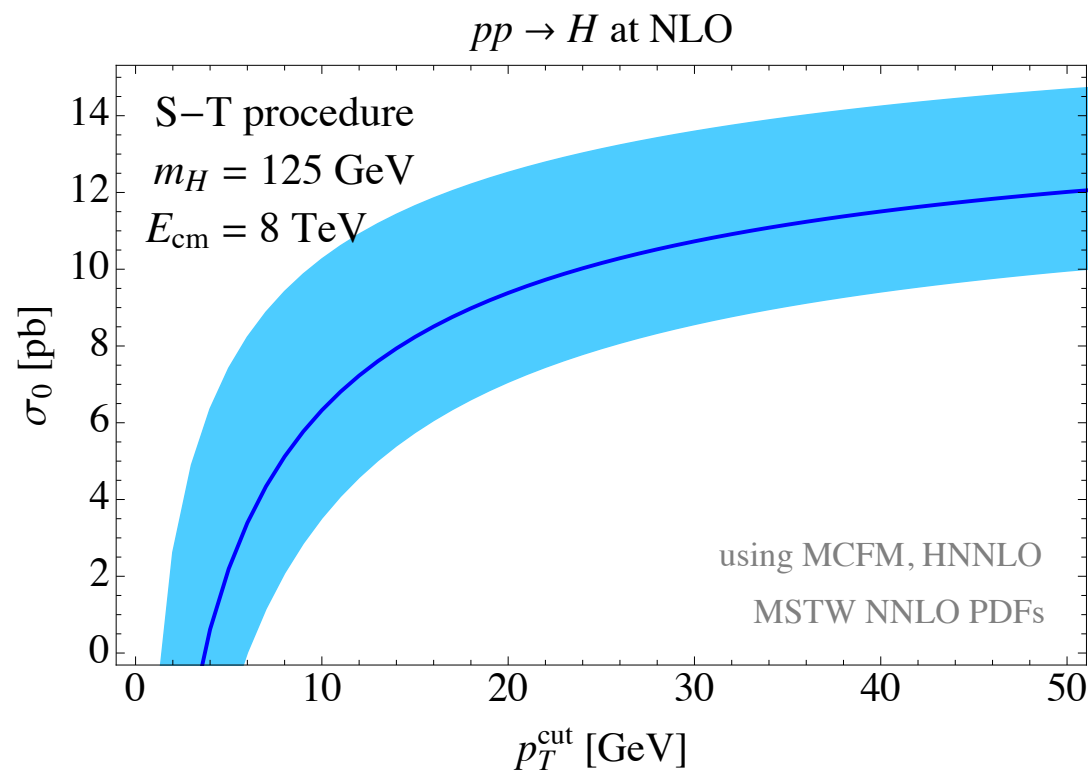
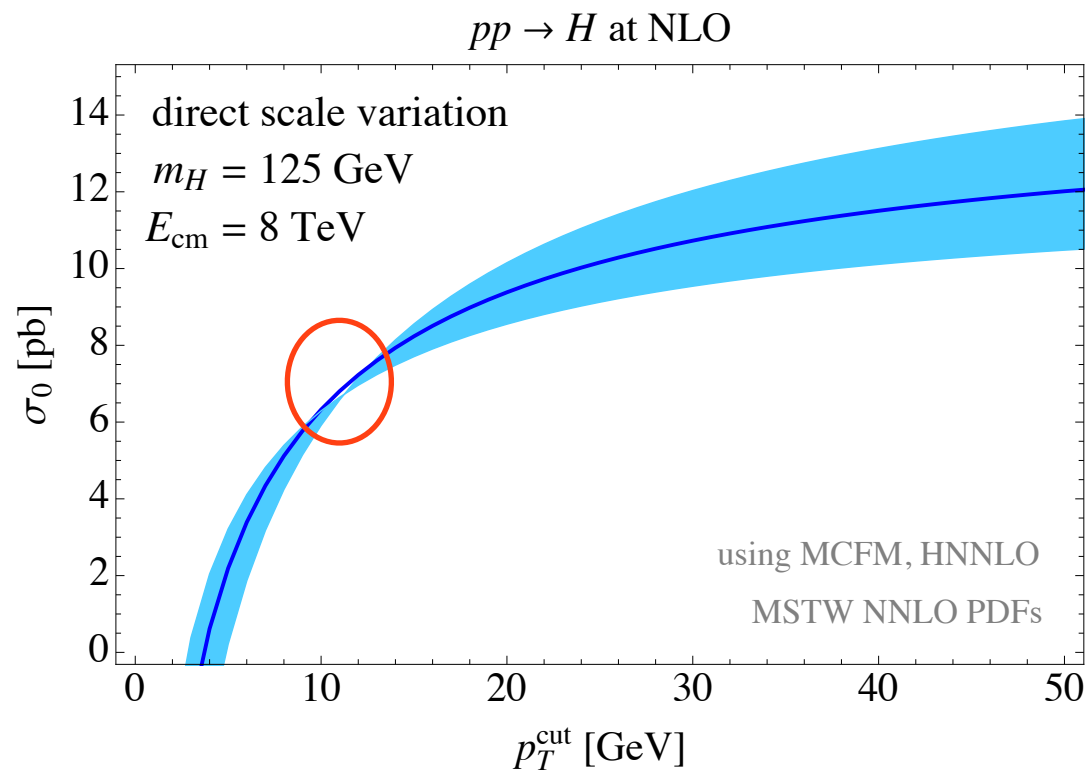
$$\sigma_0(p_T^{\text{cut}}) \propto \sigma_B \left[1 + \frac{\alpha_s}{\pi} \left(K_{\text{NLO}} - 2C_A \ln^2 \frac{m_H}{p_T^{\text{cut}}} \right) + \dots \right]$$

unphysical
cancellation between large **K-factor** and **logs**

part of the
total rate

bin cut between
0 jets, 1+ jets

Stewart, Tackmann,
1107.2117



cause of uncertainty pinch:

$$\sigma_0(p_T^{\text{cut}}) \propto \sigma_B \left[1 + \frac{\alpha_s}{\pi} \left(K_{\text{NLO}} - 2C_A \ln^2 \frac{m_H}{p_T^{\text{cut}}} \right) + \dots \right]$$

unphysical
cancellation between large **K-factor** and **logs**

part of the
total rate

bin cut between
0 jets, 1+ jets

Stewart, Tackmann,
1107.2117

solution: take these sources
of uncertainty as *uncorrelated*

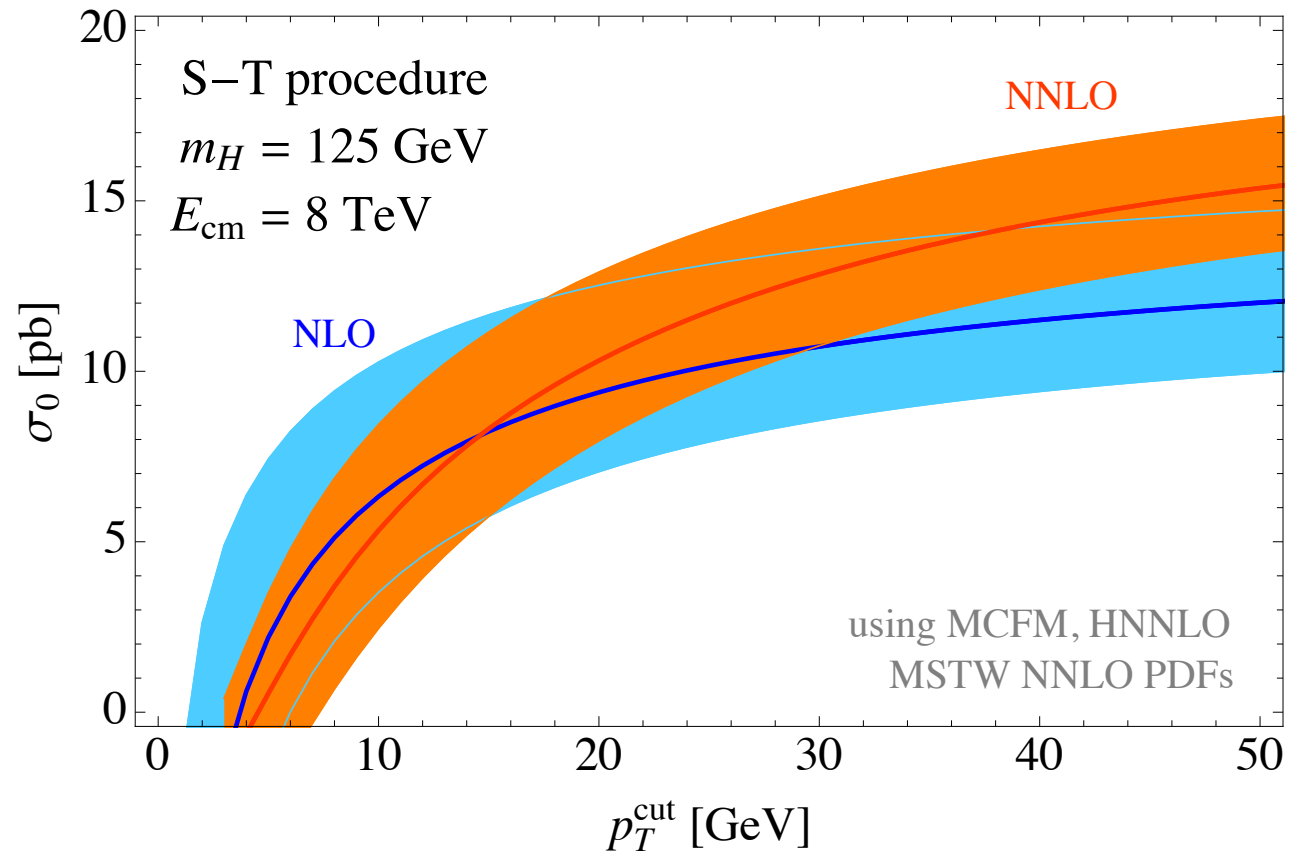
$$\Delta_0(p_T^{\text{cut}})^2 = \Delta_{\geq 0}^2 + \Delta_{\geq 1}(p_T^{\text{cut}})^2$$

robust (if conservative) estimation of
uncertainty across the spectrum

commonly used by ATLAS, CMS

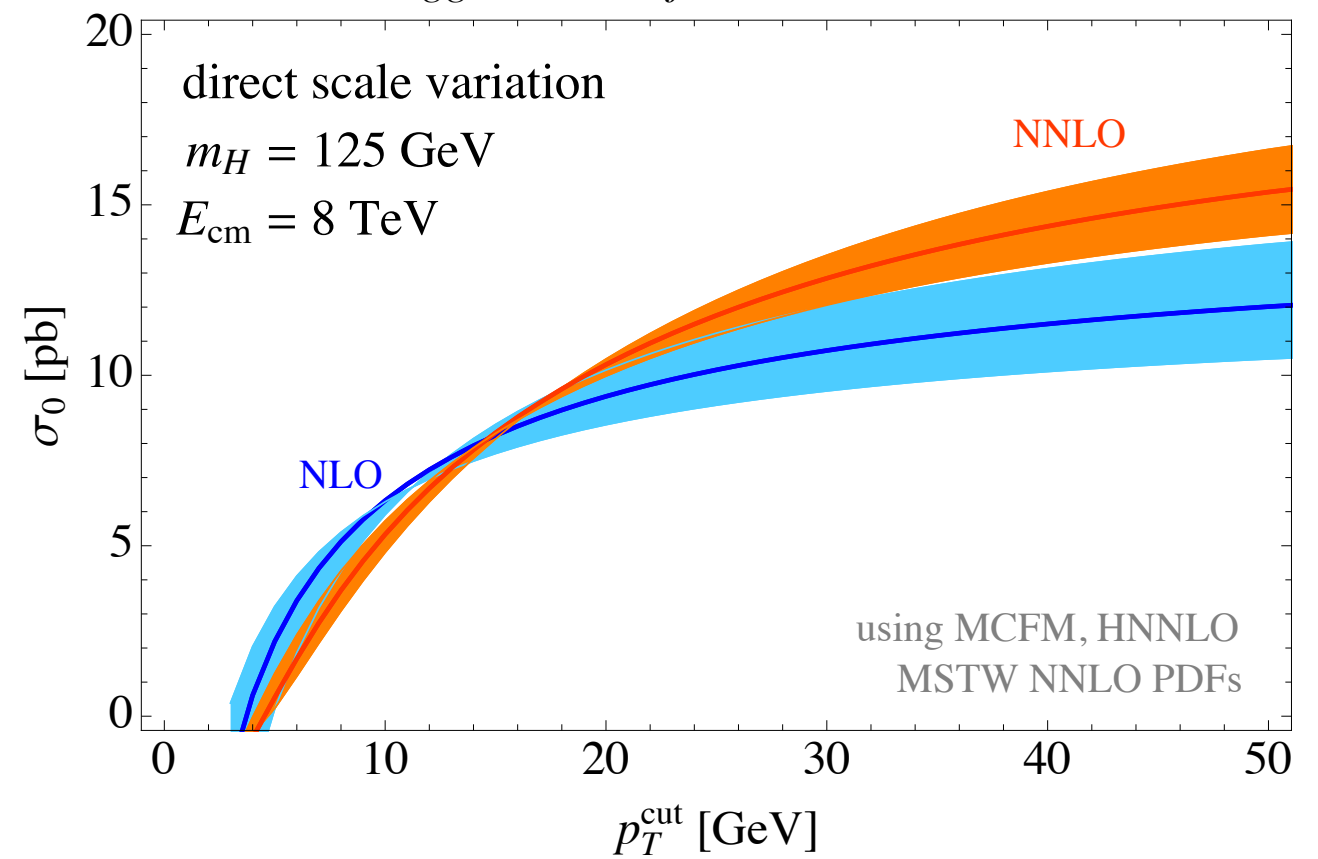
S-T procedure

$gg \rightarrow H + 0 \text{ jets}$ at fixed order

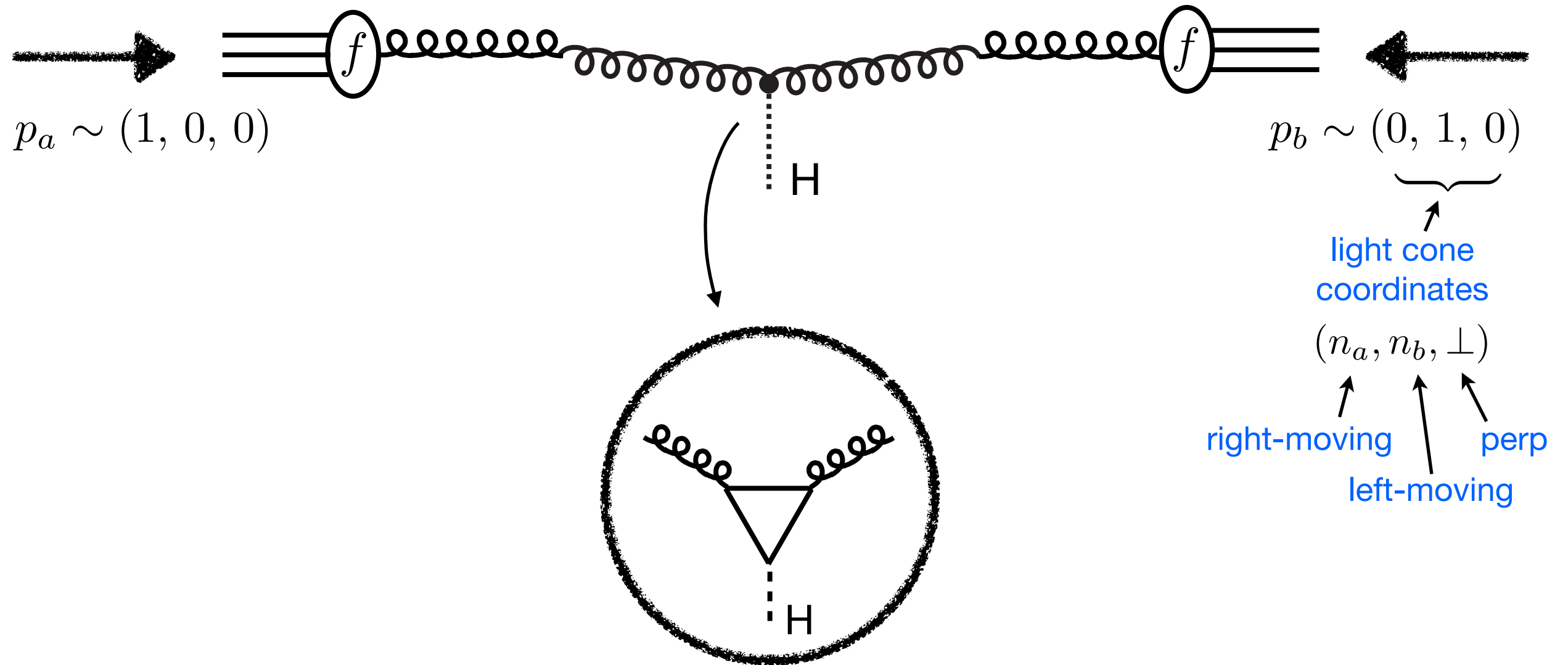


direct SV

$gg \rightarrow H + 0 \text{ jets}$ at fixed order



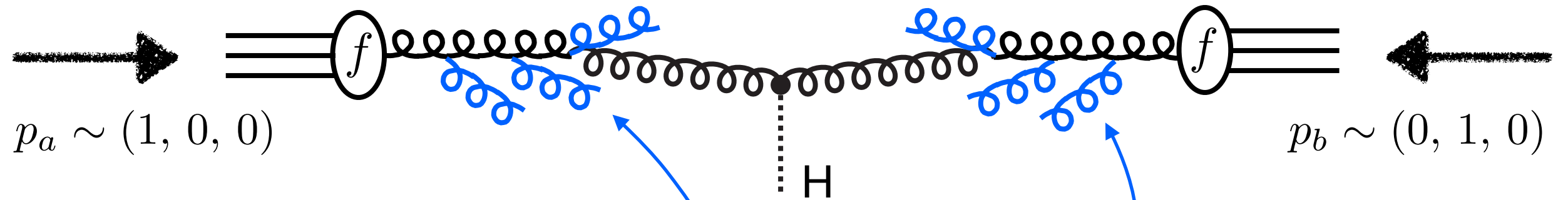
dynamics of Higgs production with 0 jets



short distance process: $gg \rightarrow H$

can integrate out the top quark to produce an effective ggH operator or treat the top exactly

dynamics of Higgs production with 0 jets

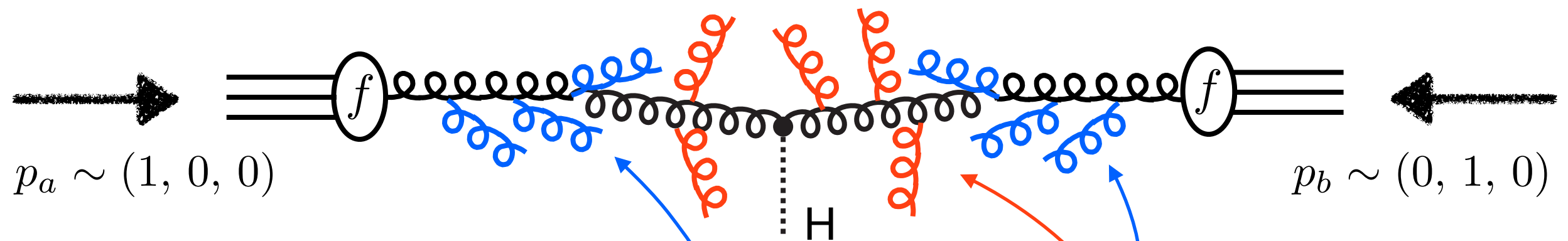


collinear radiation:

$$\begin{cases} p_c \sim m_H(1, \lambda^2, \lambda) \\ p_{\bar{c}} \sim m_H(\lambda^2, 1, \lambda) \end{cases}$$

$\lambda \sim \frac{p_T^{\text{cut}}}{m_H}$: power counting parameter in soft-collinear effective theory (SCET)

dynamics of Higgs production with 0 jets



collinear radiation:

$$\begin{cases} p_c \sim m_H(1, \lambda^2, \lambda) \\ p_{\bar{c}} \sim m_H(\lambda^2, 1, \lambda) \end{cases}$$

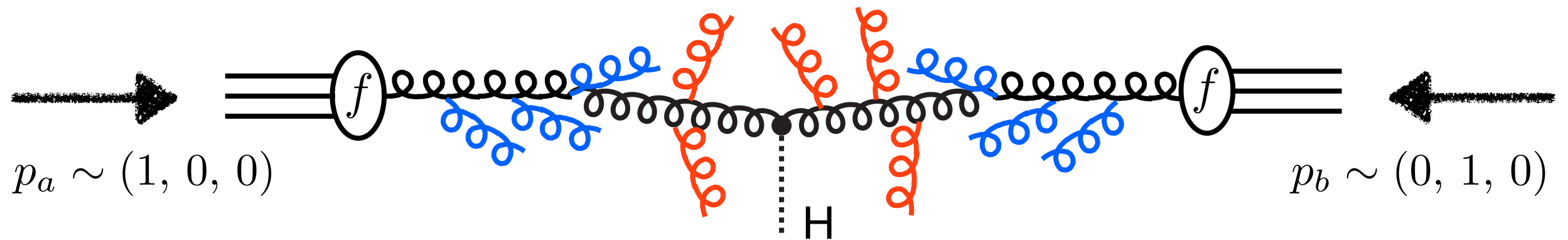
soft radiation:

$$p_s \sim m_H(\lambda, \lambda, \lambda)$$

$$\lambda \sim \frac{p_T^{\text{cut}}}{m_H} : \text{power counting parameter in soft-collinear effective theory (SCET)}$$

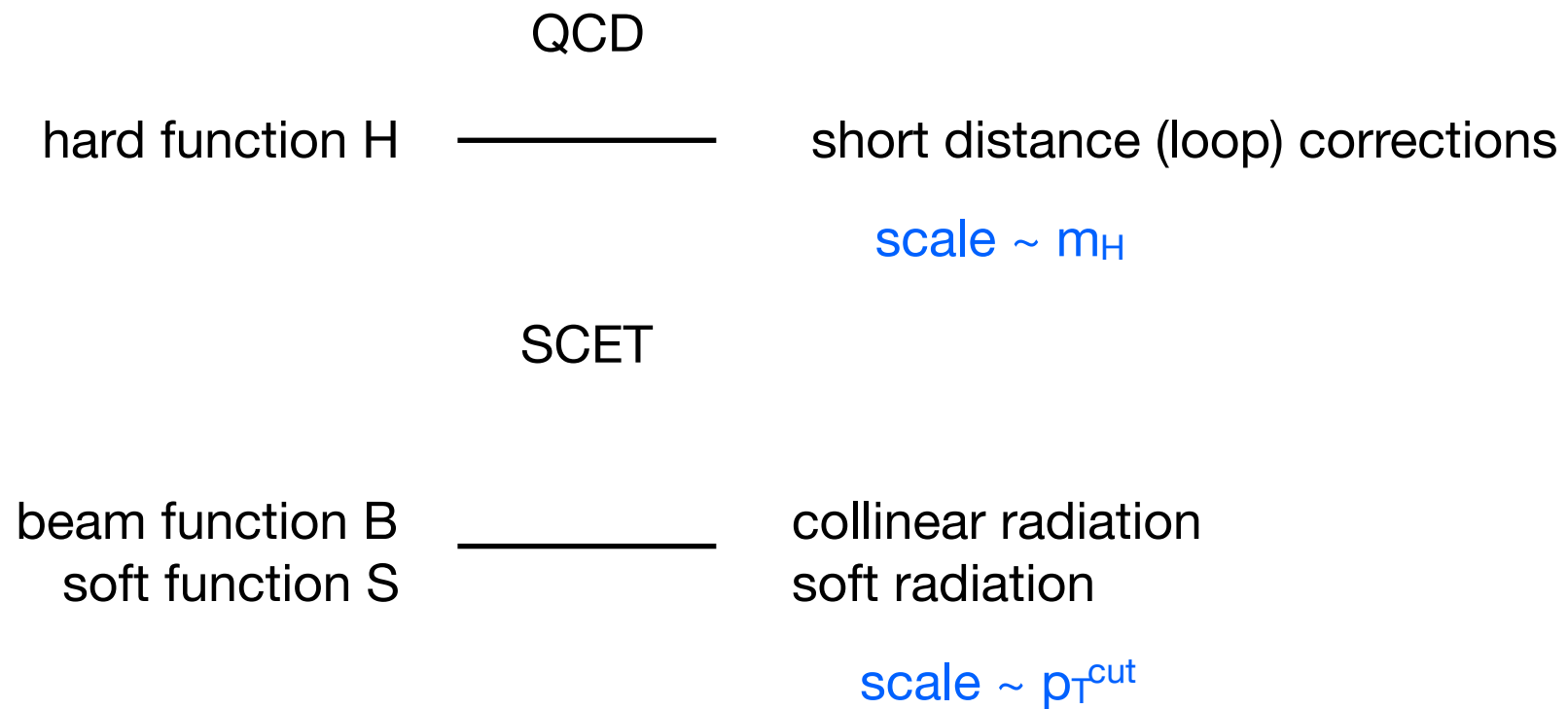
both soft and collinear modes capable of creating jets that probe the veto scale

soft-collinear effective theory (SCET)



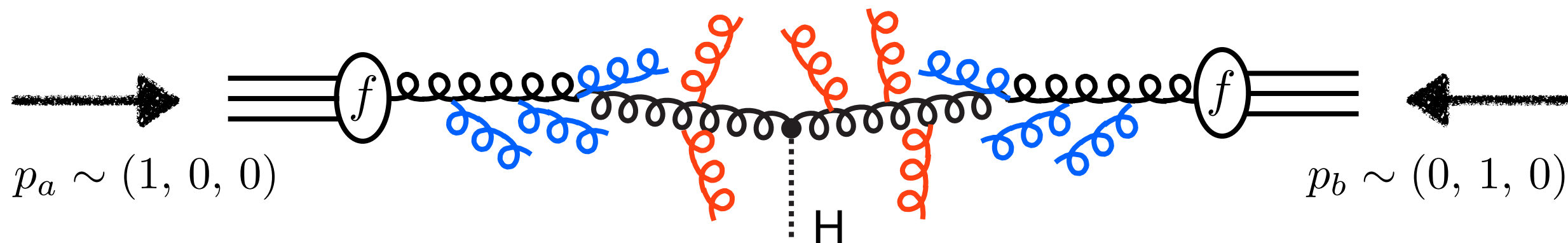
this is SCET_{II}
(not to be confused with SCET_I)

increasing
scale



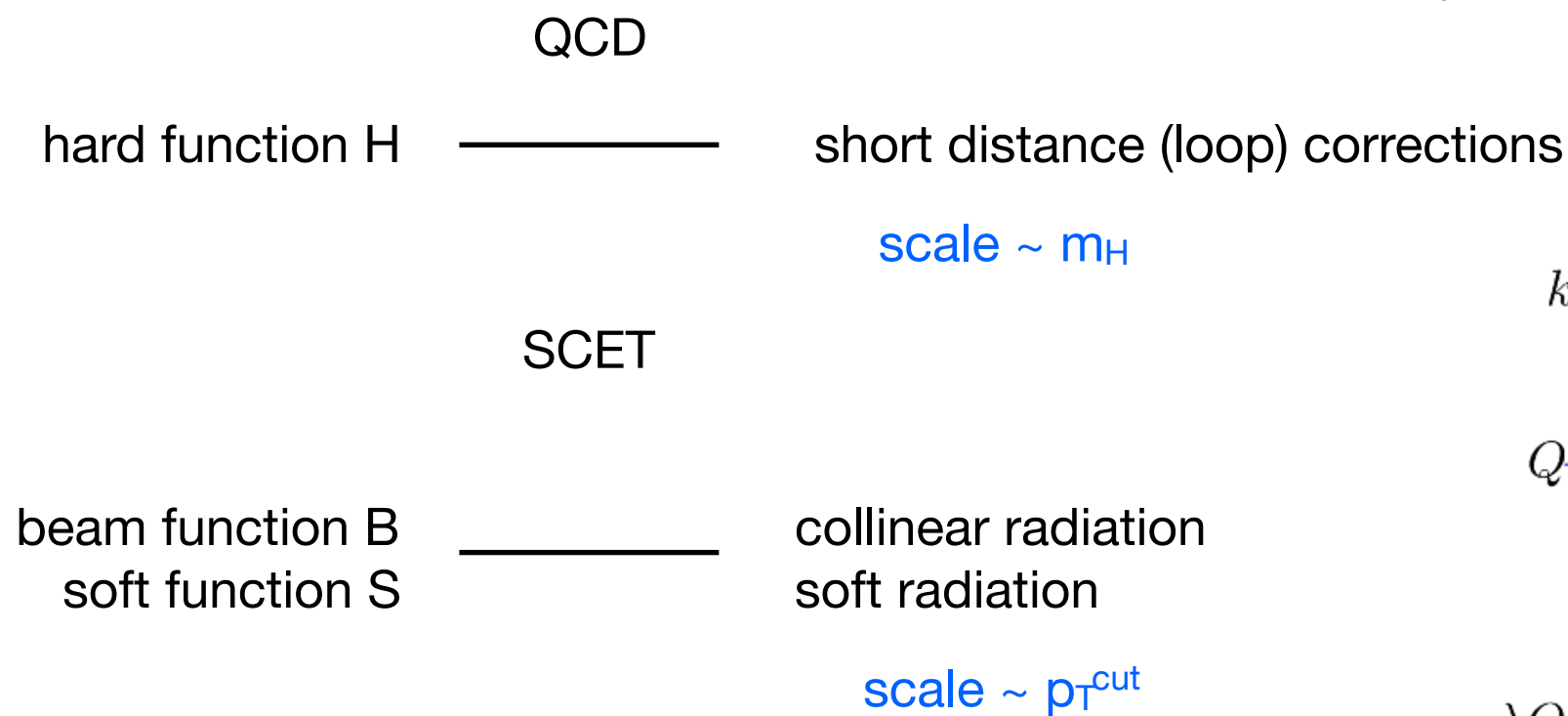
renormalization group evolution in SCET
sums logarithms of m_H / p_T^{cut}

soft-collinear effective theory (SCET)

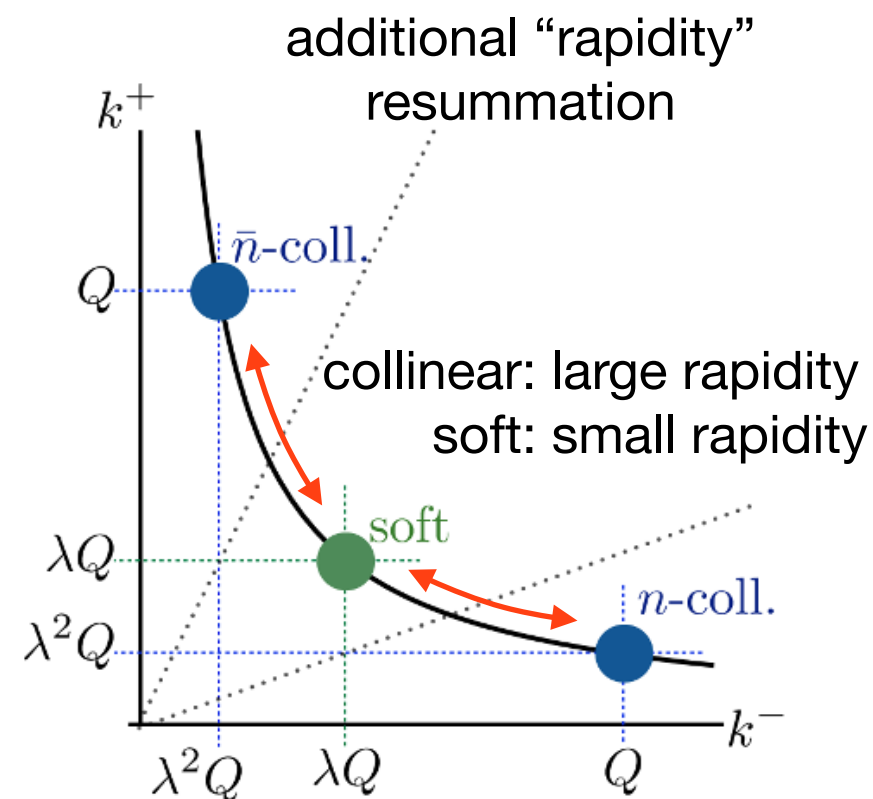


this is SCET_{II}
(not to be confused with SCET_I)

increasing
scale

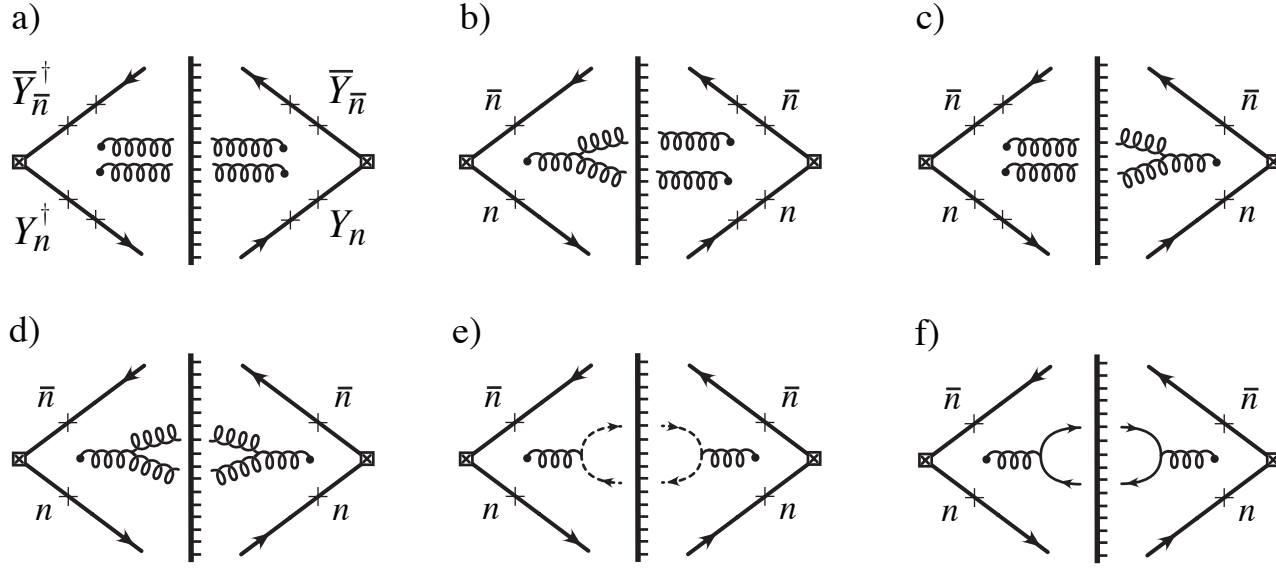


renormalization group evolution in SCET
sums logarithms of m_H / p_T^{cut}



Chiu, Jain, Neill, Rothstein,
1104.0881, 1202.0814

NNLO soft function calculation



real matrix elements

$$\begin{aligned} \tilde{\mathcal{A}}_2 = & 4(4\pi\alpha_s\mu^{2\epsilon})^2 C_A^2 \left\{ \frac{1}{2(x+u)(1+\xi u)} \left[x \left(-2 + \frac{\xi}{2}(1-2u) \right) + \left(1 + \frac{\xi}{2}(u-1) \right) \right] \right. \\ & \left. + \frac{1-\epsilon}{4(x+u)^2(1+\xi u)^2} \left[\frac{1}{4}\xi^2 u(1+u) \right] \right\} \\ & + 4(4\pi\alpha_s\mu^{2\epsilon})^2 C_A T_{Rn_f} \left\{ \frac{1}{2(x+u)(1+\xi u)} \frac{\xi}{4} - \frac{1}{4(x+u)^2(1+\xi u)^2} \left[\frac{1}{2}\xi^2 u(1+u) \right] \right\}. \end{aligned} \quad (2.10)$$

real-virtual terms, global veto

$$S_{RV}^{(2)}(E_T) = \left(\frac{\alpha_s}{\pi} \right)^2 C_A^2 \mu^{4\epsilon} \nu^\eta E_T^{-1-4\epsilon-\eta} \frac{1}{\eta} \left[-\frac{2}{\epsilon^2} + \pi^2 + \frac{16}{3}\zeta_3\epsilon - \frac{\pi^4}{60}\epsilon^2 \right]$$

full result

$$S_{gg}(p_T^{\text{cut}}, R, \mu_S, \nu_S) =$$

$$\begin{aligned} & 1 + \frac{\alpha_s(\mu_S)}{4\pi} \left[2\Gamma_0^g L_S^\mu (L_S^\mu - 2L_S^\nu) - \frac{\pi^2}{3} C_A \right] \\ & + \frac{\alpha_s^2(\mu_S)}{(4\pi)^2} \left\{ \frac{1}{2} \left[2\Gamma_0^g L_S^\mu (L_S^\mu - 2L_S^\nu) - \frac{\pi^2}{3} C_A \right]^2 \right. \\ & + 2\beta_0 L_S^\mu \left[2\Gamma_0^g L_S^\mu \left(\frac{1}{3} L_S^\mu - L_S^\nu \right) - \frac{\pi^2}{3} C_A \right] \\ & + 2\Gamma_1^g L_S^\mu (L_S^\mu - 2L_S^\nu) \\ & \left. + \gamma_{S1}^g L_S^\mu + \gamma_{\nu 1}^g(R) L_S^\nu + s_2(R) \right\}, \end{aligned}$$

2-loop anomalous dimensions

$$\begin{aligned} \gamma_{S1}^g &= 8C_A \left[\left(\frac{52}{9} - 4(1+\pi^2)\ln 2 + 11\zeta_3 \right) C_A \right. \\ & \left. + \left(\frac{2}{9} + \frac{7\pi^2}{12} - \frac{20}{3}\ln 2 \right) \beta_0 \right] \\ &= 16C_A^2 (-3.83), \\ \gamma_{\nu 1}^g(R) &= -16C_A \left[\left(\frac{17}{9} - (1+\pi^2)\ln 2 + \zeta_3 \right) C_A \right. \\ & \left. + \left(\frac{4}{9} + \frac{\pi^2}{12} - \frac{5}{3}\ln 2 \right) \beta_0 \right] + C_2(R) \\ &= 16C_A^2 (4.16) + C_2(R). \end{aligned}$$

reduced double real terms, global veto

$$\begin{aligned} S_{R,\eta}^{(2)}(E_T) &= \left(\frac{\alpha_s}{\pi} \right)^2 \frac{e^{2\gamma_E\epsilon}}{\Gamma(1-\epsilon)^2} \mu^{4\epsilon} \nu^\eta E_T^{-1-4\epsilon-\eta} \frac{2}{\eta} \left\{ \int_0^1 du \frac{1}{\sqrt{u(1+u)}} \right. \\ & \times \left[C_A^2 \left\{ I_x^{1,0}(u) I_\xi^{1,0}(u) \left[\frac{1}{2} \right] + I_x^{1,0}(u) I_\xi^{1,1}(u) \left[\frac{1}{4}(u-1) \right] + I_x^{1,1}(u) I_\xi^{1,0}(u) [-1] \right. \right. \\ & \quad \left. \left. + I_x^{1,1}(u) I_\xi^{1,1}(u) \left[\frac{1}{4}(1-2u) \right] + I_x^{2,0}(u) I_\xi^{2,2}(u) \left[\frac{1-\epsilon}{16} u(1+u) \right] \right\} \right. \\ & \left. + C_A T_{Rn_f} \left\{ I_x^{1,0}(u) I_\xi^{1,1}(u) \left[\frac{1}{8} \right] + I_x^2(u) I_\xi^{2,2}(u) \left[-\frac{1}{8} u(1+u) \right] \right\} \right] \\ & + \int_0^1 dv \frac{1}{v\sqrt{1+v}} \left[C_A^2 \left\{ I_x^{1,0}\left(\frac{1}{v}\right) I_\xi^{1,0}\left(\frac{1}{v}\right) \left[\frac{1}{2} \right] + I_x^{1,0}\left(\frac{1}{v}\right) I_\xi^{1,1}\left(\frac{1}{v}\right) \left[\frac{1}{4v}(1-v) \right] \right. \right. \\ & \quad \left. \left. + I_x^{1,1}\left(\frac{1}{v}\right) I_\xi^{1,0}\left(\frac{1}{v}\right) [-1] + I_x^{1,1}\left(\frac{1}{v}\right) I_\xi^{1,1}\left(\frac{1}{v}\right) \left[\frac{1}{4v}(v-2) \right] \right. \right. \\ & \quad \left. \left. + I_x^{2,2}\left(\frac{1}{v}\right) I_\xi^{2,2}\left(\frac{1}{v}\right) \left[\frac{1-\epsilon}{16} \frac{1}{v^2}(1+v) \right] \right\} \right. \\ & \left. + C_A T_{Rn_f} \left\{ I_x^{1,0}\left(\frac{1}{v}\right) I_\xi^{1,1}\left(\frac{1}{v}\right) \left[\frac{1}{8} \right] + I_x^{2,2}\left(\frac{1}{v}\right) I_\xi^{2,2}\left(\frac{1}{v}\right) \left[-\frac{1}{8} \frac{1}{v^2}(1+v) \right] \right\} \right] \right\}. \end{aligned} \quad (4.7)$$

$$\begin{aligned} S_{R,0}^{(2)}(E_T) &= -\frac{4}{(4\pi)^4} \frac{e^{2\gamma_E\epsilon}}{\Gamma(1-\epsilon)^2} \nu^\eta E_T^{-1-4\epsilon-\eta} \int_0^1 d\xi \frac{1}{\sqrt{1-\xi}} \left(\frac{\xi}{4} \right)^{-1-2\epsilon} \int_0^\infty du \frac{1}{\sqrt{u(1+u)}} \\ & \times \int_0^1 dx (x(1-x))^{-1/2-\epsilon} 2^{-2\epsilon} c_\phi \ln(1+\xi u) \tilde{\mathcal{A}}_2(\xi, u, x). \end{aligned} \quad (4.13)$$

renormalization group evolution

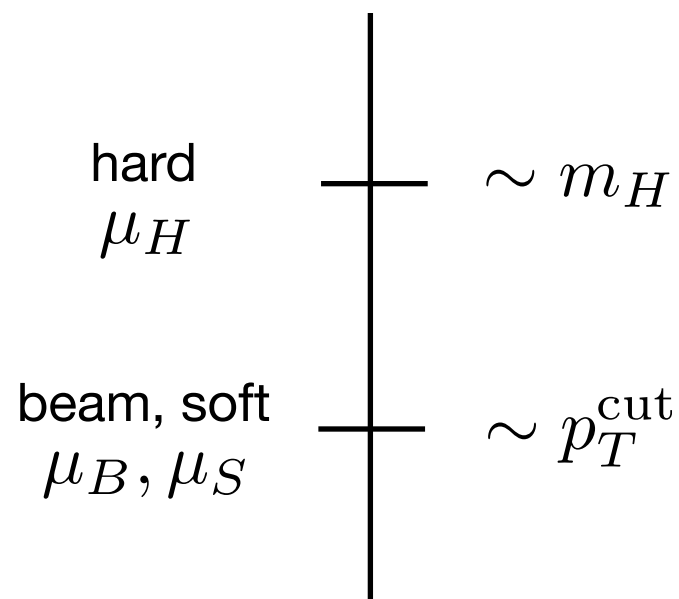
$$\sigma(p_T^{\text{cut}}) \sim H_{gg}(\mu) [B_a(p_T^{\text{cut}}, \mu, \nu) \times B_b(p_T^{\text{cut}}, \mu, \nu) \times S(p_T^{\text{cut}}, \mu, \nu)] + \sigma_{ns}(\mu)$$

RGE

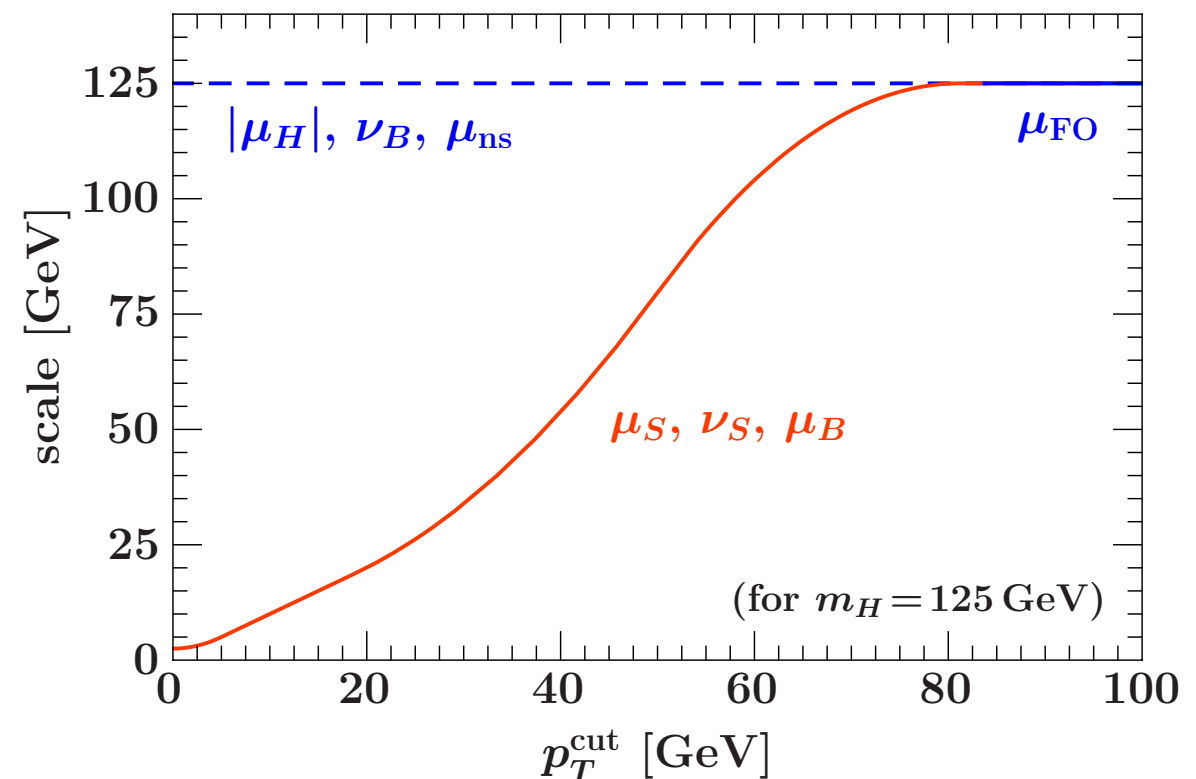
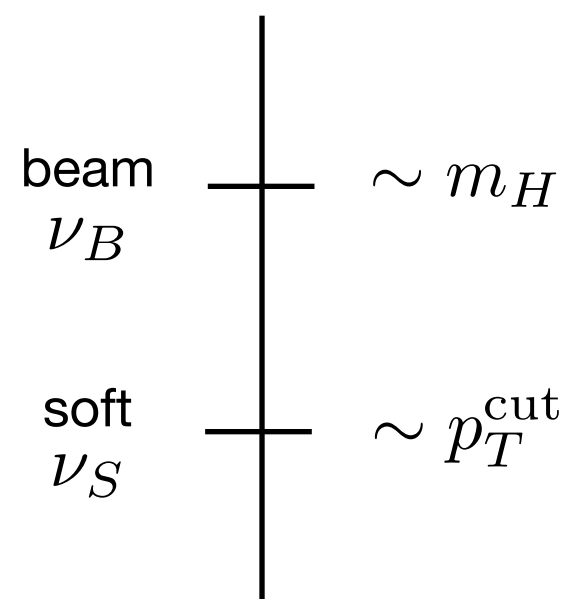
$$S(p_T^{\text{cut}}, \mu, \nu) = S(p_T^{\text{cut}}, \mu_S, \nu_S) \exp\left(\int_{\mu_S}^{\mu} \frac{d\mu'}{\mu'} \gamma_S^{\mu}(\mu', \nu)\right) \left(\frac{\nu}{\nu_S}\right)^{\gamma_S^{\nu}(p_T^{\text{cut}}, \mu_S)}$$

profile scales control the matching between resummation, fixed order

renormalization scale μ



rapidity scale ν



π^2 Resummation

virtual corrections to $gg \rightarrow H$
contain logarithms of the form

$$\ln^n \frac{-q^2 - i0}{\mu^2} \subset C_{ggH}(-q^2, \mu^2)$$

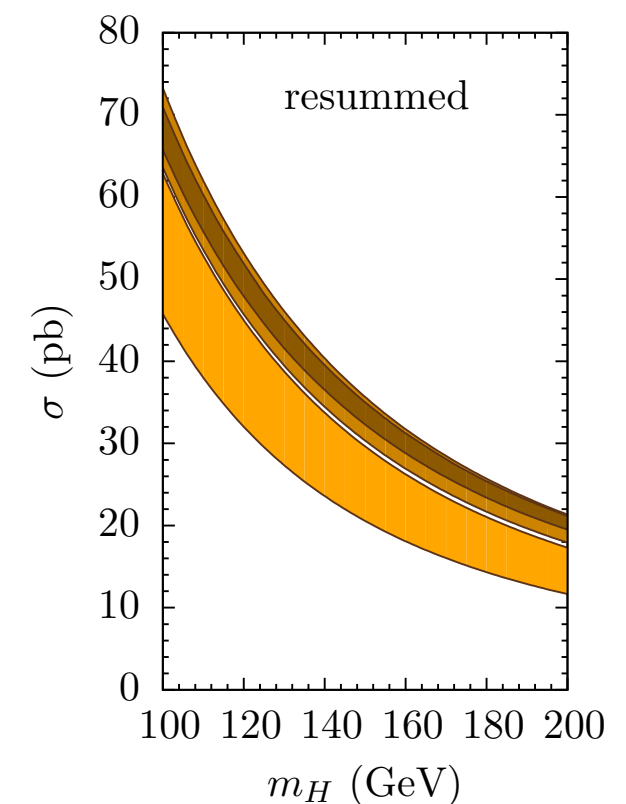
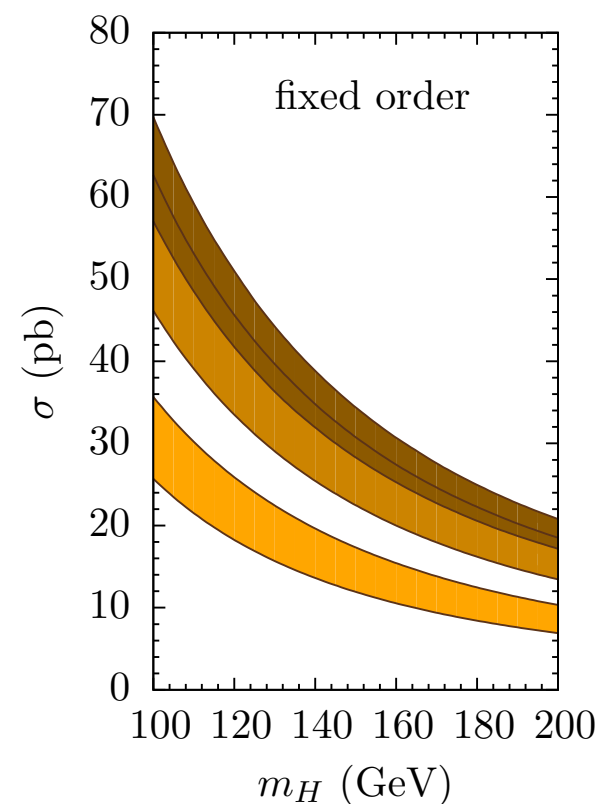
$$H(m_H, \mu_H) = |C_{ggH}(-m_H^2, \mu_H^2)|^2$$

Setting $\mu_H = m_H$ generates
large π^2 terms in H

$$\ln^2 \frac{-m_H^2 - i0}{\mu_H^2} \Big|_{\mu_H = m_H} = \pi^2$$

These terms are resummed
if one chooses $\mu_H = -im_H$

Ahrens, Becher, Neubert, Yang
0808.3008

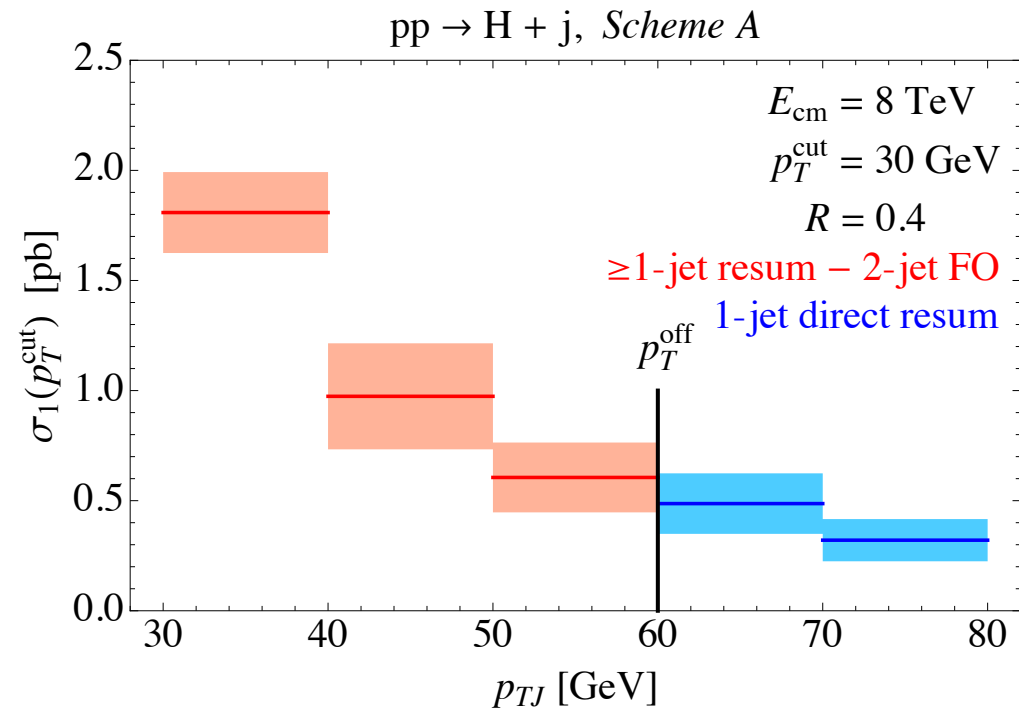


technical ingredients

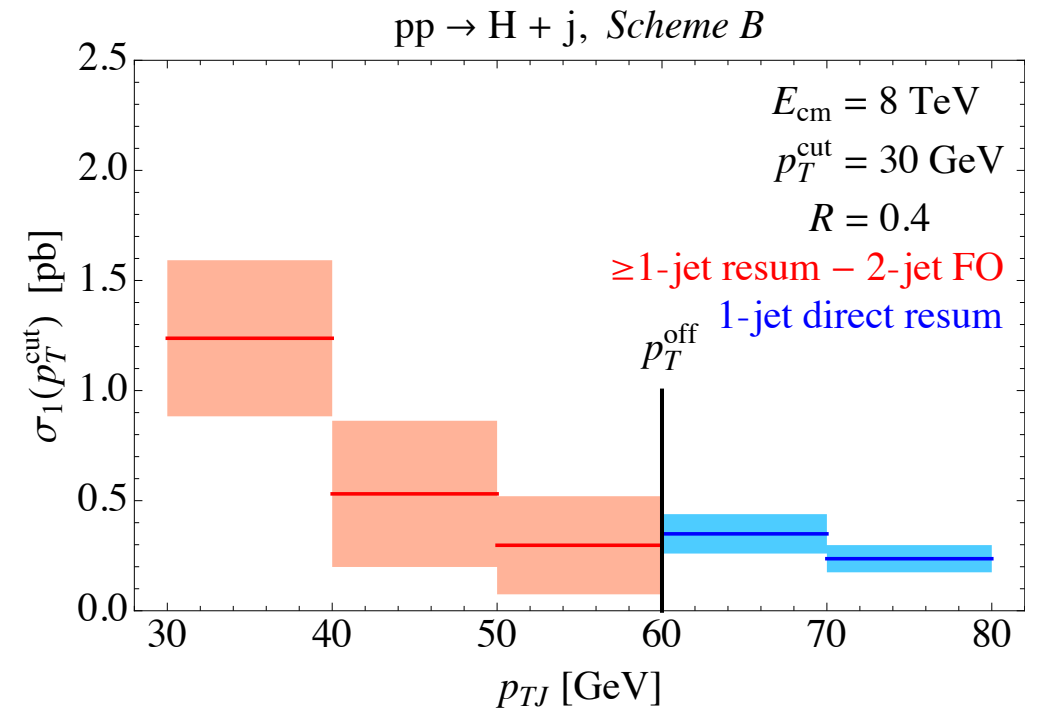
- Jet algorithm dependence and factorization properties
 - Can use a global, algorithm-independent veto
 - Complicates factorization: need to ensure soft-collinear decoupling in the jet clustering
 - Nontrivial logarithmic structure of the jet radius in the 0-jet rate
 - Factorization and RGE properties constrains form, have calculated N³LO contributions
- Details of soft, beam function calculations
 - Lorentz invariant properties of the global veto simplifies calculation
 - Can group finite and logarithmic clustering effects in beam and soft function via RGE
- Nonsingular contributions to the cross section, determined using fixed order codes
- Physical basis for uncertainty estimation, comparison to fixed order methods
- Extension of 0-jet resummation to 1-jet bin

matching the direct and indirect contributions

scheme A: π^2 resummation, H + 1j NNLO virtuals



scheme B: no π^2 resummation, H + 1j @ NLO



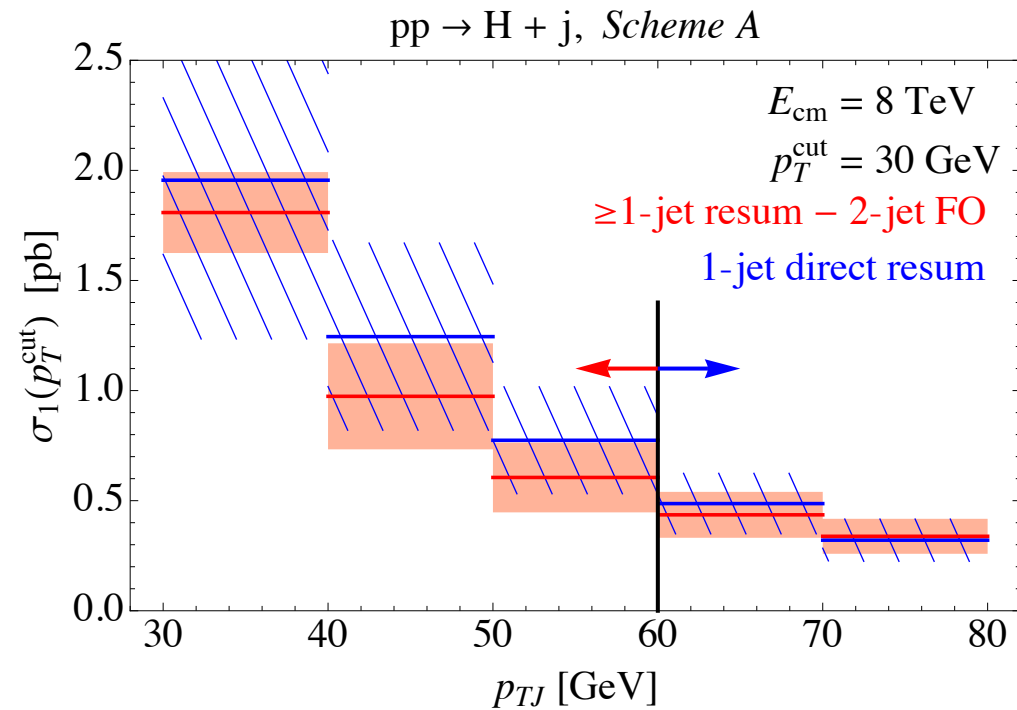
Matching of the direct and indirect approaches is smooth across p_T^{cut}

scheme A shows significantly reduced uncertainties

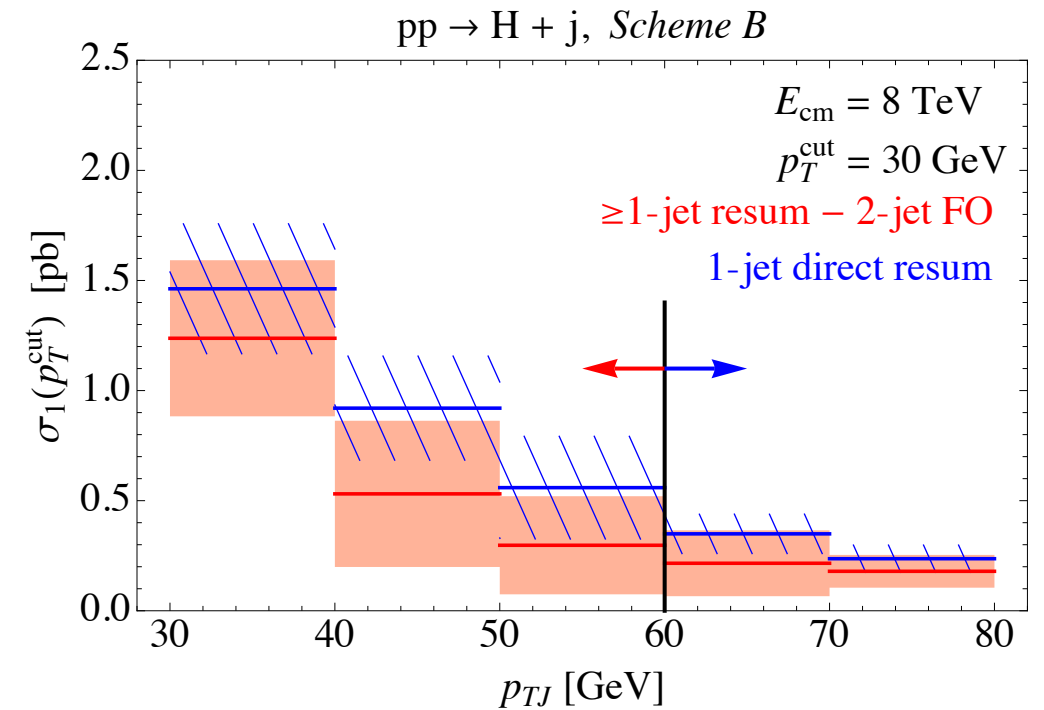
π^2 resummation \Leftrightarrow H + 1j NNLO virtuals

matching the direct and indirect contributions

scheme A: π^2 resummation, H + 1j NNLO virtuals



scheme B: no π^2 resummation, H + 1j @ NLO

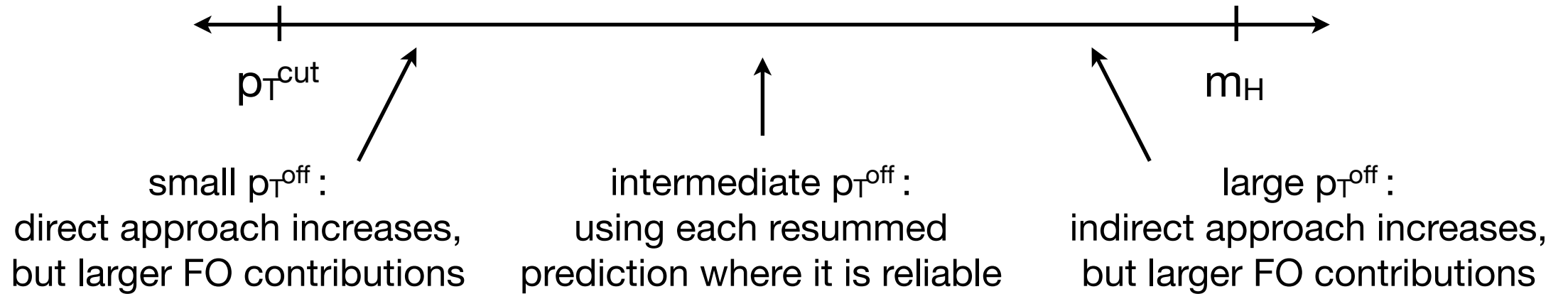


Matching of the direct and indirect approaches is smooth across p_T^{cut}

scheme A shows significantly reduced uncertainties

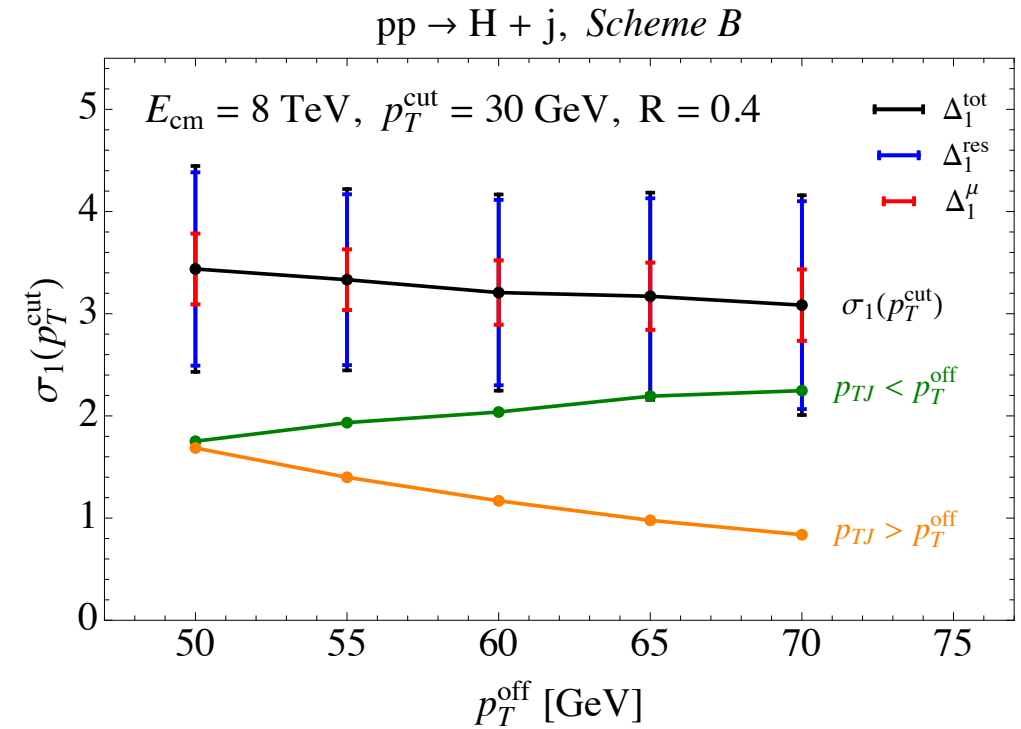
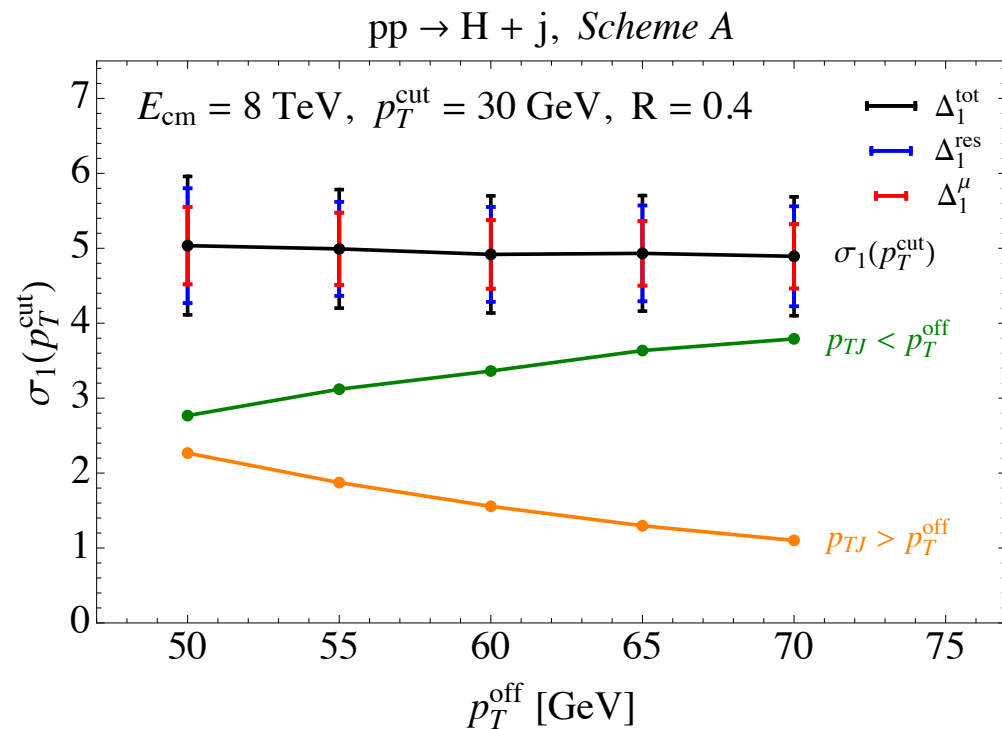
π^2 resummation \Leftrightarrow H + 1j NNLO virtuals

testing the matching



scheme A: π^2 resummation, H + 1j NNLO virtuals

scheme B: no π^2 resummation, H + 1j @ NLO



Matching scale (p_T^{off}) dependence is small

Combining Jet Bins

Signal strength: $\mu = \frac{\sigma_{\text{obs}}}{\sigma_{\text{exp}}}$

$$\sigma_{\text{exp}} = \epsilon_0^{\text{exp}} \sigma_0^{\text{exp}} + \epsilon_1^{\text{exp}} \sigma_1^{\text{exp}} + \epsilon_{\geq 2}^{\text{exp}} \sigma_{\geq 2}^{\text{exp}}$$

2-jet term
negligible for
 $gg \rightarrow H \rightarrow WW$

ATLAS measurement of signal strength in $H > WW$:

$$\begin{aligned} \mu_{\text{obs}, 8 \text{ TeV}} &= 1.26 \pm 0.24 \text{ (stat.)} \pm 0.21 \text{ (theo. syst.)} \pm 0.14 \text{ (expt. syst.)} \pm 0.06 \text{ (lumi.)} \\ &= 1.26 \pm 0.35. \end{aligned}$$

[ATLAS-CONF-2013-030](#)

Two Clustering Effects, Two Regions of Jet Radius

Jet algorithm effects:

$$\sigma \supset \mathcal{O}(R^n), \mathcal{O}(\ln^n R) \text{ terms}$$

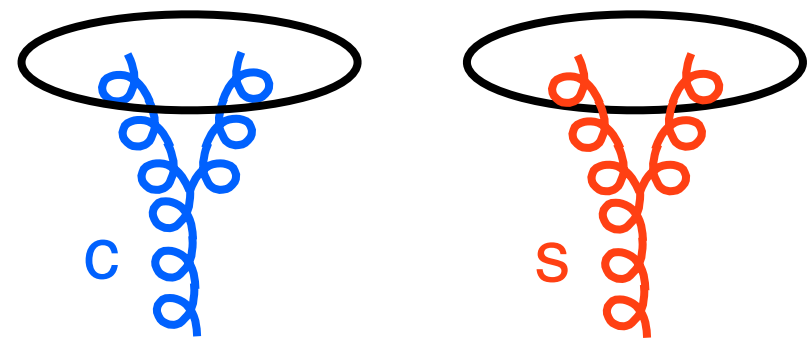
Two Clustering Effects, Two Regions of Jet Radius

Jet algorithm effects:

$$\sigma \supset \mathcal{O}(R^n), \mathcal{O}(\ln^n R) \text{ terms}$$

*Factorization theorem
valid for small jet radius*

Small jet radius
 $R \ll 1$



logarithms of jet radius important
but resummation is impossible

Two Clustering Effects, Two Regions of Jet Radius

Jet algorithm effects:

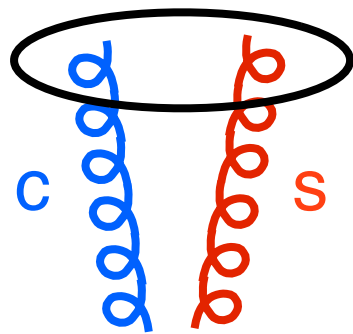
$$\sigma \supset \mathcal{O}(R^n), \mathcal{O}(\ln^n R) \text{ terms}$$

Can induce violations to naive factorization

Factorization theorem valid for small jet radius

Large jet radius

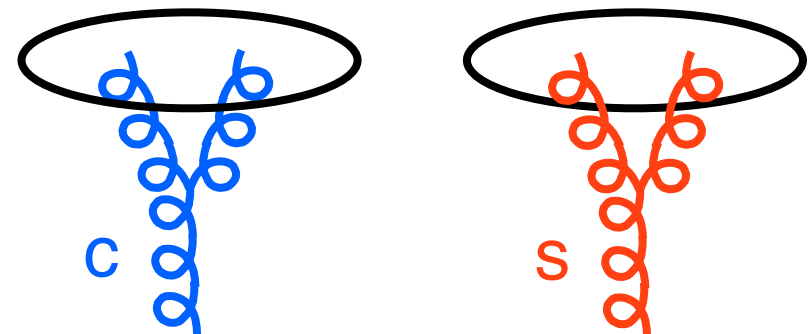
$$R \sim 1$$



complicates factorization
but numerically unimportant

Small jet radius

$$R \ll 1$$



logarithms of jet radius important
but resummation is impossible

Clustering Logs

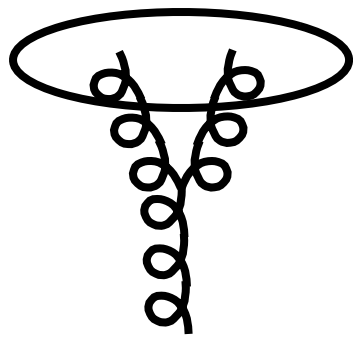
Clustering effects give rise to logs of R

E_T veto measurement at NNLO:

$$\mathcal{M} = \theta(p_{T1} + p_{T2} < p_T^{\text{cut}})$$

correction for clustering:

$$\Delta\mathcal{M} = \theta(\Delta R > R) \left[\theta(p_{T1} < p_T^{\text{cut}}) \theta(p_{T2} < p_T^{\text{cut}}) - \theta(p_{T1} + p_{T2} < p_T^{\text{cut}}) \right]$$



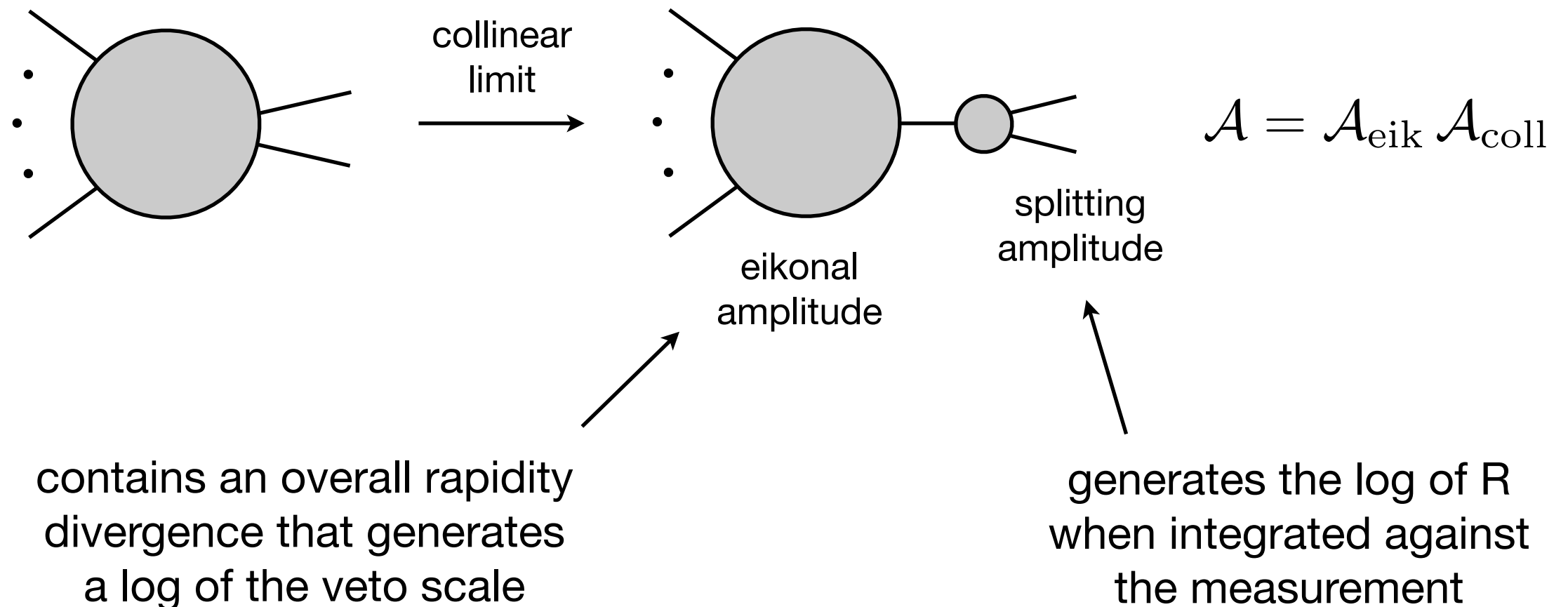
can write in terms of canceling IR collinear divergences

$$\begin{array}{l} \mathcal{M}_{sp} : \frac{1}{\epsilon} \\ \Delta\mathcal{M}_{sp} : -\frac{1}{\epsilon} R^\epsilon \end{array} \begin{array}{l} \nearrow \\ \nearrow \end{array} \ln R : \text{remnant of collinear} \\ \text{divergence sensitive} \\ \text{to jet radius}$$

Clustering Logs in the Soft Function

Tackmann, JW, Zuberi
1206.4312

can be calculated using collinear limits of eikonal matrix elements:



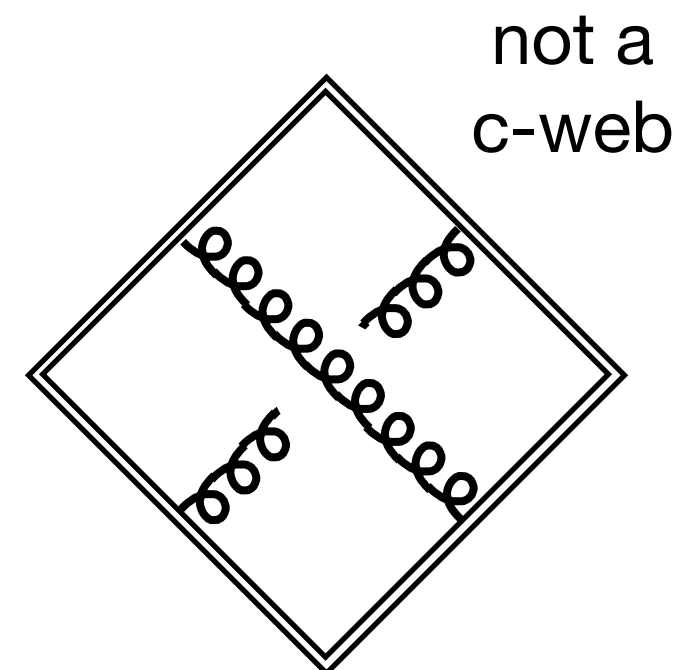
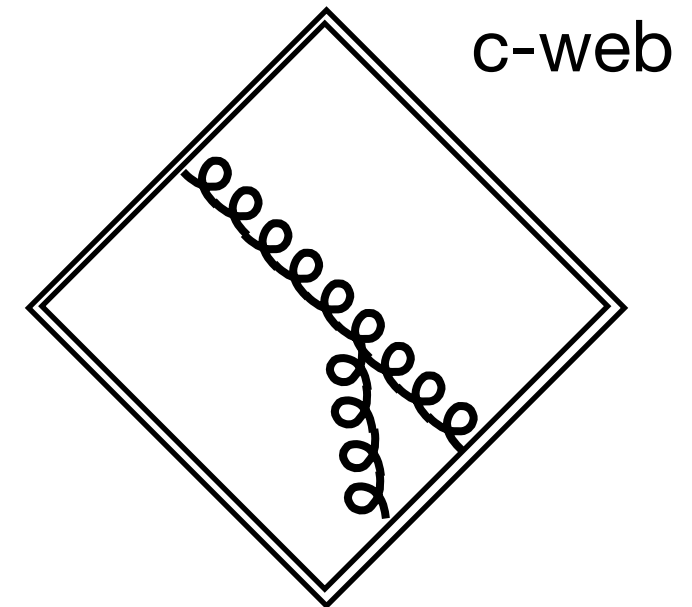
$$\Delta S = \left(\frac{\alpha_s C_A}{\pi} \right)^2 \ln \frac{\nu}{p_T^{\text{cut}}} \ln R (-4.97)$$

consistency with the jet function: $\nu \rightarrow m_H$

Clustering Logs from c-webs

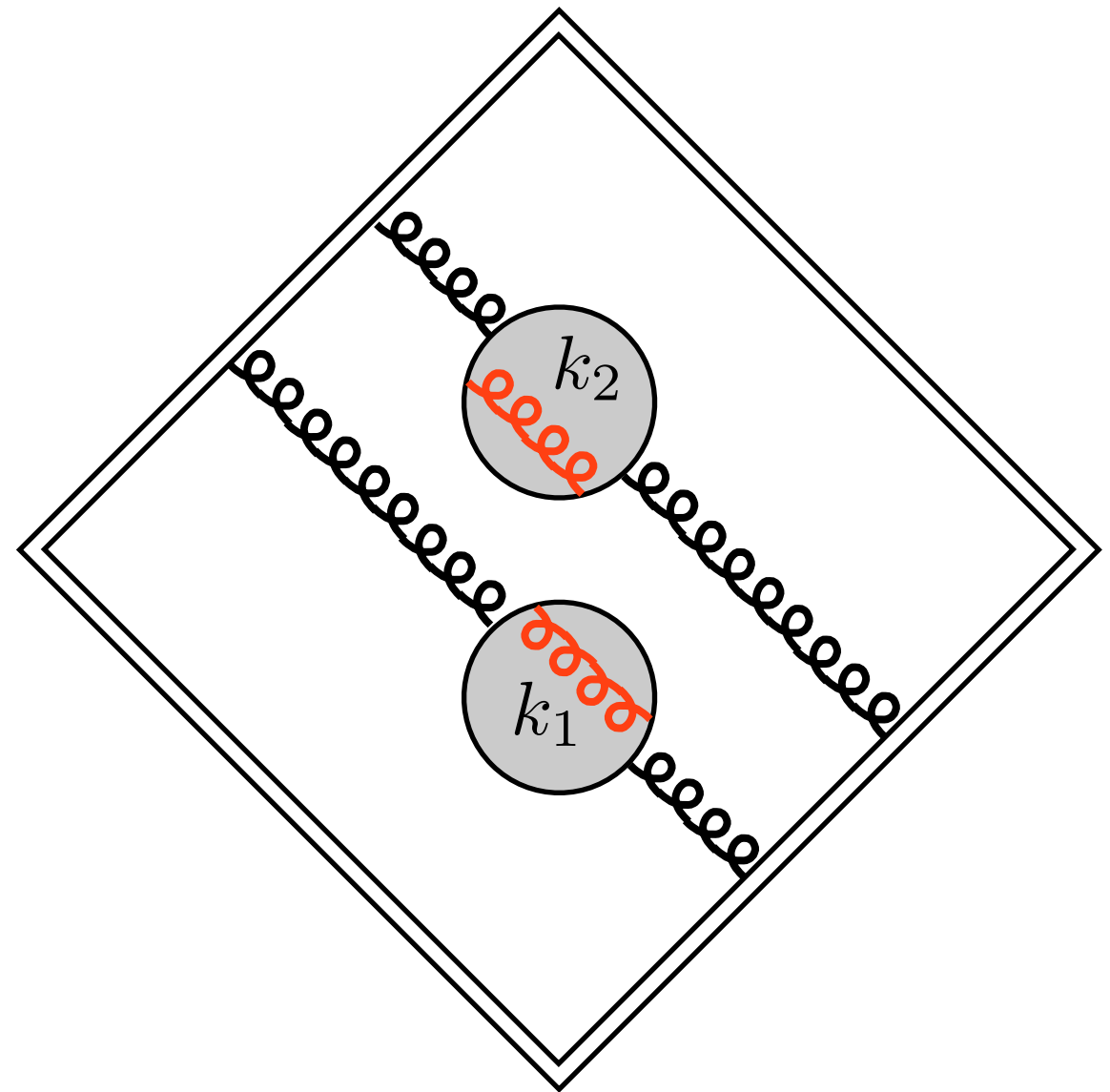
Frenkel, Taylor

- Collinear singularities between particles in the same jet give rise to logs of R from clustering
- How do we count the number of these logs?
c-webs
- Connected webs of partons that can contain collinear singularities between partons in the web



Clustering Logs from c-webs

- There is no collinear singularity between gluons in different c-webs
- Clustering between gluons in different c-webs gives power suppressed effects
- Constrains the total number of logs from clustering



$$A \not\propto \frac{1}{k_1 \cdot k_2}$$

Clustering Logs from c-webs

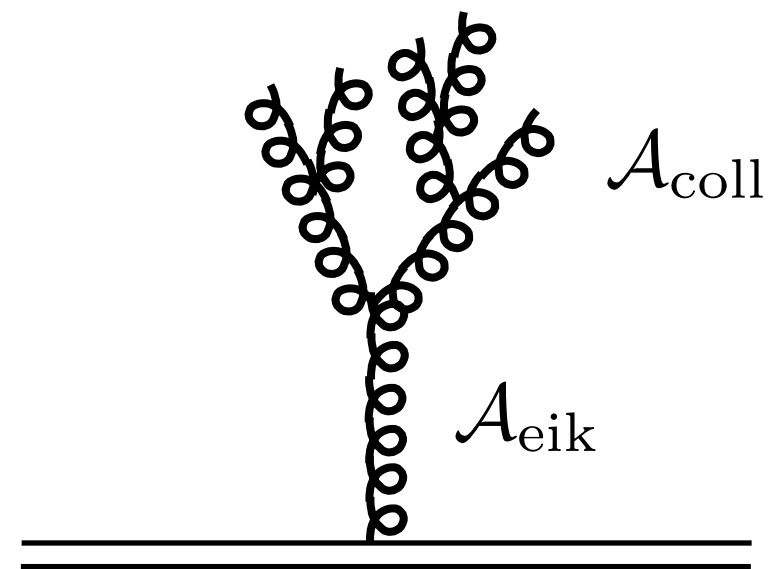
- A c-web of n gluons has $n-1$ collinear singularities
- This means the maximal clustering log is

$$\left(\frac{\alpha_s C_A}{\pi}\right)^n C_n \ln \frac{m_H}{p_T^{\text{cut}}} \ln^{n-1} R$$

- This is NLL (cannot resum) if

$$\frac{p_T^{\text{cut}}}{m_H} \sim R \sim \lambda$$

single c-web



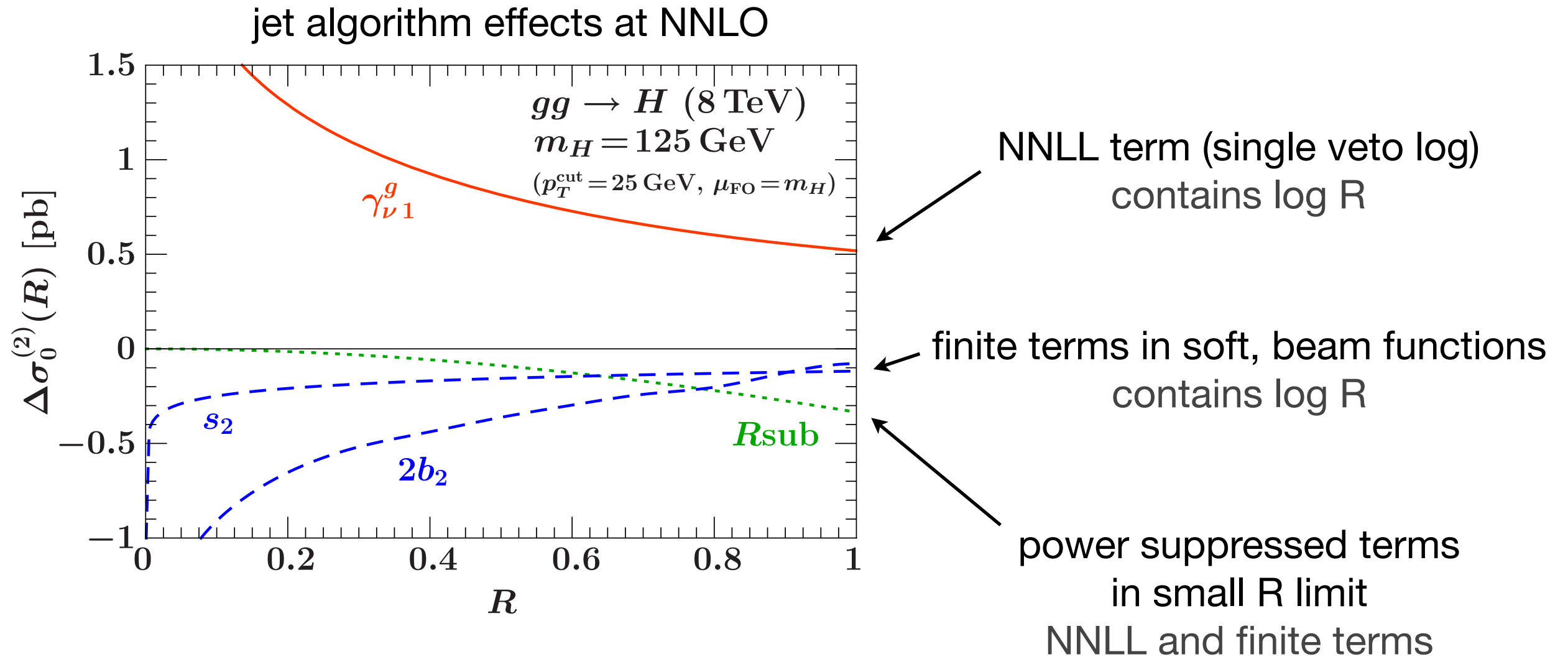
$$\mathcal{A} = \mathcal{A}_{\text{eik}} \mathcal{A}_{\text{coll}}$$

$$\mathcal{A}_{\text{coll}} \sim \left(\frac{2}{s_{\text{tot}}}\right)^{n-1} (4\pi\alpha_s\mu^{2\epsilon})^n \langle \hat{P}_{\text{coll}} \rangle$$

Catani, Grazzini

Jet Algorithm Effects

clustering effects start at NNLO
log R dependence not resummed



at NNLO, the log R effects are large

also relatively large cancellation
between NNLL and finite terms
(for $p_{T\text{cut}} = 25$ GeV)

what about at higher orders?
are the clustering terms large?
could be a source of large uncertainties

Clustering Logs

form of
leading clustering logs

$$\left(\frac{\alpha_s}{4\pi}\right)^2 \ln \frac{m_H}{p_T^{\text{cut}}} C_2 \ln R$$

$$\left(\frac{\alpha_s}{4\pi}\right)^3 \ln \frac{m_H}{p_T^{\text{cut}}} C_3 \ln^2 R$$

$$\left(\frac{\alpha_s}{4\pi}\right)^4 \ln \frac{m_H}{p_T^{\text{cut}}} C_4 \ln^3 R$$

$$m_H = 125 \text{ GeV}, \quad p_T^{\text{cut}} = 25 \text{ GeV}, \quad R = 0.4 : \\ \ln p_T^{\text{cut}} / m_H = \ln R/2$$

if we take the logs to be of the same order,
the clustering terms are of the form

$$\left(\frac{\alpha_s}{4\pi}\right)^n L^n C_n \quad \text{formally NLL, each term} \\ \text{is } \textit{equally important}$$

in this basis, $C_2 = -716.3$

contribution to
the cross section: $\sigma_{\text{clus}}^{(2)} = 0.14 \sigma_{\text{LO}}$

knowing the higher order
coefficients helpful in determining
uncertainties from clustering

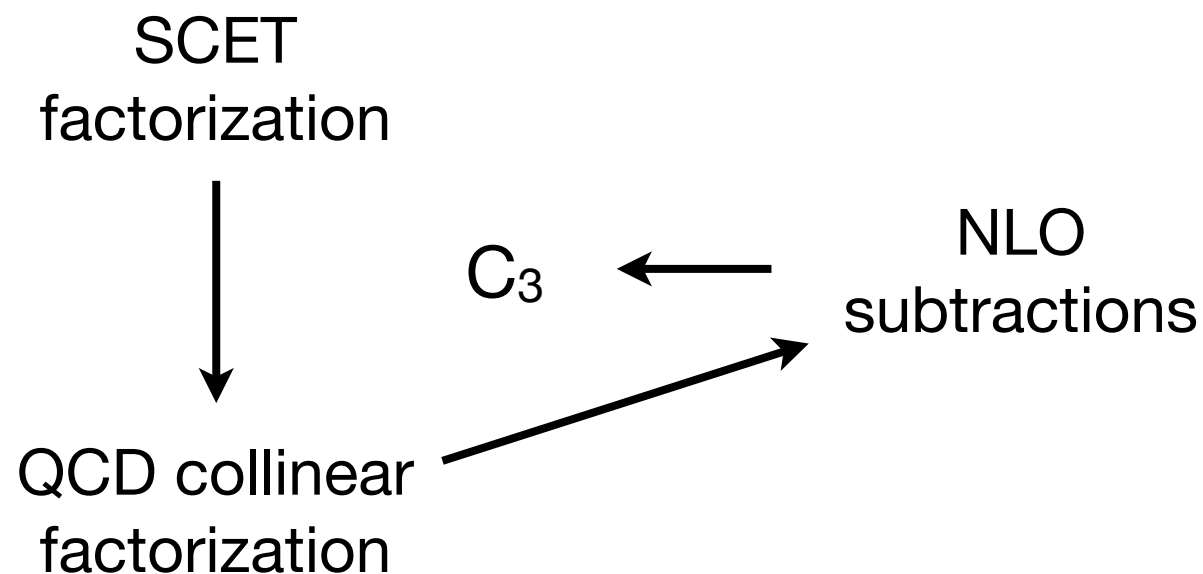
Clustering Logs at NLO

Alioli, JW - 1311.5234

C_3 can be determined via an NLO soft function calculation

$$\sigma(p_T^{\text{cut}}) \sim H_{gg}(\mu) \left[B_a(p_T^{\text{cut}}, \mu, \nu) \times B_b(p_T^{\text{cut}}, \mu, \nu) \times \underline{S(p_T^{\text{cut}}, \mu, \nu)} \right] + \sigma_{ns}(\mu)$$

relevant soft function matrix elements
can be written in terms
of universal splitting functions,
calculation done with NLO subtractions



result: C_3 is small, contribution to the resummed cross section is <1%
uncertainties under control

sample raw fits for C_3

